To the Graduate Council:

I am submitting herewith a thesis written by Darren W. Schnare entitled "Petrogenesis of Apollo 15 Olivine-Normative and Quartz-Normative Mare Basalts." I have examined the final electronic copy of this thesis for form and content and recommend that it be accepted in partial fulfillment of the requirements for the degree of Master of Science, with a major in Geology.

_____Larry A. Taylor_____

We have read this thesis
and recommend its acceptance:

___Harry Y. McSween_____

___Theodore C. Labotka___

Accepted for the Council:

_____Anne Mayhew____
Vice Chancellor and
Dean of Graduate Studies

(Original signatures are on file with official student records.)

Petrogenesis of Apollo 15 Olivine-Normative and Quartz-Normative Mare Basalts

A Thesis

Presented for the

Master of Science Degree

The University of Tennesee, Knoxville

Darren W. Schnare

December 2006

Acknowledgements

The author thanks Marc Norman, Larry Taylor, and James Day for their insightful reviews and guidance, Marc Norman and Allan Patchen for their laboratory assistance, and Dawn Taylor for technological assistance. In addition, the Department of Earth & Planetary Sciences is to be acknowledged for its support of my Graduate Teaching Assistantship; similarly, the Tennessee Space Grant Consortium is thanked for its support of my Graduate Research Assistantship.

Abstract

New data are presented for four Apollo 15 low-Ti mare basalts, two from the olivine-normative suite (15106, and 15555) and two from the quartz-normative suite (15475, and 15499). Previous studies have examined the relationships between these groups on the basis of whole-rock chemistry, many with analyses that may have been of insufficient sample-size, or of limited range of elements analyzed. To determine a relationship between these basalts, these samples have been analyzed for their mineral major-element and trace-element compositions by electron-microprobe and laser-ablation inductively-coupled-plasma mass-spectrometry, respectively.

The trace-element compositions of the main silicate phases, olivine, pyroxene, and plagioclase, are consistent with both groups of basalts having a common parental melt and the groups being related by simple fractional crystallization processes rather than coming from different sources. This observation is supported by similar radiogenic ages for the basalt groups and by petrogenetic modeling. Distribution coefficients have been used to determine the parental and evolved melt compositions for these basalts. Also, an independent set of distribution coefficients has been determined from pyroxene-melt relationships in sample 15499. The calculated parental melts are similar to measured whole-rock compositions. The calculated evolved melts are consistent with fractional crystallization of olivine. From a trace-element perspective, these basalts appear to be from a single parental melt, and related by fractional crystallization of 5-15% olivine.

Table of Contents

Section	Page
I. Introduction	1
II. Analytical Methods	5
III. Results	8
Petrography and Major-Element Mineral Chemistry	8
Olivine-Normative Basalts	8
Quartz-Normative Basalts	14
Trace-element Mineral Chemistry	17
Pyroxene	17
Plagioclase, Olivine, Spinel	21
Quenched Melt	24
IV. Discussion	26
Mineralogic Controls on Inter-Suite Variations	26
Determination of Parental Melt Compositions	27
Modal Recombination	27
Partition Coefficients	30
Calculated Evolved Parental Melts	32
Distribution Coefficients from Rim-Melt Compositions	35
V. Apollo 15 Basalt Petrogenesis: Two Magmas or Fractional Crystallization?	37
VI. What Does This Mean for Lunar Geology?	40
VII. Summary	41
List of References	42
Appendices	49
Vita	90

List of Tables

Tables Page

1. Modal Analyses of Apollo 15 Mare Basalts 9

2. Petrography and Major-Element Mineral Chemistry Summary 10

3. Representative EMP Data for Minerals 11

4. Trace-Element Data from LA-ICP-MS Analyses of Major Silicate Phases 18

5. Normalized Parental Melts and Whole-Rock Compositions 29

6. Calculated Distribution Coefficients for QNB 15499 36

A1: LA-ICP-MS Data for USGS Basaltic Glass Reference Materials 50

List of Figures

Figure Page

1. Whole-Rock Data Element Variation Diagrams 4

2. Back-Scattered-Electron (BSE) Images of the Four Thick-Sections of Apollo 15 Basalts 12

3. Pyroxene-Quadrilaterals and Olivine and Plagioclase Histograms for ONBs and QNBs 13

4. Cr-Al-2Ti Diagram for Spinels from these Apollo 15 Basalts 15

5. Plot of Ti vs Al for Pyroxenes in the Samples Analyzed 16

6. Rare-Earth-Element Plot for Pyroxenes Analyzed in this Study 19

7. Trace-Element Variation Diagrams for Pyroxene 20

8. Rare-Earth-Element Concentrations for Plagioclase 22

9. Element Variation Diagrams for Olivine 23

10. Quenched Matrix Rare-Earth-Element Plot 25

11. Modal Recombination Results 28

12. Rare-Earth-Element Diagram for Parental Melts 31

13. Photomicrograph of QNB 15499 33

14. Rare-Earth-Element Diagram for Evolved Melts 34

15. Trace-Element versus Mg# Whole-Rock Plot 39

I. Introduction

Petrologic and geochemical studies of mare basalts and highland rocks collected during the Apollo missions have shaped our present understanding of the Moon. Mare basalt studies have revealed information on the timing of volcanism, magmatic processes occurring within the lunar mantle and crust, chemical attributes of lunar-mantle source regions, and, ultimately, the origin and evolution of Earth's Moon (e.g., Taylor, 1975, 1982; Taylor, Taylor, and Taylor, 2006). Studies of these basalts have also revealed similarities and differences with basaltic magmatism that occurs on other planets, planetesimals, and moons (e.g., Ruzicka *et al.*, 2001). Indeed, for lunar petrologists, *"the significance of these mare basalts far outweighs their relative crustal volume (~1%) and surficial extent (~17%)"* (Head, 1976). The advent of new instrumentation and analytical techniques has greatly improved understanding of mare basalt petrogenesis leading to more detailed models for lunar volcanism. This thesis applies recent geochemical advances to the study of Apollo 15 basalts, allowing a more refined model for their petrogenesis.

At the Apollo 15 site, the low-Ti mare basalts have been subdivided into two distinct groups on the basis of their bulk-rock, major-element compositions. Olivine-normative basalts (ONB) possess higher FeO and TiO_2 and lower SiO_2 than quartz-normative basalts (QNB) (pyroxene-phyric basalts of Dowty *et al.,* 1973), which generally possess higher abundances of large-ion lithophile elements (Rhodes and Hubbard, 1973). The major-element compositions of ONBs appear to be more primitive than QNBs, which led to proposals that the two suites are related by fractional

crystallization of a combination of olivine, pigeonite, and chromite. However, for the last 30 years there has remained a controversy as to the relationship of the basalts: Are these magmas related or not?

Initial studies indicated that these chemically defined groups represent at least two distinct lava flows in the Hadley Rille/Appenine Front region (Apollo 15 Preliminary Examination Team, 1972). Indeed, the olivine-normative basalts are likely to overlie the quartz-normative basalts at the Apollo 15 landing site (Wilhelms, 1984; 1987), suggesting an older age for the ONBs. However, both groups have identical crystallization ages of ~3.3 ±0.1 Ga (Nyquist and Shih, 1992; Snyder et al., 1997; 1998). Snyder *et al.* (1998) reported an Rb-Sr isochron age for 15016 (ONB) of 3.34 ±0.03 Ga, and a less-precise Sm-Nd isochron age of 3.21 ±0.17 Ga. Snyder *et al.* (1997) reported an Sm-Nd isochron age for 15475 (QNB) of 3.37 ±0.05, but did not report a reliable Rb-Sr age. The similar initial strontium ratios for 15016 (QNB) of $^{87}Sr/^{86}Sr_i = 0.699410 \pm 10$ (Snyder *et al.*, 1998) and 15475 (QNB) of $^{87}Sr/^{86}Sr_i = 0.699365 \pm 10$ (Snyder *et al.*, 1997) support similarity in crystallization ages. Snyder *et al.* (1998) stated that the older Rb-Sr age for 15016 does not allow an unequivocal separation of ages between ONBs and QNBs and suggested these basalt types were essentially contemporaneous.

However, there has been controversy in the literature regarding the petrogenetic relationships between these groups and their origin within the lunar mantle (Rhodes and Hubbard, 1973; Chappell and Green, 1973; Lindstrom and Haskin, 1978; Vetter *et al.* 1989). In general, major-element compositions are compatible with olivine fractionation, whereas the whole-rock incompatible-trace element compositions show a much greater variation than can be accommodated by reasonable amounts of olivine fractionation.

However, many of the whole-rock, trace-element trends are similar in both rock types: the rare-earth elements (REE), Hf, and Sm/Eu values all increase with decreasing Mg# (Fig. 1). Some differences do occur, made evident by the QNBs, such as decreased Sc concentrations with decreasing MgO. However, one of the largest data sets (Vetter et al. (1989) for QNBs is on small rake samples that have clearly experienced sampling-size problems, as noted by Ryder and Steele (1988) and Ryder and Schuraytz (2001). The sample-size problem relates to the grain size and mass of sample analyzed. To overcome this issue, Ryder and Schuraytz (2001) recommended up to 5g sub-samples would be required for a thorough reanalysis the Apollo 15 sample suite, undertaken to understand the nature and causes of petrologic dispersion in these rocks. This was not carried out as planned due to the untimely death of Graham Ryder.

The present study addresses the relationship of Apollo 15 olivine- and quartz-normative basalts using the major- and trace-element chemistry of the individual minerals. This methodology utilizes electron microprobe and laser-ablation inductively-coupled-plasma mass-spectrometry and does not rely on possibly erroneous whole-rock data, although some comparisons are drawn with these data. With this new data set, the causes of chemical dispersion within, and the relationships between, the Apollo 15 olivine-normative and quartz-normative basalts are explored. Preliminary results of this study have been presented at the Meteoritical Society Annual Meeting and the Lunar and Planetary Science Conference (Schnare *et al.*, 2005, 2006).

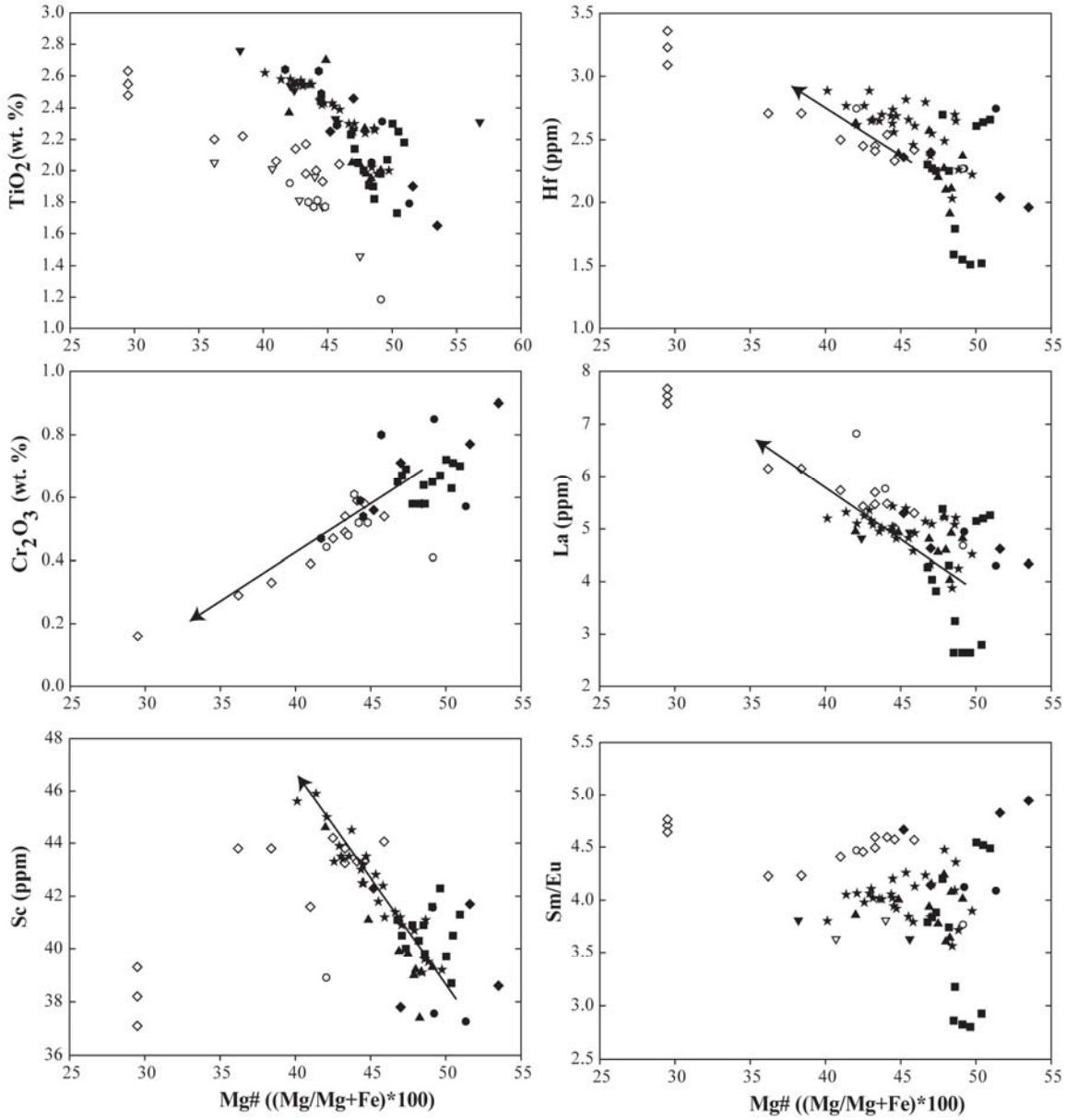


Figure 1. Whole-Rock Data Element Variation Diagrams. Open symbols are QNBs. Closed symbols are ONBs. Circles - Day *et al.* (2006); Triangles - Ryder & Steele (1988); Squares - Shervais et al. (1990); Diamonds - Vetter *et al.* (1988); Inverted Triangles - Rhodes and Hubbard (1973); Stars - Ryder and Shuraytz (2001); Hexagons - Chappell and Green (1973). Arrows indicate concurrent trends. After Vetter *et al.* (1993).

II. Analytical Methods

Modal abundances of minerals were determined on four polished thin sections (15016,10; 15555,257; 15475,147; 15499,125), using the *Feature Scan Phase Distribution* software package of an Oxford instrument energy dispersive spectrometer (EDS) interfaced to the CAMECA SX-50 electron microprobe (EMP) at the University of Tennessee. Modal analysis acquisition was performed using an accelerating potential of 15 keV, a 4 nA beam current, and 70 ms count times sampling every 8 μm (Taylor et al., 1996).

Four polished thick sections (15016, 221a; 15555, 955a; 15475, 174a; and 15499, 154a; the 'a' indicates they are in-house made thick sections) were prepared from larger sub-samples, provided by NASA's allocation committee. Mineral major-element compositions were determined using an automated CAMECA SX-50 electron microprobe analyzer (EMP) at the University of Tennesee**.** Mineral compositions were determined in wavelength dispersive spectral (WDS) mode with the EMP using an accelerating potential of 15 keV, 20 nA beam current, 1 μm beam size, peak and background counting times of 20-30s and standard ZAF (PAP) correction procedures. WDS counting times were generally 20s for all elements. Detection limits (3σ above background) are typically <0.03 wt. % for SiO_2, TiO_2, Al_2O_3, MgO, CaO, Na_2O, K_2O, and Cl, <0.05 wt. % for Cr_2O_3, MnO, FeO, P_2O_5 NiO, and Co, and <0.05–0.1 wt% for all other oxides and elements listed.

Minerals within polished thick sections (i.e., polished sections ~ 150 μm thick) were analyzed initially by EMP and subsequently for their trace-element abundances by laser-ablation inductively-coupled-plasma mass-spectrometry (LA-ICP-MS) at the

Australian National University, Canberra. I performed the analyses using an Excimer (193nm wavelength) laser-ablation system attached to an Agilent 7500 ICP-MS. Analytical procedures and data reduction generally followed those described by Norman *et al*. (1996). Trace-element abundances were determined on individual spots using a 54 μm-diameter laser beam and a laser repetition rate of 5 Hz**.** Ablation was conducted under a helium atmosphere to enhance production of fine aerosols and the ablated sample mixed with argon prior transport to the ICPMS. Each analysis consisted of 60 seconds of data collection. Backgrounds on the ICPMS sample gas were collected for approximately 20 seconds followed by approximately 40 seconds of laser ablation of the sample. Data were collected in time-resolved mode so that effects of inclusions, mineral zoning, and possible penetration of the laser beam to underlying phases could be evaluated for each analysis. Plots of counts per second versus time were examined for each analysis and integration intervals for the gas background and the sample analysis were selected manually. Each LA-ICP-MS analysis was normalized to a major-element oxide, measured by EMP, as an internal standard to account for variable ablation yield (CaO for pyroxene, plagioclase, and melt; MgO for olivine; TiO_2 for spinels and ilmenite). Analyses of mesostasis, thought to represent quenched residual melt, in sample 15499 were performed with an 86 μm-diameter laser beam size and rastering the sample beneath the laser beam. For all data, the NIST 612 glass standard was used for calibration of relative element sensitivities using values given by Norman *et al.* (2004). Replicate LA-ICP-MS analyses of the USGS basaltic glass standards BCR-2G, BHVO-2G, and BIR-1G (Table A1), run at intervals during analysis, yielded an external precision of 1-4% (1σ relative standard deviation) for all trace- and major-element

compositions (with the exception of Fe = ~7%). Detection limits calculated according to the procedures of Longerich et al. (1996) were 1-30 ppb for Sr, Y, Nb, Ba, La, Ce, Pr, Eu, Tb, Ho, Lu, Ta; 2-50 ppb for Er, Th, U; 10-40 ppb for Zr; 7-80 ppb for V, Nd, Dy, Hf; 7-100 ppb for Gd, Yb; 15-170 ppb for Rb, Sm; 15-300 ppb for Sc; 20-265 ppb for Ga; 0.06-0.58 ppm for Sc; 0.04-0.7 ppm for Ni; and 0.18-2.7 ppm for Cr.

III. Results

Petrography and Mineral Major-Element Chemistry

The petrography and mineral chemistries of ONB and QNB samples analyzed during the course of this study are herein summarized. Modal data, petrography and major-element compositions and representative mineral EMP analyses for these samples are presented in Tables 1-3.

Olivine-Normative Basalts

Two medium-grained olivine-normative basalts, 15016 and 15555, were selected for analysis in this study (Fig. 2). Modal data of all rocks are presented in Table 1. Sample 15555 is both the largest and most intensively studied of the Apollo 15 rocks. The petrography and major-element compositions are summarized in Table 2. In short, 15016 has a subophitic texture, and 15555 has a plagioclase-poikolitic texture. Both samples contain olivine, pyroxene, and plagioclase as major silicate minerals. Representative mineral EMP analyses for these samples are presented in Table 3. In addition to the major silicate minerals, these rocks contain minor amounts of ilmenite, spinel, troilite, FeNi metal, merrillite, and tridymite. Sample 15555 also contains minor amounts of fayalite, as a late-stage crystallization product. The crystallization sequence of both rocks is: chromite → chromite + olivine → olivine + pyroxene + ulvöspinel → pyroxene + plagioclase + ilmenite. This crystallization sequence was determined from petrographic textural evidence and experimental crystallization studies on starting liquids of ONB composition (Walker *et al.*, 1977; Bianco and Taylor, 1977; Ryder, 1985). Pyroxenes range from low-Ca (Wo_{11}) pigeonites to high-Ca (Wo_{41}) augites (Fig. 3).

Table 1: Modal Analyses of Apollo 15 Mare Basalts

Samples	15016, 10	15555, 257	15475, 147	15499, 125
volume %	ONB	ONB	QNB	QNB
Pigeonite	39.1	31.1	36.0	44.9
Plagioclase	20.9	23.7	30.2	13.1
Clinopyroxene	18.5	21.3	18.4	31.5
Olivine	14.5	14.7	0.6	1.9
Fe-Px	1.3	0.8	5.3	4.3
Fayalite	0.8	2.5	<0.1	<0.1
Ilmenite	1.9	1.8	1.0	0.6
K-glass	<0.1	0.5	0.2	0.1
FeNi Metal/Troilite	0.2	0.2	0.2	0.1
Chromite	0.6	0.3	0.2	0.4
Ulvöspinel	1.7	1.7	0.7	1.3
Phosphate	0.2	0.3	3.6	0.1
Silica	0.3	1.3	3.6	1.8
	100	100	100	100

Table 2. Petrography and Major-Element Mineral Chemistry Summary

	Whole-Rock MgO (wt. %)*	Textures/Features	Chromite**	Olivine	Pyroxene	Plagioclase
15016	12.3	ophitic-subophitic	Cr # = 69-72	Fo_{62-16} (0.1 to 0.5 mm)	$Wo_{9-30}En_{12-58}$ (0.2 to 2 mm)	An_{89}-An_{94} (0.2 to 2 mm)
15555	11.7	plagioclase-poikolitic	Cr # = 64-74	Fo_{61-26} to Fayalite ($Fo_{1.2}$) (0.2 to 1 mm)	$Wo_{11-42}En_{2-59}$ (0.2 to 2 mm)	An_{87}-An_{93} (0.2 to 4 mm)
15475	10.6	subophitic	—	—	$Wo_{5-33}En_{0.5-69}$ (0.5 up to 2 mm)	An_{84}-An_{93} (1 to 2 mm)
15499	7.9	Vitrophyric Skeletal Px	Cr #= 70-76	— Fo_{69-44} (0.5 to 1 mm)	$Wo_{5-39}En_{13-67}$ (0.5 to 1 cm)	— —

**from Day et al. (2006), solution ICP-MS analyses.*

***Cr#=100*(Cr/(Cr+V+Al))*

Table 3. Representative EMP Data for Minerals

Phases:	Pyroxene				Fe-Px			Olivine		
Sample:	15106	15555	15475	15499	15475	15475	15475	15106	15555	15499
SiO_2	52.3	51.5	51.5	52.3	45.9	46.2	46.5	35.8	35.8	35.9
TiO2	0.37	0.46	0.35	0.38	0.43	0.40	0.38	<0.05	<0.05	<0.05
Al_2O_3	0.99	0.90	1.37	1.60	0.34	0.32	0.26	—	—	—
Cr_2O_3	0.44	0.46	0.70	1.01	<0.05	<0.05	<0.05	0.35	0.20	0.31
MgO	19.9	18.3	19.7	21.8	1.13	2.25	1.62	29.0	29.0	29.5
CaO	5.59	5.04	6.03	4.04	5.43	5.53	5.95	0.32	0.35	0.36
MnO	0.40	0.44	0.35	0.28	0.53	0.64	0.57	0.29	0.36	0.29
FeO	19.7	22.0	19.3	18.4	45.9	44.0	44.6	34.1	33.5	33.4
Na_2O	<0.03	<0.03	<0.03	<0.03	<0.03	<0.03	<0.03	—	—	—
V_2O_3	—	—	—	—	—	—	—	<0.03	<0.03	<0.03
Total	99.7	99.1	99.3	99.8	99.7	99.3	99.8	99.8	99.2	99.7
Mg#	64.3	59.8	64.5	67.9	4.17	8.32	6.08	60.2	60.7	61.1

Phases:	Plagioclase			Ulvöspinel				Chromite		
Sample:	15016	15555	15475	15016	15555	15475	15555	15016	15555	15499
wt%										
SiO_2	47.1	46.5	46.6	0.05	<0.03	<0.03	29.0	0.06	0.08	<0.03
TiO2	—	—	—	31.9	27.9	32.4	0.13	3.89	4.81	2.47
Al_2O_3	32.3	33.0	32.8	1.83	3.53	1.78	—	11.3	10.8	11.4
Cr_2O_3	—	—	—	3.01	12.2	0.51	0.01	46.5	45.1	51.8
MgO	—	—	—	0.12	1.83	0.14	0.55	1.00	1.01	7.23
CaO	17.9	18.1	18.1	0.07	<0.03	0.03	0.79	<0.03	0.08	0.05
MnO	—	—	—	0.31	0.24	0.31	0.75	0.24	0.27	0.20
FeO	0.67	0.80	0.57	61.8	53.1	64.0	67.7	35.2	36.5	24.8
Na_2O	1.08	1.08	1.14	—	—	—	—	—	—	—
V_2O_3	—	—	—	0.30	0.47	0.23	<0.03	0.84	0.86	1.18
K_2O	0.04	0.04	0.04	—	—	—		—	—	—
Total	99.0	99.5	99.2	99.4	99.3	99.4	98.9	99.1	99.4	99.1

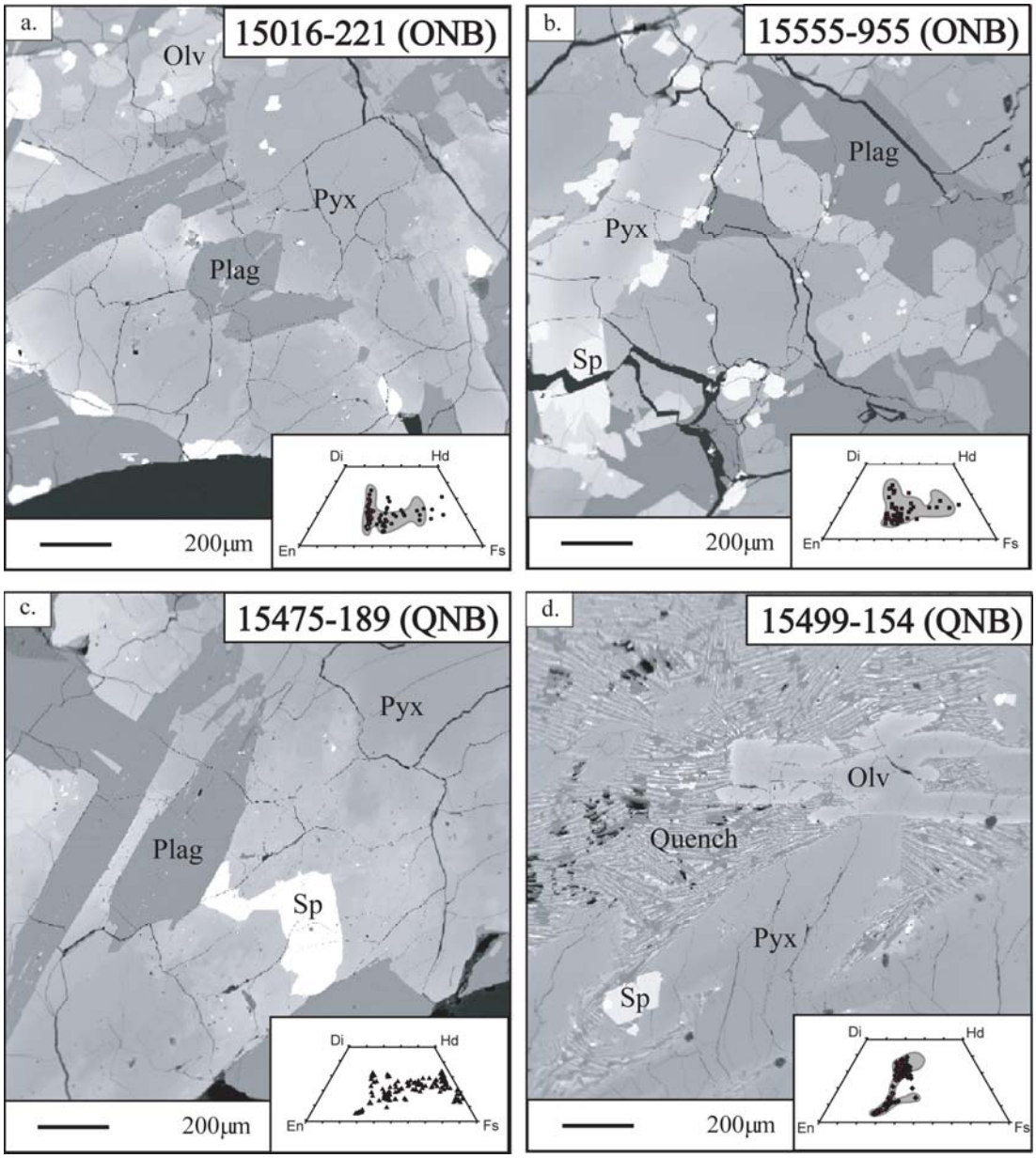


Figure 2. Back-Scattered-Electron (BSE) Iimages of the Four Thick-Sections of Apollo 15 Basalts. Vitrophyric 15499 contains pyroxene phenocrysts and olivine xenocrysts in a quenched matrix. Dark phases are plagioclases, gray areas are pyroxene and olivine, and light-colored phases are spinel, ilmenite, troilite, and FeNi metal. Pyroxene quadrilaterals (from Fig. 3) are inset to highlight degrees of pyroxene chemical variability and zonation.

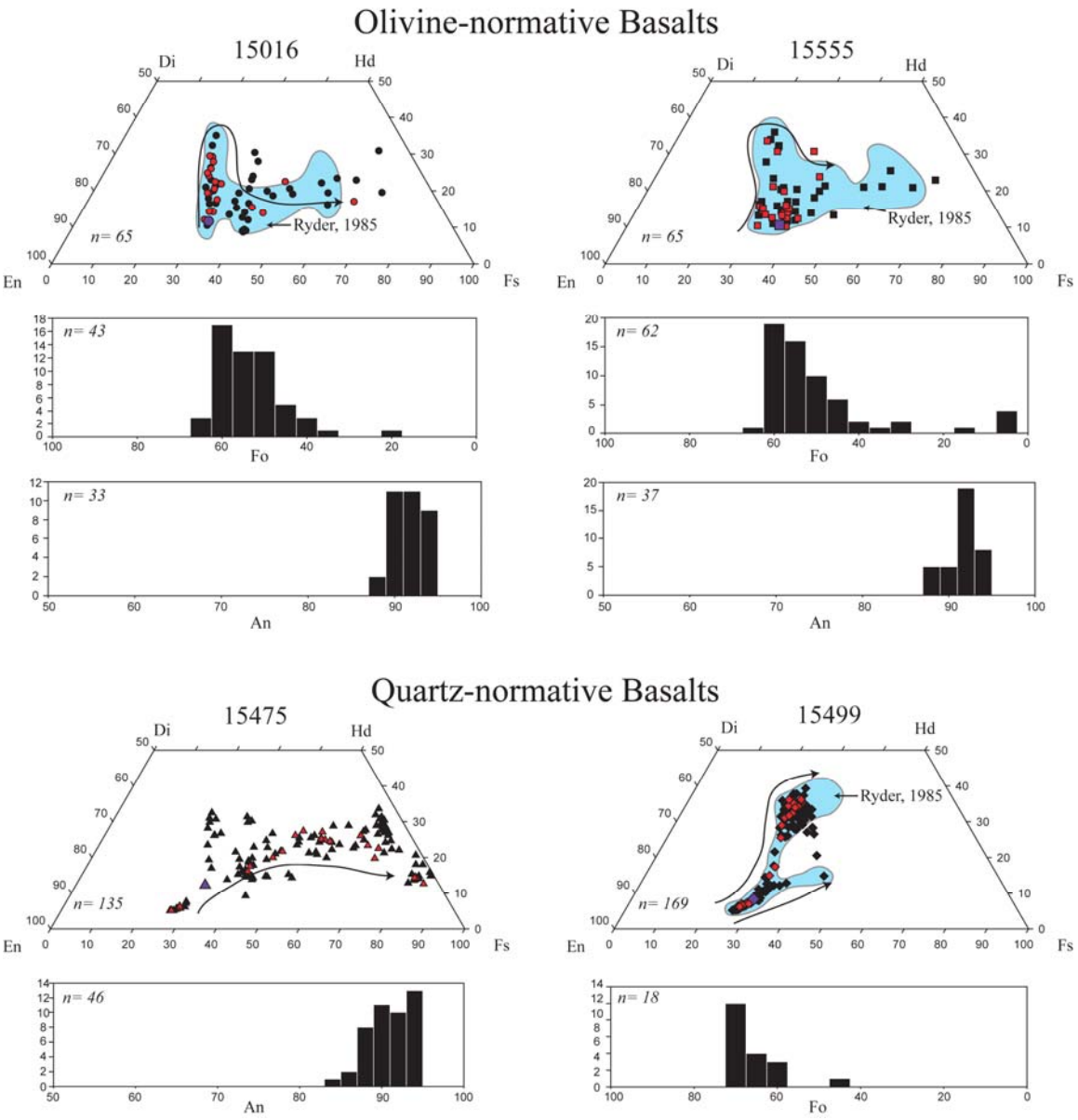


Figure 3. Pyroxene-Quadrilaterals and Olivine and Plagioclase Histograms for ONBs and QNBs. For all but 15499, pyroxene compositions show fractionation from high-Mg, low-Ca cores to Fe-rich rims. Note that 15475 contains no olivine, and 15499, a vitrophyre, has not crystallized plagioclase phenocrysts, but has plagioclase in its matrix. Lines shown are fractionation trends from Ryder (1985). Previous data from Ryder (1985) are plotted as fields.

Quartz-Normative Basalt

The QNBs include samples 15475, a coarse-grained pigeonite-porphyritic basalt, and 15499, a vitrophyric basalt. The petrography and major-element compositions are summarized in Table 2. The main silicate phases for these basalts are pyroxene and plagioclase in 15475 and pyroxene in 15499. Representative mineral EMP analyses for these samples are presented in Table 3. Basalt 15475 contains minor amounts of ilmenite, spinel, troilite, FeNi metal, merrillite, and silica. The wide range of pyroxene compositions present in 15475 records an extensive fractionation sequence (Fig. 3). The crystallization sequence of 15475 is pyroxene → plagioclase → ilmenite (Grove, 1977). The opaque minerals first appear with pyroxene and follow the sequence chromite→ ulvöspinel→ ilmenite. Ilmenite began crystallizing after plagioclase started, and ended prior to the cessation of pyroxene growth (Engelhardt, 1979).

An interesting feature of vitrophyre 15499 is that, unlike 15475, it contains zoned olivine phenocrysts and euhedral chromite (Fig. 4), often trapped within the cores of pyroxenes. The zoned olivine is grossly out of equilibrium with the melt, evidenced by its high Fo-contents. Pyroxenes lack significant major-element zoning, a feature expected if they crystallized quickly. Also present are tridymite and small (<0.3 mm long-axis) plagioclase laths within the fine-grained matrix. The determined crystallization sequence is olivine → olivine + pigeonite → pigeonite + augite -> augite + plag (Bence and Papike, 1972). The pyroxenes in 15499 show no exsolution; phenocrysts are well-developed with no evidence for resorption, consistent with a late-stage quench (Bence and Papike, 1972). Steady increase in Al_2O_3 (to ~10 wt. %) in the rims of pyroxene phenocrysts (Fig. 5),

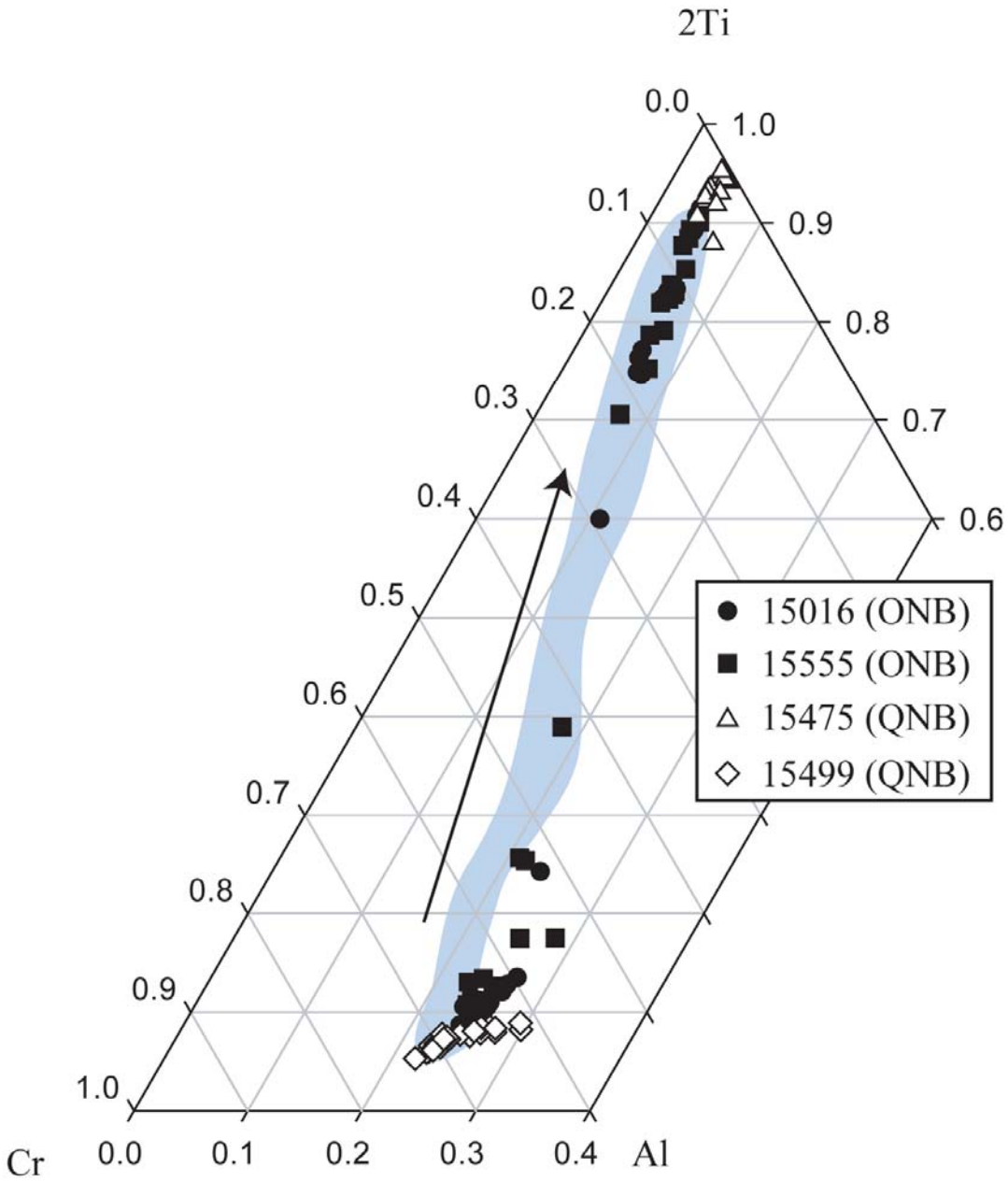


Figure 4. Cr-Al-2Ti Diagram for Spinels from these Apollo 15 Basalts. Envelope of spinel data from mare basalts is from El Goresy (1976). A characteristic mare basalt gap exists between ulvöspinel and high-Al chromite populations.

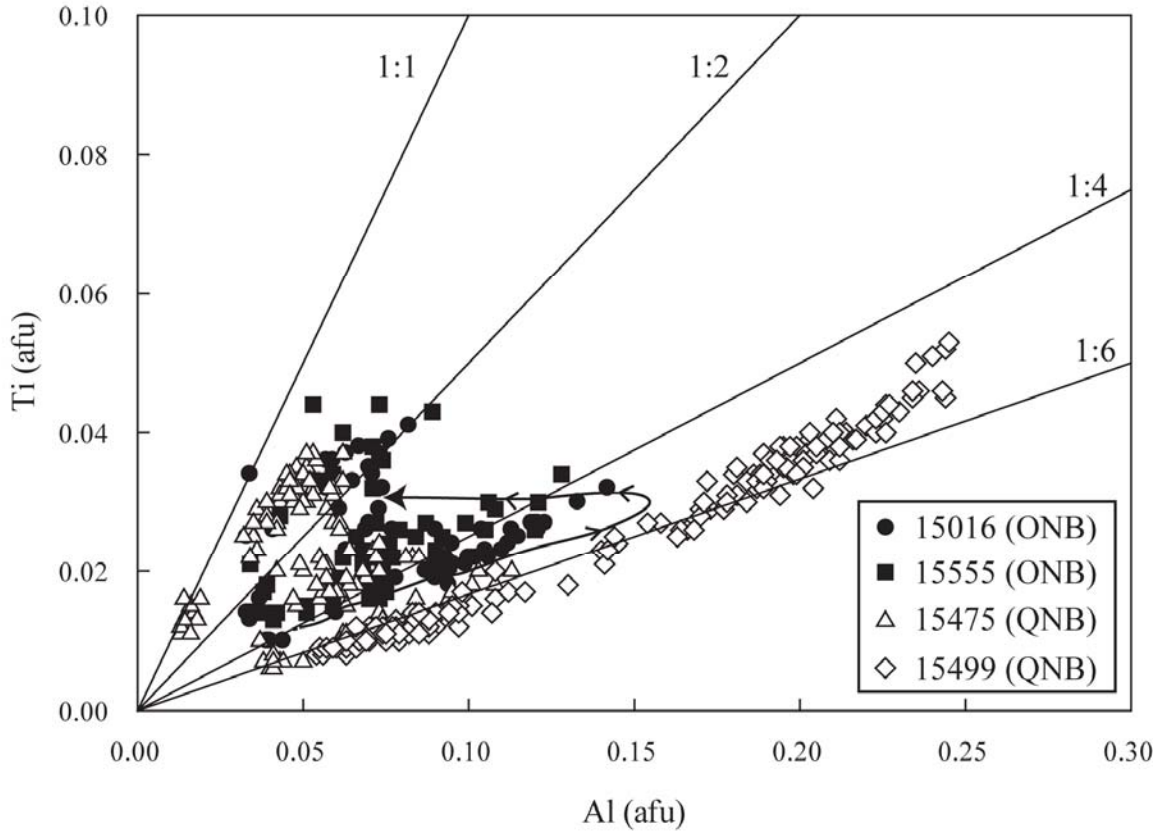


Figure 5. Plot of Ti vs Al for Pyroxenes in the Samples Analyzed. Note the 1:6 relationship of 15499 pyroxenes, a result of the sample being quenched. The trend line is that of standard pyroxene crystallization, free of resorption.

(Bence and Papike, 1972) indicates that plagioclase did not precipitate until the phenocrysts stopped crystallizing, and then only as minute crystals in the matrix (Ryder, 1985).

Trace-Element Mineral Chemistry

Pyroxene

LA-ICP-MS data for pyroxenes from the four Apollo 15 thick-sections analyzed during the course of this study are presented in Table 4. Pyroxene rare-earth-element (REE) profiles, normalized to CI chondrite have convex-upward, sub-parallel patterns, large negative Eu anomalies, and increasing REE abundances with Fe-enrichment (Fig. 6). Excluding a few high-REE content pyroxenes from sample 15475, pyroxenes contain, in ppm, La (0.008 - 1.48), Ce (0.02 - 4.27), Pr (0.008 - 0.819), Nd (0.052 - 5.5), Sm (0.045 - 2.65), Eu (0.011 - 2.62), Gd (0.102 - 4.25), Tb (0.030 - 0.833), Dy (0.227 – 5.72), Ho (0.066 – 1.23), Er (0.171 – 3.32), Yb (0.212 – 3.44), Lu (0.04-5.44 ppm). Scandium content in pyroxene (21.6-168 ppm) tracks fractionation (Fig. 7a). In particular, pyroxenes within 15475 follow their major-element fractionation trend seen in Figure 3. Additional elements track fractionation to some degree and have wide ranges such as Co (7.7 - 140 ppm), Ni (0.3 - 63.7 ppm), and Sr (0.2 - 22 ppm). A plot of La/Sm versus La/Yb for pyroxenes (Fig.7b) serves to illustrate that variation in slope of the rare-earth-elements follows a constant trend, one that is nonspecific to either group. Olivine- and quartz-normative basalts possess similar ranges in $(La/Yb)_n$ = 0.02-0.46 and 0.02-0.57, respectively, $(La/Sm)_n$ = 0.04-0.46 and 0.05-0.50, respectively, and $(Sm/Yb)_n$

Table 4: Trace-Element Data from LA-ICP-MS Analyses of Major Silicate Phases

Sample	15016			15555			15475		15499	
Phases	Pyroxene	Olivine	Plagioclase	Pyroxene	Olivine	Plagioclase	Pyroxene	Plagioclase	Pyroxene	Olivine
p.p.m.										
Sc	31.1	9.6	2.91	39.8	10.9	3.5	49.9	2.81	49.8	9.96
Ti	1729	224	321	2610	248	373	2267	266	2326	147
V	166	63	2.16	162	71.1	0.842	280	3.43	345	91.9
Cr	2473	1178	5.31	2714	1507	2.41	3998	9.01	6526	2588
Mn	2183	2646	69	2605	2348	70.4	2060	83.2	2314	2038
FeO	16.5	34.5	0.562	20.8	31	0.599	16.7	0.735	19.7	27.7
Co	38.9	104	1.03	49.4	107	1.44	34.7	0.861	54.1	114
Ni	16.5	124	0.351	17.1	112	<0.386	5.38	0.423	23.1	203
Ga	0.36	0.07	8.48	0.45	<0.053	10.7	0.597	7.15	0.653	<0.063
Rb	<0.027	<0.038	<0.075	<0.066	<0.044	0.177	<0.039	<0.123	<0.048	<0.033
Sr	0.39	0.0063	277	0.546	<0.0060	385	1.13	260	0.407	<0.0077
Y	2.22	0.78	0.2	3.13	0.258	0.237	4.29	0.212	4.01	0.223
Zr	0.91	0.076	0.109	1.21	0.064	<0.028	2.3	<0.026	2.37	0.094
Nb	0.024	0.015	0.017	0.026	0.015	<0.013	0.048	0.012	0.069	0.024
Ba	0.0048	<0.0076	19.7	<0.0052	<0.0060	34.1	0.075	19.4	<0.013	<0.0062
La	0.0093	<0.0069	0.237	0.01	<0.0081	0.345	0.035	0.241	0.016	<0.0072
Ce	0.048	<0.0063	0.534	0.062	<0.0038	0.785	0.181	0.581	0.09	<0.0067
Pr	0.015	<0.0073	0.074	0.017	<0.0060	0.088	0.044	0.078	0.025	<0.0056
Nd	0.133	<0.020	0.25	0.167	<0.048	0.354	0.34	0.354	0.21	<0.043
Sm	0.071	<0.030	<0.090	0.106	<0.038	<0.091	0.226	<0.072	0.178	<0.030
Eu	0.014	<0.0061	1.7	0.014	<0.011	2.42	0.027	1.51	0.014	<0.011
Gd	0.227	<0.029	<0.083	0.302	<0.033	<0.085	0.503	0.066	0.346	<0.044
Tb	0.049	0.01	<0.014	0.065	<0.0078	<0.029	0.093	<0.012	0.086	<0.0064
Dy	0.39	0.114	0.045	0.507	0.031	0.082	0.747	<0.054	0.666	<0.024
Ho	0.095	0.019	<0.014	0.13	0.0084	<0.027	0.162	<0.014	0.154	<0.0053
Er	0.26	0.094	<0.045	0.363	<0.020	<0.035	0.481	<0.041	0.44	0.029
Yb	0.401	0.157	<0.062	0.388	0.05	<0.082	0.494	<0.050	0.504	0.084
Lu	0.061	0.022	<0.017	0.064	0.012	<0.015	0.073	<0.016	0.095	0.017
Hf	0.076	<0.016	<0.036	0.057	<0.013	<0.051	0.117	<0.037	0.121	<0.017
Ta	0.005	<0.0060	<0.010	<0.0050	<0.0069	<0.015	<0.0083	<0.017	<0.0071	<0.0081
Th	<0.0076	<0.011	<0.015	<0.0065	<0.0088	<0.033	<0.013	<0.022	<0.024	<0.017
U	<0.0059	<0.0068	<0.011	<0.0089	<0.0067	<0.023	<0.0058	<0.020	<0.0075	<0.0089

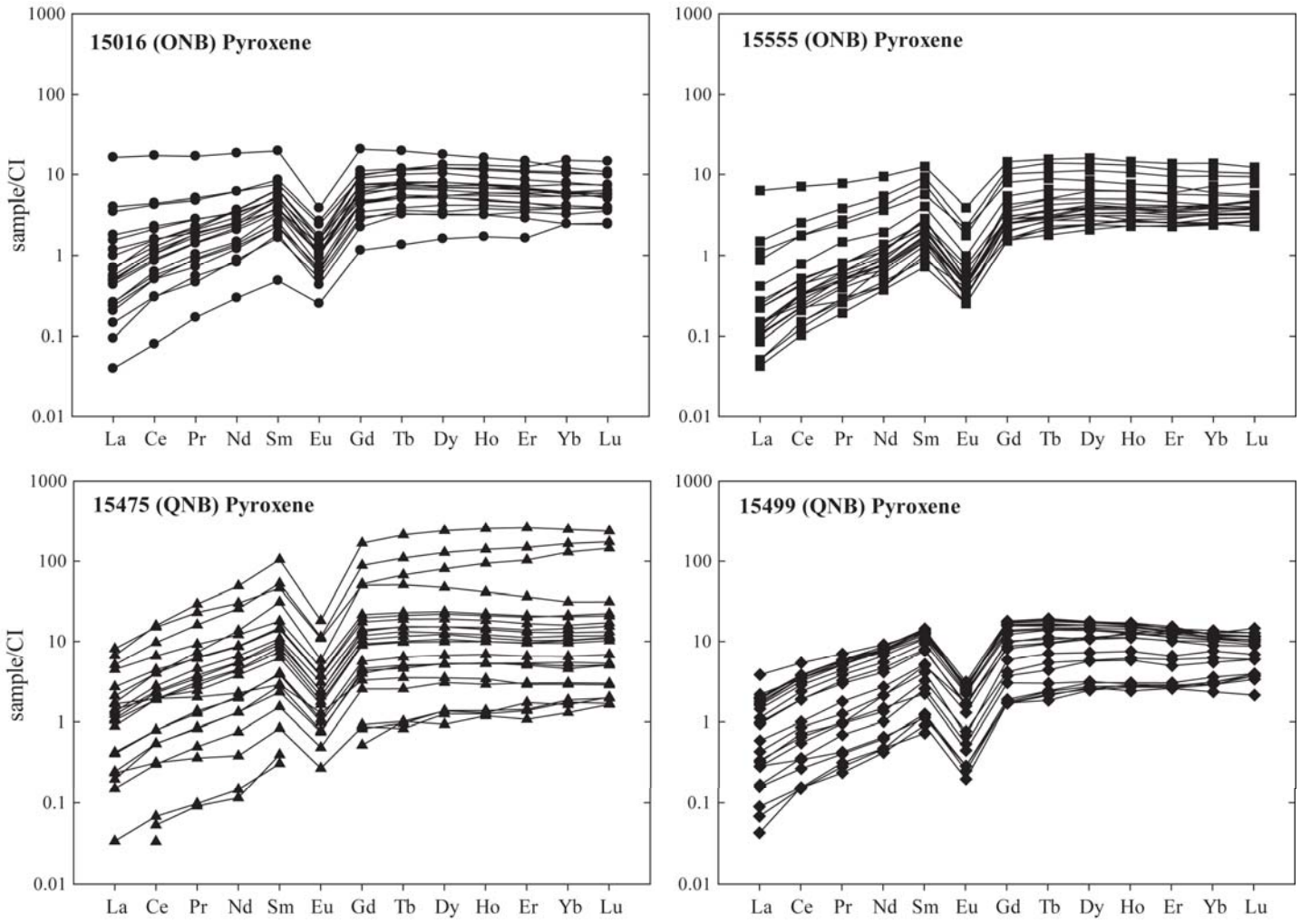


Figure 6. Rare-Earth-Element Plot for Pyroxenes Analyzed in this Study.

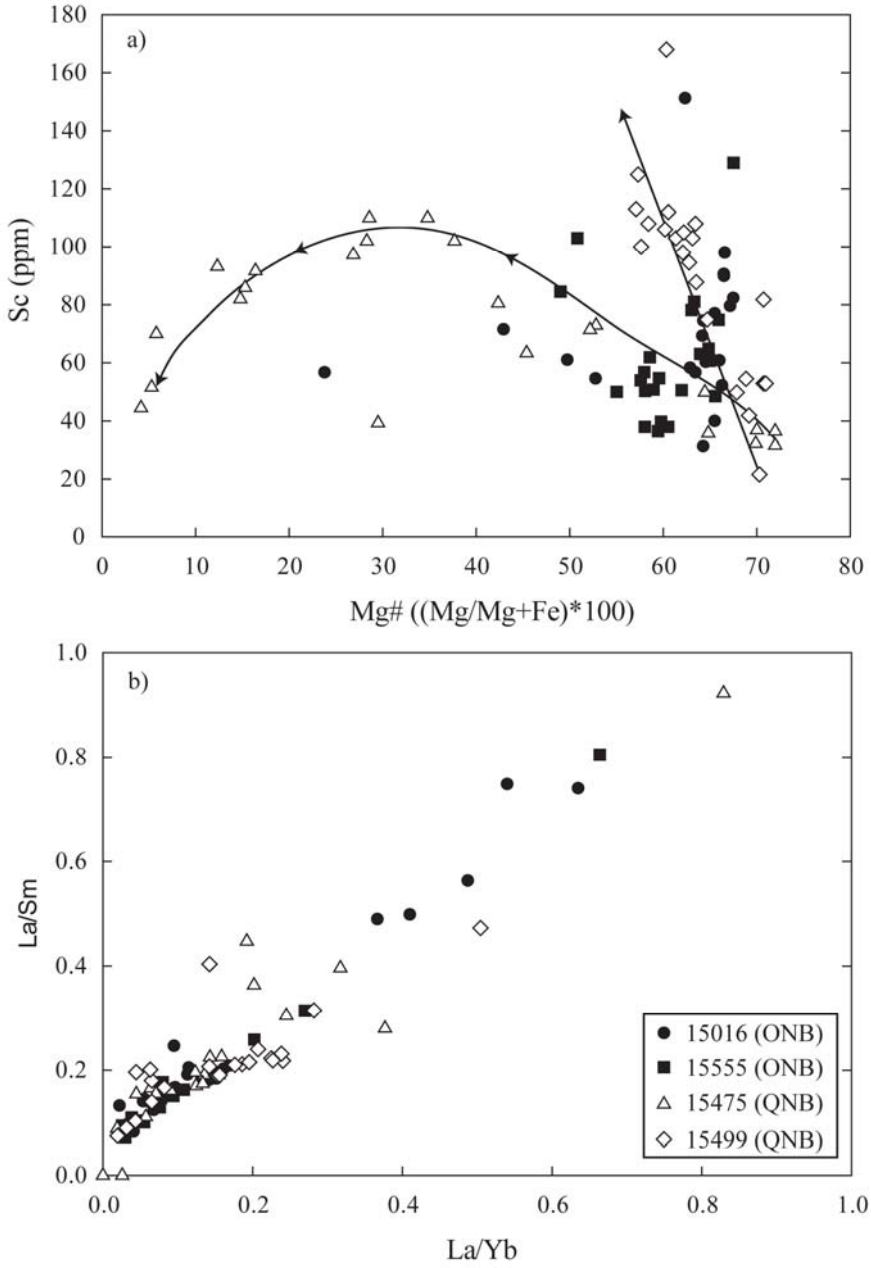


Figure 7. Trace-Element Variation Diagrams for Pyroxene. a) A plot of Sc vs Mg# for pyroxenes shows two fractionation trends. In 15475 the trend tracks long-term depletion in Sc; in 15499 the trend is due to rapid quenching. b) Plot of La/Sm vs La/Yb for pyroxenes shows that there is little difference between slope variations on REE element plots for these pyroxenes, suggesting similarities between the basalt types.

= 0.08-0.95 to 0.23-1.49. Discounting the maximum ratio from Fe-rich pyroxenes from QNBs further tightens ranges such as $(Sm/Yb)_n$ to 0.23-1.20.

Plagioclase, Olivine, and Spinel

Plagioclases have relatively flat LREE patterns, with positive europium anomalies (0.82 – 3.4 ppm) (Fig 8). Many HREEs are below detection limits. As expected from studies of REE behavior (see Jones (1995) for a comprehensive review), REE contents increase with decreasing anorthite content of the plagioclase. Plagioclase contains 136 - 500 ppm Sr, 10 -56 ppm Ba, and 4.2 – 13.3 ppm Ga. Many trace-elements in olivine and spinel are below detection limits. Olivines, including those from quartz-normative basalt 15499, have trace-element correlations with vanadium (28 -136 ppm) and chromium (675 - 6050 ppm) consistent with fractional crystallization (Fig. 9). Olivines also contain 33.8 – 203 ppm Ni, 86 – 148 ppm Co, and 8 – 44 ppm Sc. Most spinels analyzed have detectable contents of Sr (1.3-2.25 ppm), Y (0.2-0.4 ppm), Zr, Nb, Lu, Hf, and Ta, with the exception of the 15499 chromites, which do not have appreciable contents of Lu, Hf, and Ta. In ulvöspinels, Nb/Ta ranges from 17 to 25. In general, the high-field-strength elements (HFSEs) are enriched relative to the REEs. The apparent enrichment in strontium may be due to the presence of small plagioclase inclusions.

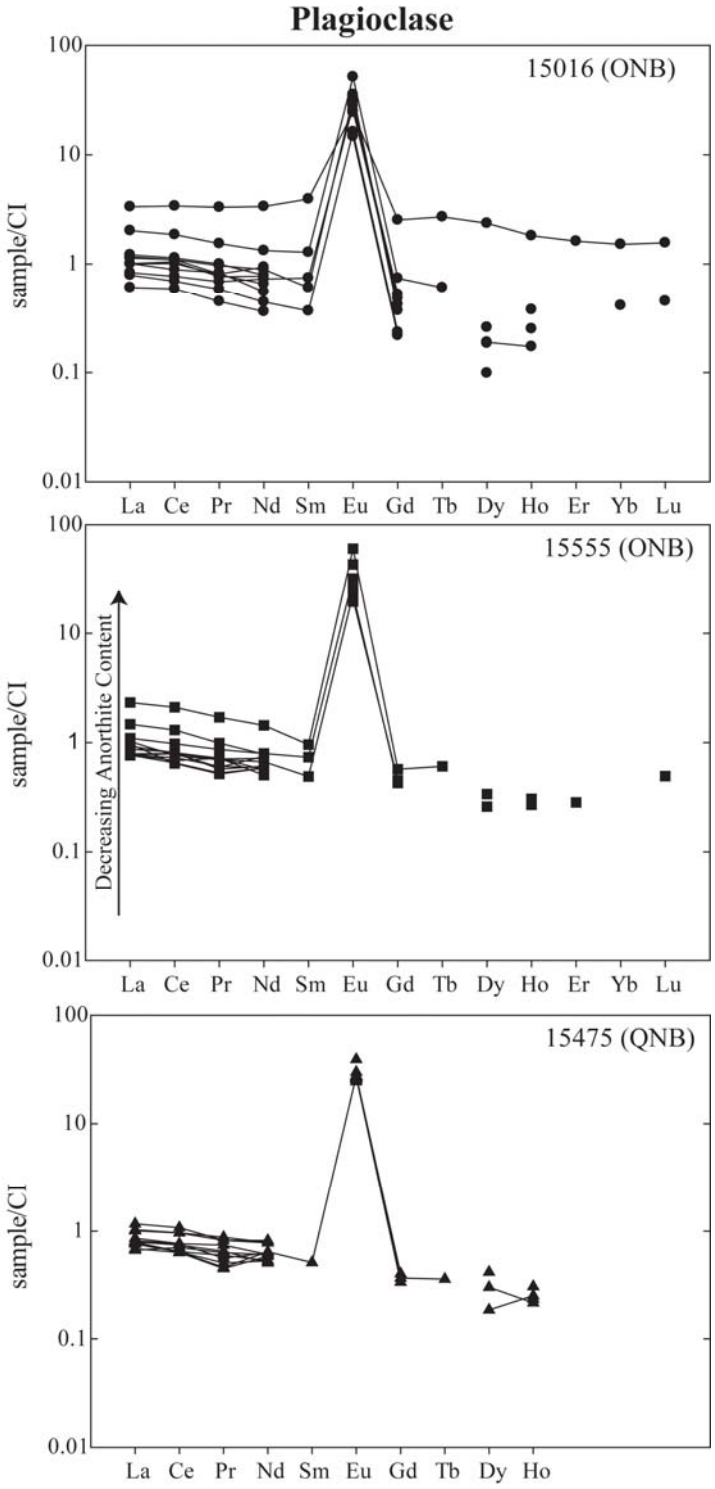


Fig. 8. Rare-earth-element concentrations for plagioclase. REE contents increase with decreasing anorthite content.

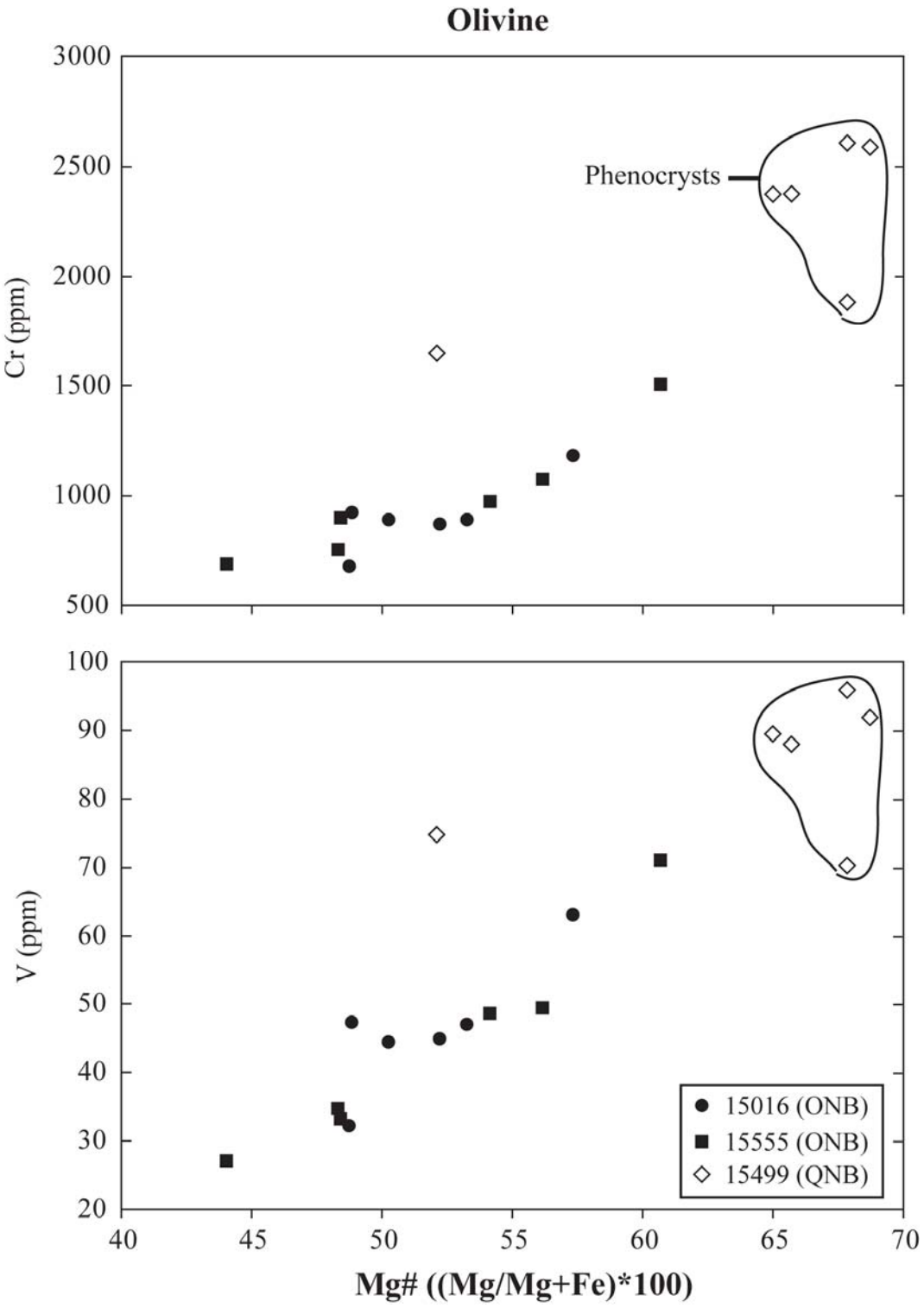


Figure 9. Element Variation Diagrams for Olivine. Trace-elements are consistent with melt evolution.

Quenched Melt

The quenched-melt martix of QNB 15499 was anlayzed for its trace-element contents by LA-ICP-MS (Figure 10). This evolved melt contains enriched REE contents on the order of: La (10 – 20 ppm), Ce (27 – 53 ppm), Pr (3.8 – 7.5 ppm), Nd (20 - 37ppm), Sm (6 - 11 ppm), Eu (1.7 – 2 ppm), Gd (7.5 - 13 ppm), Tb (1.3 – 2.1 ppm), Dy (7.9 – 12.8 ppm), Ho (1.6 – 2.6 ppm), Er (4.2 – 6.5 ppm), Yb (3.7 – 5.6 ppm), and Lu (0.5 – 0.7 ppm). These quenched-melt compositions can be used in conjunction with pyroxene rims to estimate an evolved melt composition for basalt 15499.

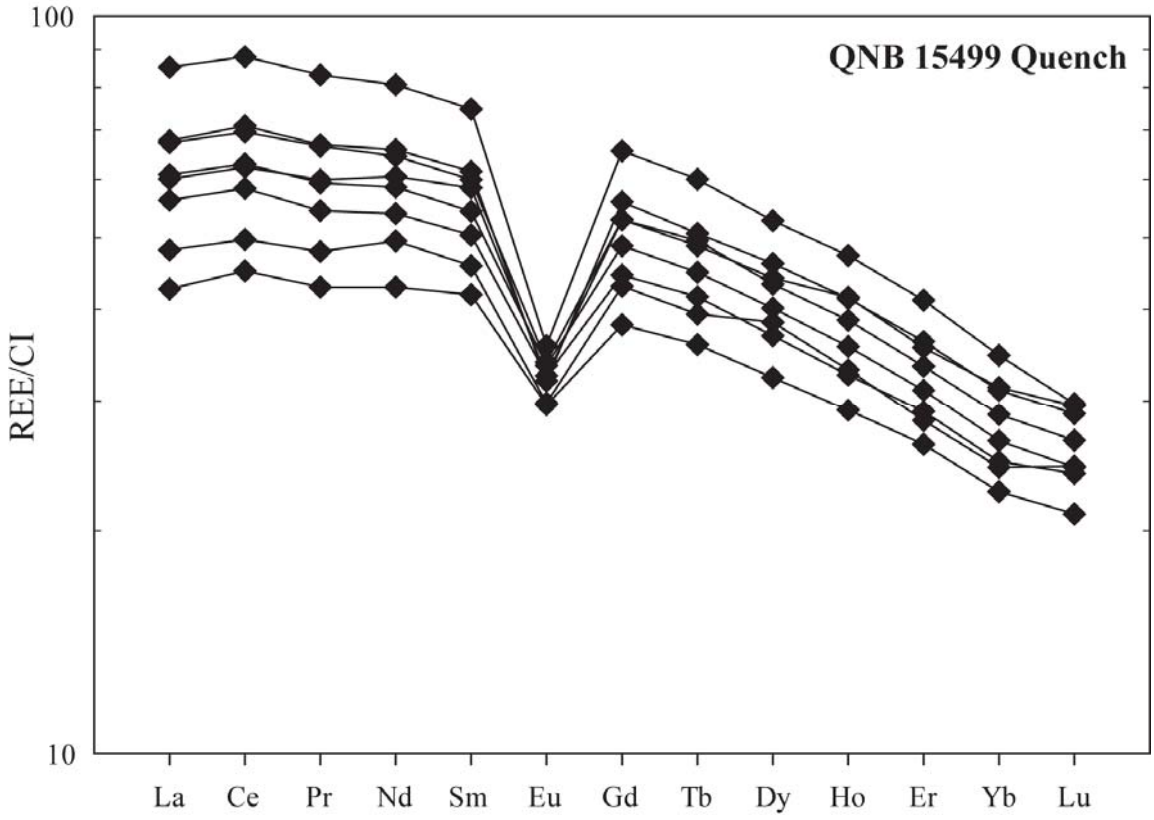


Figure 10. Quenched Matrix Rare-Earth-Element Plot. Rare-earth-element concentrations normalized to chondrite for multiple analyses on the quenched matrix of quartz-normative mare basalt 15499.

IV. Discussion

The control of mineral fractionation on inter-suite chemical variations and chemical trends is a well known phenomenon in many planetary magmatic settings. On the basis of the new data presented here, this process has been significant in the petrogenesis of Apollo 15 low-Ti basalts. In the following discussion, this important petrologic process in understanding the relationship between ONBs and QNBs is considered. Furthermore, to establish a relationship between the ONBs and QNBs, modeled parental melts using distribution coefficients and whole-rock compositions determined by modal recombination are compared.

Mineralogic Controls on Inter-Suite Variations

Mineral major- and trace-element data for the ONBs are qualitatively consistent with simple fractional crystallization. In olivine, the trace-elements chromium, nickel, and vanadium, all decrease in concentration with decreasing Mg#, which is used as a fractionation indicator (Fig. 9). Because of the lack of olivine in most QNBs, we consider pyroxene in both suites to provide direct comparisons of fractionation trends within ONBs and QNBs. The pyroxene-compatible trace-element scandium also follows expected fractionation trends (Fig. 7a). The REE contents of pyroxenes in both suites are generally sub-parallel (Fig. 6), and the slopes of the REE elements follow a similar trends, demonstrated by a plot of La/Sm versus La/Yb (Fig. 7). All increases in LREE/HREE and incompatible trace-element ratios are also consistent with crystallization from an increasingly fractionated or evolved residual melt. $(La/Yb)_n$, $(La/Sm)_n$, and $(Sm/Yb)_n$ ratios in pyroxene cover nearly the same ranges and suggest that

on the basis of REE content in pyroxene, there is no significant difference in REE content in pyroxene within, or between, the ONB and QNB lavas.

Determination of Parental Melt Compositions

Modal Recombination

The whole-rock REE compositions of the Apollo 15 mare basalts studied herein have been calculated by modal recombination and are presented in Figure 11. Modal recombination of vitrophyric sample 15499 was not possible because the elevated REE contents in the constituent phases of the quench material can not be accurately accounted for. In addition, thin section 15475, 147 has a high apparent concentration of phosphates (3.6%) uncharacteristic of the sample as a whole. We have used a value of 0.26% phosphates for 15475 in the calculation, the value from 15555, because both samples have near identical calcium and phosphate contents. The calculated whole-rock REE contents of both the ONBs and the one QNB are near-identical, as are the whole-rock compositions determined by ICP-MS (Day *et al.* 2006), (Fig. 11, and Table 5). Both the calculated and determined compositions are similar in abundances and sub-parallel in patterns to each other. One notable feature is the pronounced negative europium anomaly in the calculated compositions, probably because of some trace Eu-containing phases involved in the calculation. The similarities of the calculated whole-rock trace-element data for these ONBs and QNBs further suggest that these groups are likely related. Relative abundances of the REE and subtle differences in the REE patterns (e.g., slight enrichment in LREE in the QNBs) are qualitatively consistent with a fractional crystallization relationship.

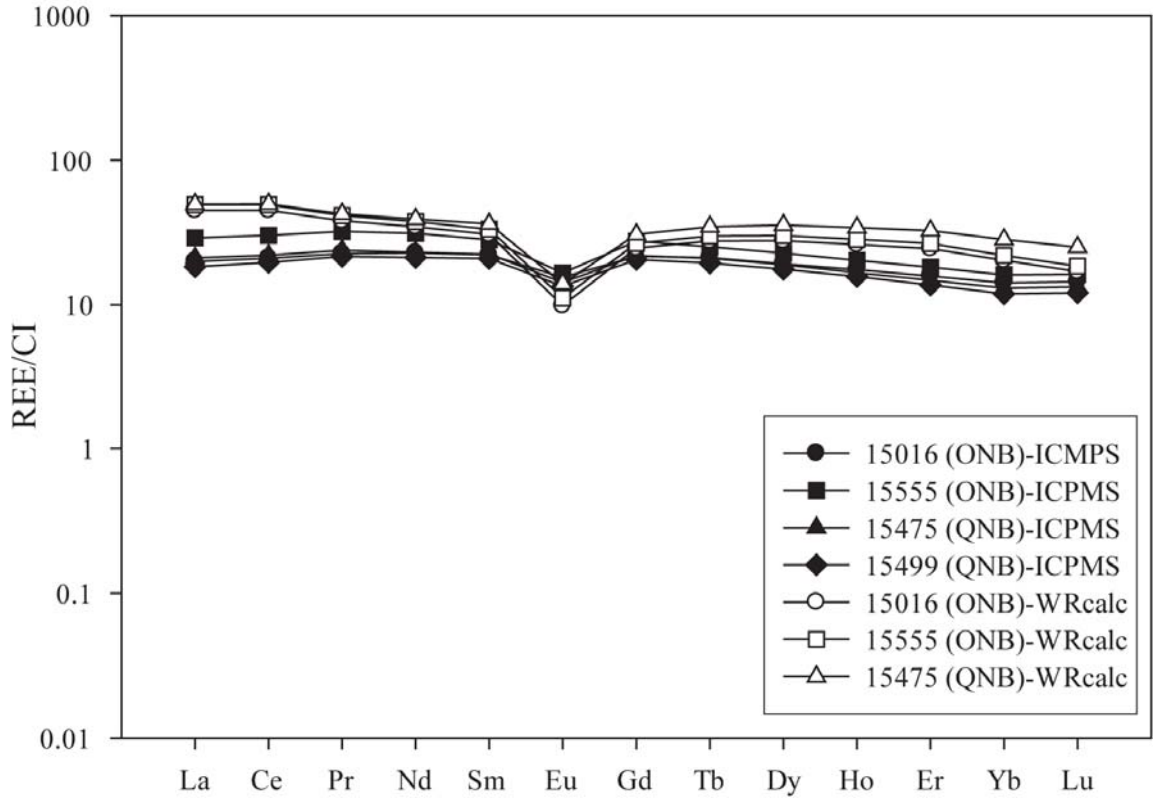


Figure 11. Modal Recombination Results. Whole-rock REE/CI calculated values (open circles) plotted for comparison with Whole-rock REE/CI obtained by solution ICP-MS (Day *et al.*, 2006).

Table 5. Normalized Parental Melts and Measured Whole-Rock Compositions

	Whole-Rock*				Parental Melts			
	15016	15555	15475	15499	15016	15555	15475	15499
ppm								
La	19.92	29.03	21.04	18.30	19.81	21.30	74.56	34.09
Ce	20.94	30.11	22.00	19.62	19.89	25.70	75.02	37.30
Pr	22.54	32.11	23.79	21.58				
Nd	22.78	31.21	23.06	21.19	15.47	19.43	39.56	24.43
Sm	22.13	28.15	22.32	20.87	15.57	23.25	49.56	39.03
Eu	15.44	16.57	14.23	13.41	15.63	15.63	30.13	15.63
Gd	21.59	27.53	21.84	20.49	26.85	35.72	59.50	40.93
Tb	21.14	25.19	20.94	19.42				
Dy	19.17	22.74	18.91	17.56				
Ho	17.47	20.25	16.62	15.66				
Er	15.77	18.15	14.78	13.70				
Yb	14.14	16.10	13.02	11.87	18.98	18.37	23.38	23.86
Lu	14.44	16.26	13.29	12.08	19.31	20.26	23.11	30.07

*Source: Day *et al.* (2006)

Partition Coefficients

The REE compositions of individual augite cores in these Apollo 15 mare basalts can be used to estimate compositions of their parental liquids because these rocks cooled quickly, and the cores have not re-equilibrated (evidenced by Fig. 5 – the pyroxenes show pure crystallization trends on a plot of Ti versus Al.). We have calculated the parental-melt REE compositions of these pyroxenes by inverting LA-ICP-MS data of the most primitive pyroxenes using the experimentally derived distribution coefficients (D = min/melt) of McKay *et al.* (1986), and a D_{Eu} value estimated graphically from McKay *et al.* (1991). These D values have been regularly used on lunar rocks in such studies as Anand *et al.* (2006). Choosing a good set of distribution coefficients is always complicated (cf., Jones (1995)), as D values vary based on a number of factors, including but not limited to temperature, pressure, mineral, and melt compositions. The D values used are La = 0.002, Ce = 0.004, Nd = 0.019, Sm = 0.031, Eu = 0.016, Gd = 0.043, Er = 0.092, Yb = 0.13, Lu = 0.13. These D values were selected because they were determined for low oxygen fugacity (~ IW) and $\mathbf{Wo_{12}}$ pyroxenes, similar to those found in the Apollo 15 basalts. The average Wo content of the pyroxenes compositions inverted is ~11 %. The primitive pyroxene compositions used for the inversion, along with their respective calculated parental melts, are presented in Figure 12.

The parental-melts calculated by this method have REE contents similar to but slightly elevated above their whole-rock compositions. Offsets between the parental melts calculated from pyroxenes and the measured whole-rock compositions, suggest that either the whole-rock compositions do not represent melts or the D values are somewhat in error.

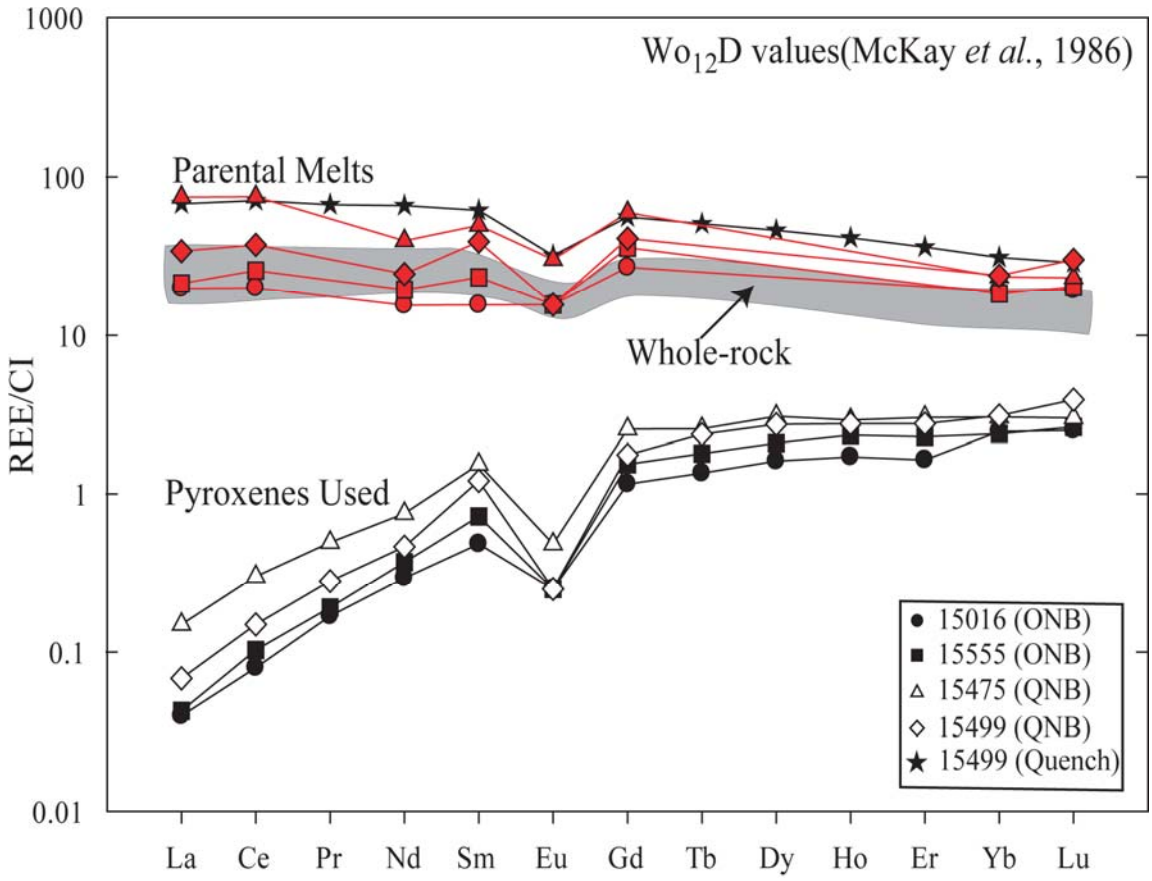


Figure 12. Rare-Earth-Element Diagram for Parental Melts. Rare-earth-element contents normalized to chondrite (using Anders and Grevesse, 1989) for Wo_{12} pyroxenes, equilibrium parental melts calculated from those pyroxenes, data from a raster analysis of the 15499 quench matrix, and the whole-rock data-field range (gray envelope) for all four samples.

Problems associated with D values have been noted above. Olivine-pyroxene accumulation would reduce the REE content of the bulk rock relative to the calculated melt composition, and its effect on the whole-rock compositions cannot be discounted. The QNB calculated parental melts possess higher REE contents than do the ONBs. This is supporting evidence, albeit qualitative, for a hypothesis that the QNBs represent higher degrees of fractionation products from parental melts that are almost identical to olivine-normative basalts. In addition, data from a raster (essentially moving the laser along the sample) analysis (Fig. 13) performed on the quenched matrix in sample 15499 plots above the equilibrium melts and whole-rock data in Figure 12. This is consistent with enrichment of incompatible trace-elements concentrated into the residual melt of the 15499 melt as it crystallizes out pyroxene phenocrysts and subsequently is quenched. The results here suggest that the ONBs and QNBs are indeed directly related from a trace-element perspective.

Calculated Evolved Parental Melts

Following the same method as discussed above, evolved melts have been calculated using D values from McKay *et al.* (1986) but for **Wo_{32}** pyroxenes. These evolved melts and the pyroxenes used in the calculations are presented in Figure 14. The REE patterns of the calculated evolved melt are flatter than the least evolved calculated melts (Fig. 12). The absolute abundance differences between the melts from each rock are partially due to the Wo-contents of the pyroxenes not being exactly Wo_{32}. In general, the evolved compositions have higher abundances of HREEs and lower LREEs,

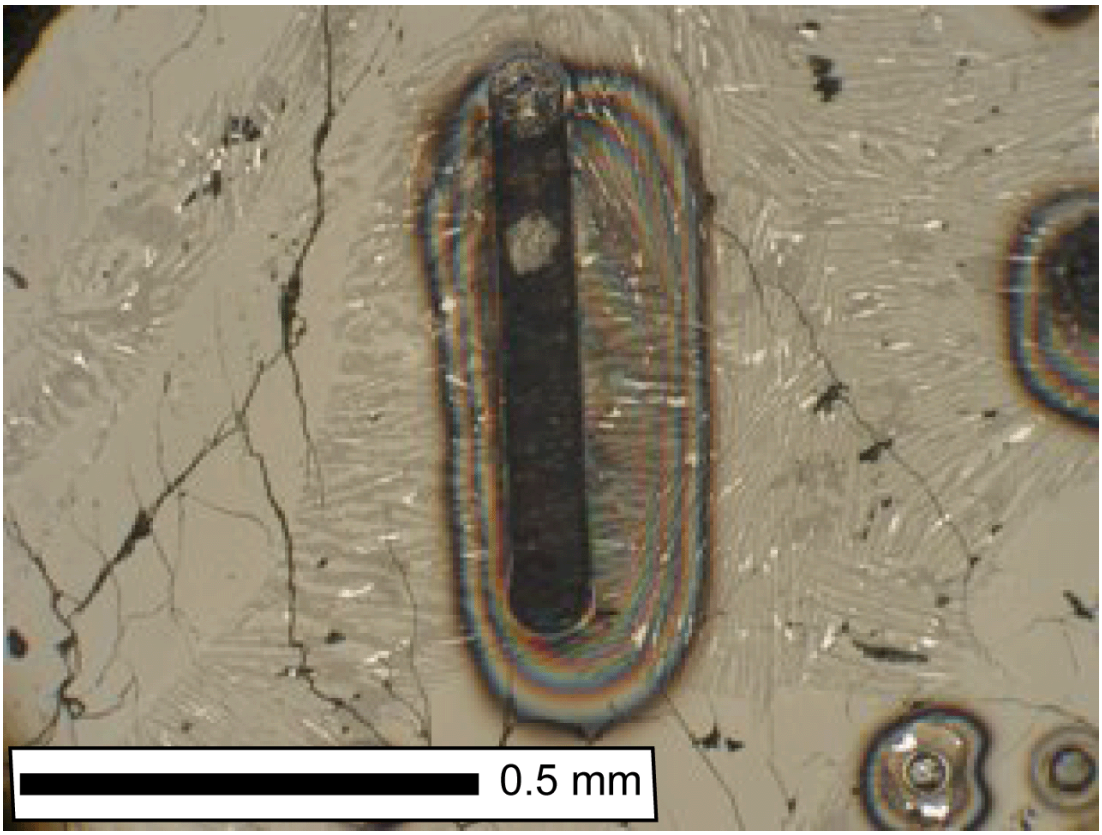


Figure 13. Photomicrograph of QNB 15499. This shows the area of raster analysis of the quenched matrix.

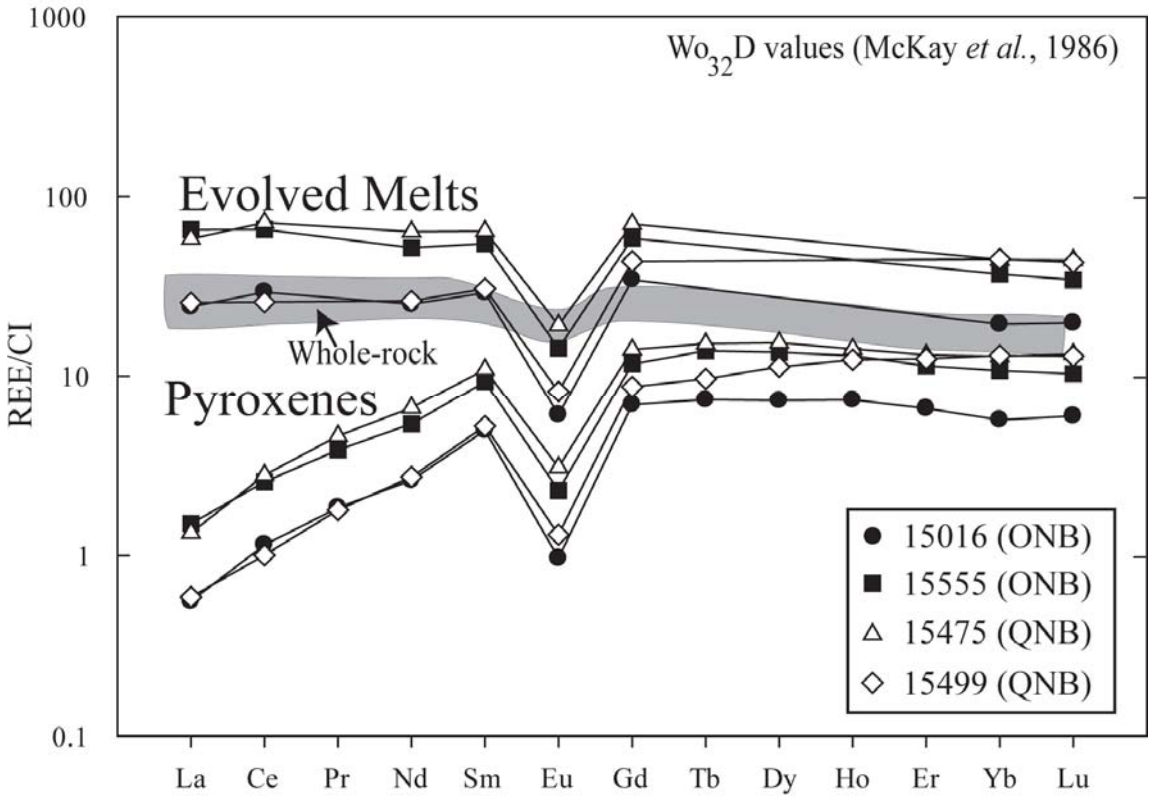


Figure 14. Rare-Earth-Element Diagram for Evolved Melts. Plotted are rare-earth-element concentrations for ~Wo_{32} pyroxenes, the evolved melts calculated from those pyroxenes, and the parental melts calculated above (gray field).

compared to the calculated parental melts (Figure 12), consistent with melt evolution. Abundances of LREEs in the evolved melts may be underestimated due to co-competition with phosphate crystallization. The close correspondence between the calculated melt and measured whole-rock composition is consistent with all samples representing melt compositions. This argues against an accumulation model such as the one proposed above to explain the disparities between bulk-rock analyses and calculated whole-rock compositions.

Distribution Coefficients from Rim-Melt Compositions

Distribution coefficients have been determined for sample 15499 for a range of elements. They are calculated for each element as: $D = X_i^{Mineral} / X_i^{Melt}$, where the mineral composition is that of an evolved pyroxene analyzed, and the melt composition is from an analysis of the 15499 quenched matrix. Ideally, the pyroxene composition would be on the rim, which is the last thing in direct contact with the melt before it quenches. The spot size of laser-ablation used within makes it difficult to analyze these small rims, but the pyroxenes in this sample are not finely zoned enough to the point where this becomes a problem. Distribution coefficients (D) calculated using the above equation where X_i^{Melt} = raster analysis composition, are presented in Table 6, along with the composition of the pyroxene they were calculated from, and the experimentally determined D values used in this study for pyroxenes of similar wollastonite content. Readers are cautioned that potential kinetic effects during cooling are not addressed. However, these distribution coefficients could prove useful for quenched mare basalt studies.

Table 6. Calculated Distribution Coefficients for QNB 15499

	Distribtuion Coefficients					Pyroxenes**				
	Experimental*	D_{Calc} (D3)	D_{Calc} (D6)	D_{Calc} (D15)	D_{Calc} (D19)	Pyx-D3	Pyx-D6	Pyx-D15	Pyx-D19	Raster-Analysis
	Wo_{32}	$Wo_{34.3}$	$Wo_{35.8}$	$Wo_{36.2}$	$Wo_{31.7}$	$Wo_{34.3}$	$Wo_{35.8}$	$Wo_{36.2}$	$Wo_{31.7}$	
Co		1.563	1.809	1.540	1.679	33.6	38.9	33.1	36.1	21.5
Ni		3.054	3.713	2.605	3.744	7.9	9.58	6.72	9.66	2.58
Ga		0.359	0.375	0.357	0.313	2.0	2.07	1.97	1.73	5.52
Sr		0.029	0.031	0.035	0.024	6.0	6.3	7.17	4.84	204
Y		0.419	0.445	0.441	0.343	20.9	22.2	22	17.1	49.9
Zr		0.165	0.164	0.174	0.129	26.4	26.3	27.9	20.7	160
Nb		0.009	0.012	0.011	0.012	0.085	0.124	0.108	0.121	10
Ba		0.000	0.000	0.001	—	0.018	0.059	0.209	—	142
La	0.023	0.026	0.027	0.031	0.019	0.376	0.393	0.45	0.265	14.3
Ce	0.039	0.051	0.056	0.059	0.038	1.930	2.11	2.24	1.44	38
Pr		0.086	0.088	0.098	0.065	0.453	0.465	0.518	0.343	5.29
Nd	0.104	0.130	0.137	0.137	0.094	3.450	3.64	3.62	2.49	26.5
Sm	0.17	0.223	0.234	0.253	0.174	1.780	1.87	2.02	1.39	7.99
Eu	0.16	0.081	0.075	0.080	0.066	0.153	0.141	0.151	0.125	1.88
Gd	0.2	0.336	0.351	0.356	0.251	3.220	3.37	3.41	2.41	9.59
Tb		0.374	0.398	0.398	0.310	0.609	0.649	0.649	0.505	1.63
Dy		0.397	0.426	0.431	0.343	3.870	4.15	4.2	3.34	9.74
Ho		0.436	0.462	0.450	0.355	0.863	0.915	0.891	0.702	1.98
Er		0.440	0.465	0.477	0.365	2.170	2.29	2.35	1.8	4.93
Yb	0.29	0.470	0.519	0.465	0.395	2.020	2.23	2	1.7	4.3
Lu	0.3	0.475	0.524	0.478	0.439	0.281	0.31	0.283	0.26	0.592
Hf		0.322	0.327	0.353	0.302	1.260	1.28	1.38	1.18	3.91

* McKay et al. (1986), **All elements in ppm

V. Apollo 15 Basalt Petrogenesis: Two Magmas or Fractional-Crystallization?

From the perspective of mineral trace-element chemistry, the contents, slopes (Fig. 7b), and patterns (Fig. 6) of REE in pyroxenes suggest that the ONBs and QNBs are similar and can be related. Elemental trends in olivine (Fig. 9), and REE-contents of plagioclase (Fig. 8) support this. Sample QNB 15499 is a puzzle, since it contains euhedral chromite and high-Mg olivine, yet an evolved groundmass in equilibrium with the whole rock. This seems to indicate crystal accumulation (i.e., xenocrysts) prior to eruption and quenching. The QNBs are definitely more evolved than the ONBs, suggesting a simple relationship by fractional crystallization processes. This is evidenced by their general lack of olivine, extensive pyroxene major-element evolution sequence [from pigeonite to Fe-Px (Fig. 3)], and elevated pyroxene REE contents (Fig. 6). Modeling of our large trace-element mineral dataset has elaborated on the particular relationship between the two basalt suites (Figs. 11, 12, 14). This modeling has shown these rocks to have calculated parental melt compositions, similar to their whole-rock compositions, to the point that, within error, both rock types are likely derived from the same parental magma. Modeling of evolved melts has shown that the QNBs are then just a step further than the ONBs by simple fractional crystallization processes in the evolution of this parental melt.

Numerous scenarios have been put forth to explain the petrogenesis of these basalts (Rhodes and Hubbard, 1973; Chappell and Green, 1973; Lindstrom and Haskin, 1978; Vetter et al. 1989). In our scenario, olivine fractionally crystallizes in the parental melt and settles out, and the residual melt is tapped subsequently to form the QNBs. QNB 15499 is a sample that has captured some of the settling xenocrysts, but is mostly

composed of the QNB magma. Initial modeling used a simplistic approach by subtracting out olivine (Mg# predicted by $K_D^{Fe/Mg} = 0.325$ (from Delano, 1980)), from the ONB magma. Subtraction of 5-20% of crystallizing olivine will account for all QNB compositions (Fig. 15). This result was subsequently verified by running the MELTS modeling program of Ghiorso and Sack (1995), whereby a primitive ONB could be used to arrive at the QNB compositions by simple olivine fractionation. This quantitative modeling is confirming evidence for the crystallization of QNB rocks from the original ONB magma.

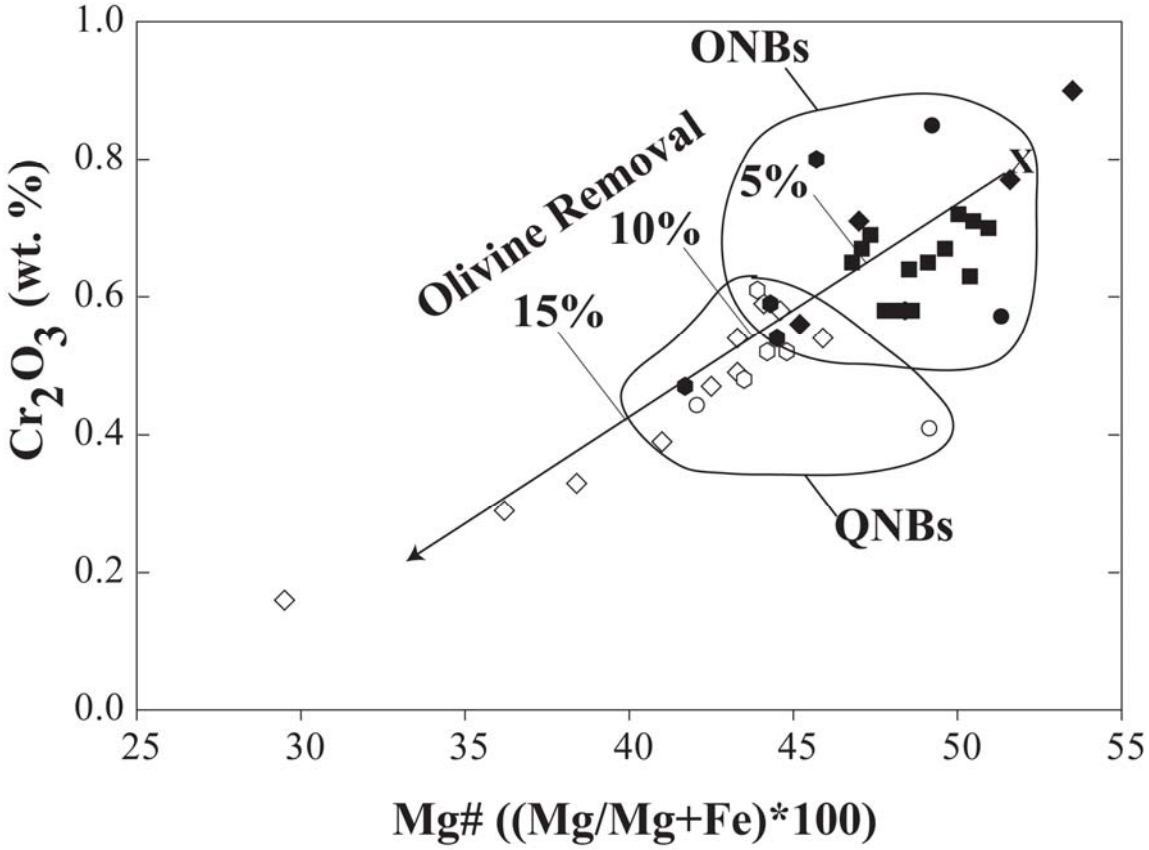


Figure 15. Trace-Element versus Mg# Whole-Rock Plot. This shows the progression of ONBs to QNBs with removal of olivine by fractional crystallization as their common parental melt (represented by X) evolves.

VI. What Does This Mean for Lunar Geology?

Much has been learned about the origin and evolution of the Moon from sample return missions, remote-sensing, and lunar meteorite studies. Despite all the accomplishments, pairing of basalts types at a single Apollo site has been a rarity due to the aforementioned complexities inherent to mare basalts. Reducing these complexities has been made possible by advances in technology. Here we take into account whole-rock and mineral chemistries in conjunction with petrography. The implication of pairing groups by a simple magmatic process is a direct reduction in basalt genesis complexity. Mare basalt samples returned in upcoming missions will be initially analyzed by methods unavailable 30 or 40 years prior. It is beneficial to have a basis using these newer methods on planetary samples for future studies.

Studies of this nature demonstrate that systematic, detailed analyses integrating petrography, major- and trace- element chemistry, and thermodynamic modeling, can lead to a simple solution to a complex problem. This study began with a complex problem and now brings to light this central idea: Mare basalt magmatism at some sites clearly involves heterogeneous sources, but at others, like the Apollo 15 site, fractional crystallization has clearly been operative. Relationships between mare basalts, or other highland rocks, in new missions to the Moon could prove simpler to establish, in turn reducing the complexity involved in basalt petrogenesis as a whole, which reflects greatly on models of the Moon's origin and evolution.

VII. Summary

- Basalts form Apollo 15 Hadley Rille have been classified based on whole-rock chemistry as olivine-normative and quartz-normative basalts - ONB & QNB.
- Two theories have been put forth to explain these two suites of basalts: different magma sources versus fractionated melts of one magma.
- Major- and trace-element chemistry of minerals in these basalts provide the data for quantitative modeling of their parental melts.
- Modeling of new data demonstrate that QNBs are single derivatives of the ONB magma with 5-20% olivine-fractionation - i.e., Ockham's Razor rules again.
- New analytical instrumentation developed over time allows sophisticated quantification and solution of old problems in lunar petrogenesis.

References

List of References

Anand, M., Talyor L.A., Floss, C., Neal, C.R., Terada, K., Tanikawa, S. (2006) Petrology and Geochemistry of LaPaz Icefield 02205: A Unique Low-Ti Mare Basalt Meteorite, *Geochimica and Cosmochimica Acta* 70, 246-264.

Anders E. and Grevesse N. (1989) Abundances of the elements: Meteoritic and solar. *Geochimica et Cosmochimica Acta* 53:197–214.

Apollo 15 Preliminary Examination Team (1972) The Apollo 15 lunar samples: A preliminary description, *Science*, 175, 363-375.

Asimow PD, Ghiorso MS (1998) Algorithmic Modifications Extending MELTS to Calculate Subsolidus Phase Relations. American Mineralogist 83, 1127-1131

Bence, A. E. and J.J. Papike (1972) Pyroxenes as recorders of lunar basalt petrogenesis: Chemical trends due to liquid-crystal interaction. *Proc. Lunar Sci. Conf. III*, 431-469.

Bianco, A. and L. A. Taylor (1977) Applications of dynamic crystallization studies: Lunar olivine-normative basalts. *Proc. Lunar Sci. Conf.* XIII, 1593-1610

Chappell, B. W., and D. H. Green (1973) Chemical composition and petrogenetic relationships in Apollo 15 mare basalts, *Earth Planet. Sci. Lett*., 18, 237-246

Day, J.M.D. et al. (2006) Evidence for age-progressive melting of increasingly incompatible-element-enriched mantle reservoirs on the Moon? *Lunar Planet. Sci. Conf.* XXXVII, CD-ROM Abs. 2235

Delano, J.W. (1980) Chemistry and liquidus phase relations of Apollo 15 red glass: Implications for the deep lunar interior. *Proc. Lunar Sci. Conf.* XI, 251-288

Dowty, E., M. Prinz, and K. Keil (1973) Composition, mineralogy, and petrology of 28 mare basalts from rake samples, *Proc. Lunar Sci. Conf. 4th*, 423-444.

Engelhardt, W. (1979) Ilmenite in the crystallization sequence of lunar rocks. *Proc. Lunar Sci. Conf. X* 677-694

El Goresy A., Prinz M., Ramdohr P. (1976) *LPS VII* pp. 1261-1279.

Ghiorso, Mark S., and Sack, Richard O. (1995) Chemical Mass Transfer in Magmatic Processes. IV. A Revised and Internally Consistent Thermodynamic Model for the Interpolation and Extrapolation of Liquid-Solid Equilibria in Magmatic Systems at Elevated Temperatures and Pressures. Contributions to Mineralogy and Petrology, 119, 197-212

Head J. W. (1976) Lunar volcanism in space and time, *Rev. Geophys. Space Phys.*,14, pp. 265-300.

Herrell, K., K. Nakamura, G. Ryder, and B. Schuraytz (1997), Olivine crystals and the petrogenesis of the Apollo 15 olivine-normative mare basalts, 1, Petrography (abstract), Lunar Planetary Science Conf. XXVIII, 553-554.

Jones, J. H. (1995) Experimental Trace Element Partitioning, Rock Physics and Phase Relationships, A Handbook of Physical Constants, American Geophysical Union, pp. 74-104

Lindstrom, M. M., and L. A. Haskin (1978) Causes of compositional variations within mare basalt suites, *Proc. Lunar Planet. Sci. Conf. 9th*, 465-486.

Lofgren, G. E.; Usselman, T. M., Donaldson, C. H. (1975) Geology, petrology, and crystallization of Apollo 15 quartz-normative basalts, *Proc. Lunar Sci. Conf. 6th*, 79-99.

Grove, T.L. and Walker D.W., Cooling historys of Apollo 15 quartz-normative basalts. *Proc. Lunar Sci. Conf. 8th,* 1501-1520.

Ma, M. S., R. A. Schmitt, R. D. Warner, G. J. Taylor, and K. Keil (1978) Genesis of Apollo 15 olivine normative mare basalts: Trace element correlations, *Proc. Lunar Planet. Sci. Conf. 9th,* 523-533.

Ma, M. S., A. V. Murali, and R. A. Schmitt, Chemical constraints for mare basalt genesis, *Proc. Lunar Sci Conf. 7th*, 1673-1695, 1976.

McKay, G., Wagstaff, J., Yang, S.-R. (1986) Clinopyroxene REE distribution coefficients for shergottites: the REE content of the Shergotty melt. *Geochim. Cosmochim Acta* 50, 927–937.

McKay (1991), Le, L., and Wagstaff J. (1991) Constraints on the Origin of the Mare Basalt Europium Anomaly: REE Partition Coefficients for Pigeonite. Abstracts of the Lunar and Planetary Science Conference, volume 22, page 883,

Norman M.D., Pearson N.J., Sharma A., and Griffin W.L. (1996) Quantitative analysis of trace elements in geological materials by laser ablation ICPMS: instrumental operating conditions and calibration values of NIST glasses Geostandards Newsletter 20, 247-261.

Norman M.D., Griffin W.L., Pearson N.J., Garcia M.A., O'Reilly S.Y. (1998) Quantitative analysis of trace element abundances in glasses and minerals: a comparison of laser ablation ICP-MS, solution ICP-MS, proton microprobe, and electron microprobe data. *Journal of Analytical Atomic Spectrometry*, **13**, 477-482

Norman M.D., Garcia M.O., and Bennett V.C. (2004) Rhenium and chalcophile elements in basaltic glasses from Ko'olau and Molokai volcanoes: magmatic outgassing

and composition of the Hawaiian plume. Geochimica et Cosmichimica Acta 68, 3761-3777

Nyquist, L.E., and C. Y. Shih (1992) The isotopic record of lunar volcanism, *Geochim. Cosmochim. Acta,* 56, 2213-2234.

Rhodes, J. M., and N. J. Hubbard (1973), Chemistry, classification and petrogenesis of Apollo 15mare basalts, *Proc. Lunar Sci. Conf. 4th*, 1127-1148.

Ruzicka A., Snyder G.A., Taylor L.A. (2001) *Geochimica et Cosmochimica Acta*, 65, 979-997.

Ryder, G., Catalog of Apollo 15 Rocks (1985), JSC 20787, 1296 pp., NASA Lydon B. Johnson Space Center, Houston, TX.

Ryder, G., and T. C. Burling (1986) An Apollo 15 mare basalt fragment and lunar mare provinces, *Meteorit. Planet. Sci.* **21**, 50-59.

Ryder G., and Schuraytz, B.C. (2001) Chemical variation of the large Apollo 15 olivine-normative mare basalt rock samples. *Journal of Geophysical Research,* **106**, 1435-1451.

Ryder, G., and A. Steele (1988), Chemical dispersion among Apollo 15 olivine-normative mare basalts, *Proc. Lunar Planetary Science Conf. XVIII*, 273-282.

Perkins W. T., N. J. G. Pearce and T. E. Jeffries (1993), Laser ablation inductively coupled plasma mass spectrometry: A new technique for the determination of trace and ultra-trace elements in silicates , *Geochimica et Cosmochimica Acta*, 57, 475-482

Schnare D.W., Norman M.D., Day J.M.D., Taylor L.A. (2005). 68th Annual meeting of the Meteoritical Society. Abstract #5214

Schnare D.W., Taylor L. A., Day J.M.D., Norman M.D. (2006)

Petrogenesis of Apollo 15 olivine- and quartz- normative mare basalts.

LPSC XXXVII Abstract #2212

Shervais, J. W., S. K. Vetter, and M. M. Lindstrom (1990) Chemical differences between small subsamples of Apollo 15 olivine-normative basalts, *Proc. Lunar Planet. Conf. 20th*, 109-126.

Snyder, G. A., L. E. Borg, L. A. Taylor, L. E. Nyquist, and A. N. Halliday (1997)

Nd-Sr-Hf isotopic and geochronologic studies of Apollo 15 basalts, Lunar Planet. Sci. Conf. XXVIII, 1347-1348.

Snyder, G. A., L. E. Borg, L. A. Taylor, L. E. Nyquist, and A. N. Halliday (1998),

Volcanism in the Hadley-Appenine Region of the Moon: Geochronology, Nd-Sr isotopic systematics, and depths of melting, Lunar Planet. Sci. XXIX, abstract 1141.

Taylor S.R. (1975) *Lunar Science: A Post-Apollo view.* Pergamon press, New York, 372pp.

Taylor S.R. (1982) *Planetary science: A lunar perspective.* Lunar and Planetary Institute, Houston, 481 pp.

Taylor S.R., Taylor G.J. and Taylor L.A. (2006) The Moon: A Taylor-made perspective. *Geochim. Cosmochim. Acta.* In press.

Taylor L.A., Patchen A., Taylor D.H.S., Chambers J. G., and McKay D. S. (1996). X-ray digital imaging petrography of lunar mare soils: Modal analyses of minerals and glasses. *Icarus* 124:500-512

Vetter, S. K., and J. W. Shervais (1989), A dynamic melting model for the origin of

Apollo 15 olivine-normative and quartz-normative mare basalts, Lunar Plant. Sci. Conf. XX, 1152-1153.

Walker, D., Longhi J., Lasaga A., Stopler E. M., Grove T. L., Hays J.F. (1977) Slowly cooled micrograbbros 15555 and 15065. *Proc. Lunar Sci. Conf. XIII*, 1521-1547

Wilhelms, D.E. (1984) Moon in The Geology of Terrestrial Planets, edited by M. Carr, NASA Spec. Publ., SP-469, 107-205.

Wilhelms, D.E. (1987) The geologic history of the Moon, U.S. Geol. Surv. Prof. Pap., 1348, 302 pp.

Appendices

A-1. Standards

Table A1. LA-ICP-MS Data for USGS Basaltic Glass Reference Materials

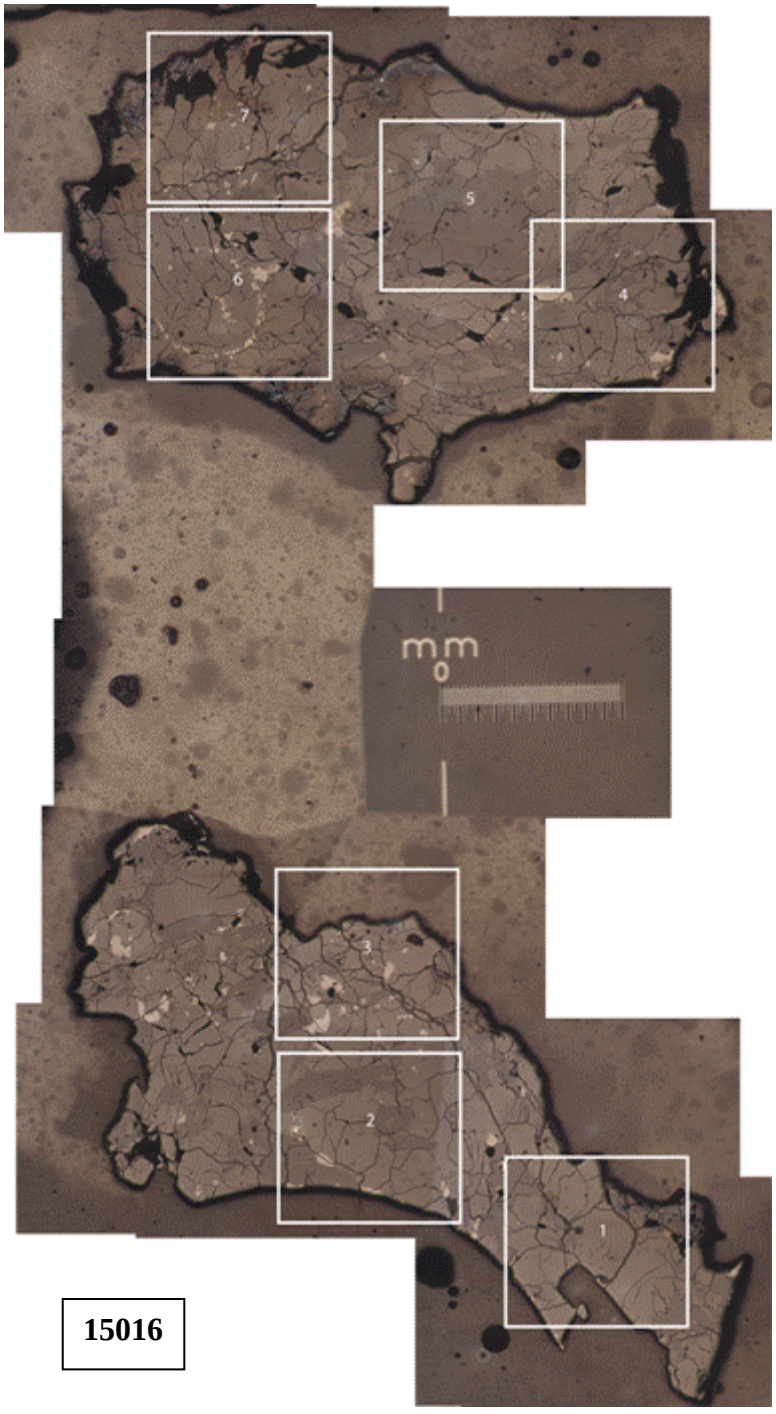
	BCR-2G				BHVO-2G				BIR-1G			
	avg	1s, n=12	%RSD	PV	avg	1s, n=11	%RSD	PV	avg	1s, n=12	%RSD	PV
MgO	3.32	0.09	2.8	3.59	6.85	0.15	2.2	7.23	9.38	0.20	2.2	9.70
MgO	3.60	0.02	0.7	3.59	7.47	0.06	0.8	7.23	10.3	0.11	1.1	9.70
Al_2O_3	13.5	0.14	1.0	13.5	13.4	0.10	0.7	13.5	15.7	0.10	0.6	15.5
CaO	7.10	0.00	0.0	7.10	11.4	0.00	0.0	11.4	13.3	0.00	0.0	13.2
Sc	33.8	0.28	0.8	33.8	32.1	0.24	0.8	31.8	43.3	0.31	0.7	43.8
Ti	14292	249	1.7	13671	17143	430	2.5	16908	6041	131	2.2	6048
V	373	2.81	0.8	379	282	2.09	0.7	285	295	2.57	0.9	286
Cr	15.6	0.43	2.8	16.4	281	4.52	1.6	280	390	3.93	1.0	370
Mn	1445	60.4	4.2	1520	1253	42.6	3.4	1290	1323	42.8	3.2	1357
FeO	12.1	0.87	7.2	12.43	11.05	0.75	6.8	11.1	10.3	0.74	7.2	10.2
Co	36.8	0.52	1.4	37.7	44.5	0.60	1.3	45	54.6	0.37	0.7	53
Ni	11.9	0.27	2.3	12.8	120	4.46	3.7	120	186	2.31	1.2	175
Ga	22.0	0.24	1.1	21.9	21.1	0.20	0.9	21	15.2	0.20	1.3	15.2
Rb	47.7	0.70	1.5	46.4	9.24	0.09	1.0	9.5	0.20	0.02	12.5	0.195
Sr	335	1.24	0.4	338	394	1.66	0.4	396	110	0.67	0.6	108
Y	34.1	0.10	0.3	34.3	24.6	0.19	0.8	24.9	14.8	0.17	1.1	14.4
Zr	190	1.16	0.6	193	173	1.29	0.7	175	14.7	0.19	1.3	14.1
Nb	12.9	0.08	0.6	12.7	18.5	0.08	0.4	18.8	0.55	0.02	3.5	0.54
Ba	679	5.90	0.9	670	131	0.40	0.3	133	6.59	0.09	1.3	6.52
La	25.4	0.19	0.7	25.2	15.4	0.13	0.9	15.5	0.61	0.02	3.7	0.604
Ce	52.5	0.43	0.8	51.7	37.4	0.24	0.6	38	1.93	0.04	2.3	1.9

Table A1. Continued

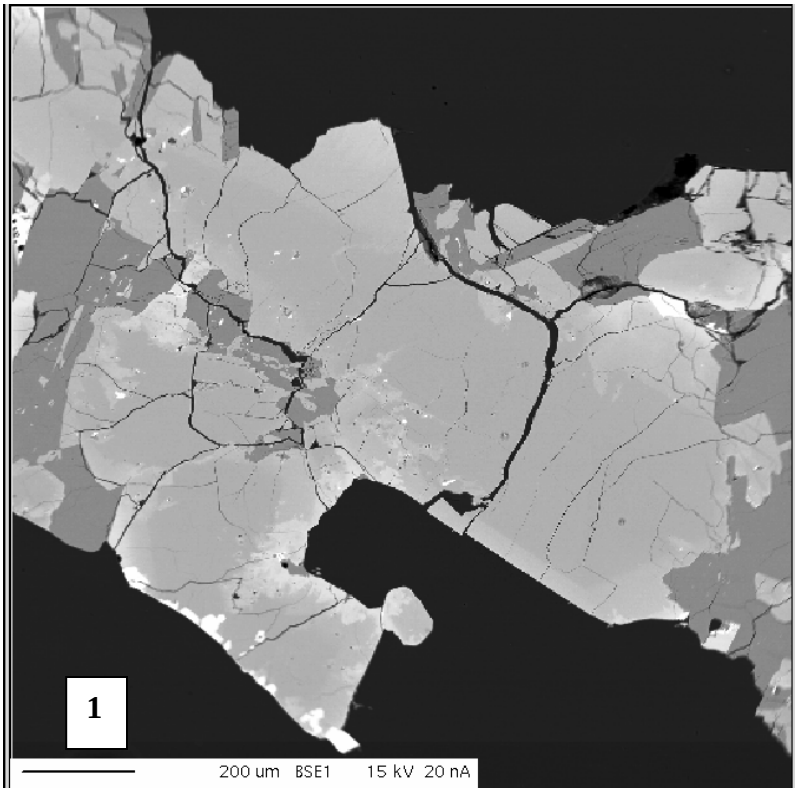
Pr	6.47	0.07	1.1	6.2	5.07	0.03	0.6	5.2	0.36	0.01	3.0	0.36
Nd	28.6	0.42	1.5	28.2	24.4	0.24	1.0	24.7	2.41	0.06	2.6	2.38
Sm	6.74	0.15	2.2	6.6	6.05	0.14	2.3	6.17	1.11	0.06	5.2	1.12
Eu	1.96	0.03	1.7	2	2.09	0.03	1.6	2.06	0.53	0.01	2.5	0.524
Tb	6.75	0.13	1.9	6.8	6.22	0.11	1.8	6.22	1.88	0.06	3.2	1.85
Gd	1.08	0.03	2.5	1.02	0.94	0.03	3.4	0.95	0.38	0.02	4.3	0.379
Dy	6.38	0.12	2.0	6.16	5.21	0.13	2.5	5.25	2.53	0.09	3.5	2.53
Ho	1.33	0.02	1.7	1.29	0.99	0.03	3.0	1	0.59	0.02	2.6	0.585
Er	3.52	0.08	2.1	3.38	2.38	0.07	3.1	2.42	1.60	0.05	3.3	1.60
Yb	3.36	0.09	2.5	3.27	1.96	0.07	3.5	1.98	1.68	0.07	3.9	1.65
Lu	0.49	0.01	2.3	0.48	0.28	0.01	3.4	0.28	0.24	0.01	4.5	0.247
Hf	4.81	0.06	1.3	4.71	4.26	0.08	2.0	4.3	0.56	0.02	3.7	0.562
Ta	0.82	0.03	3.1	0.79	1.18	0.02	2.0	1.2	0.04	0.00	10.6	0.041
Th	6.01	0.11	1.9	6.12	1.21	0.03	2.4	1.26	0.03	0.01	19.6	0.03
U	1.60	0.04	2.54	1.60	0.43	0.02	5.2	0.42	0.02	0.00	16.1	0.01

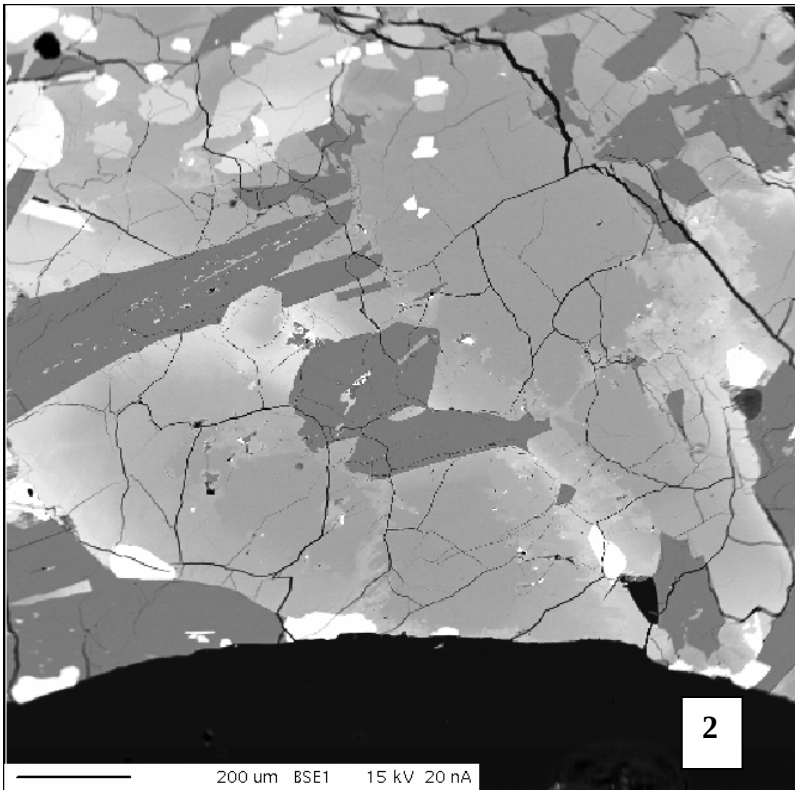
Oxides in wt%, all other data in ppm. CaO used for internal normalization of each analysis. Preferred values (PV) are based on data for the corresponding rock powders (Raczek, 2001; Eggins et al. 1997; Robinson et al. 1999)

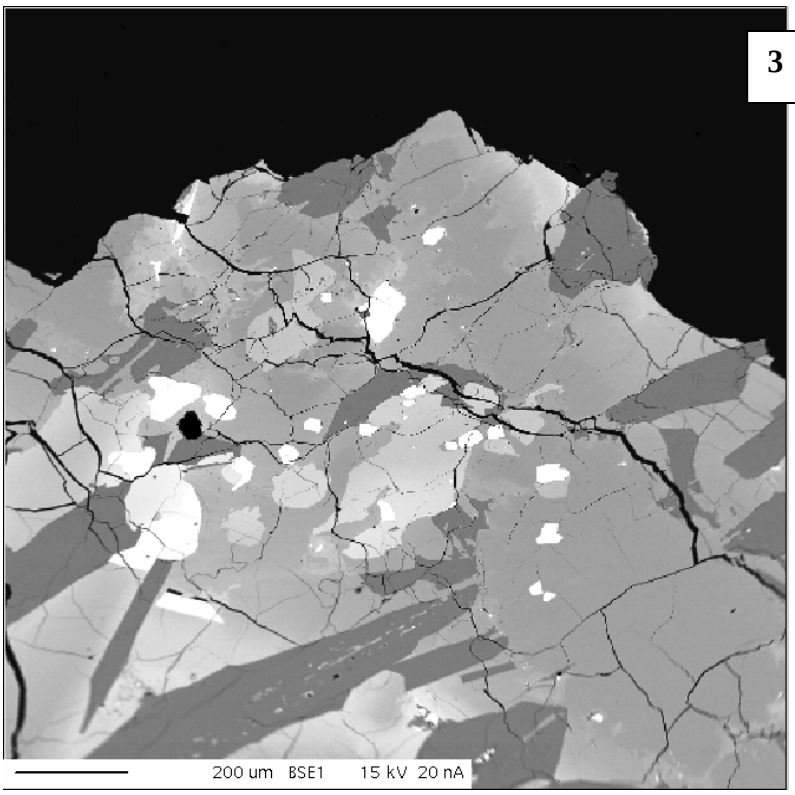
A-2: Back Scattered-Electron Images

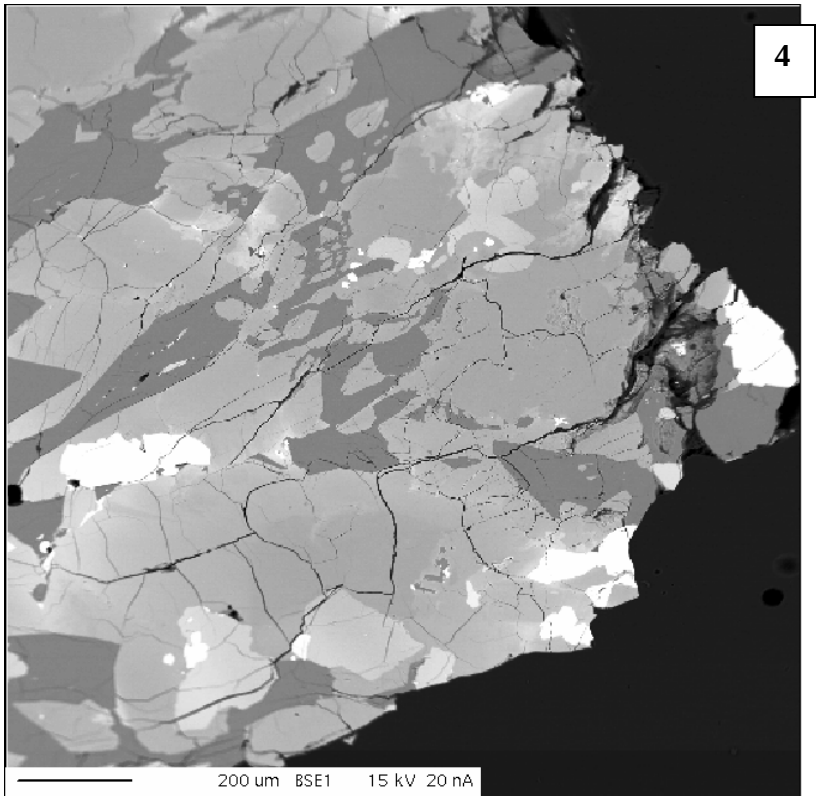


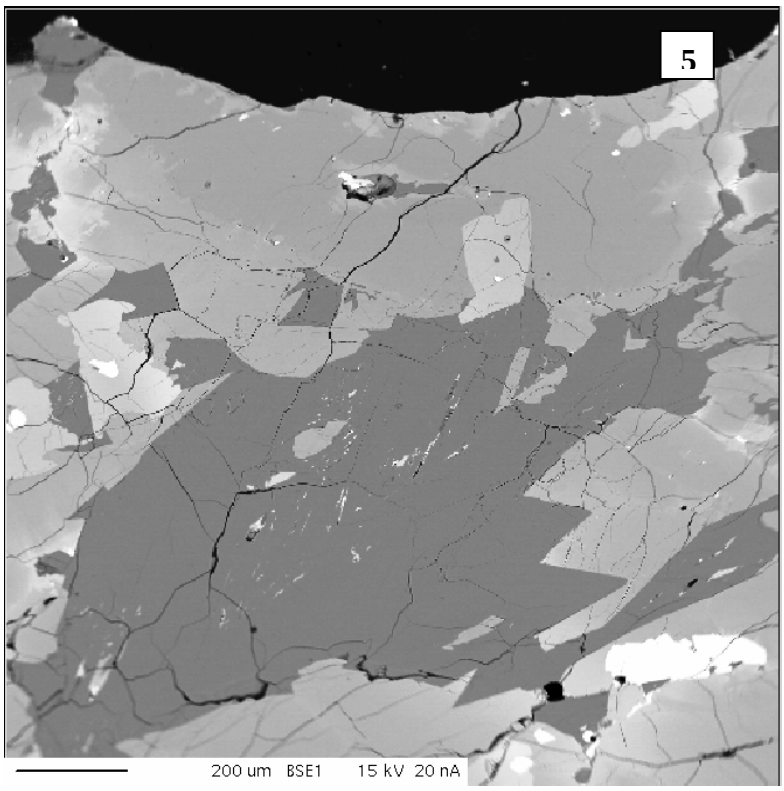
15016

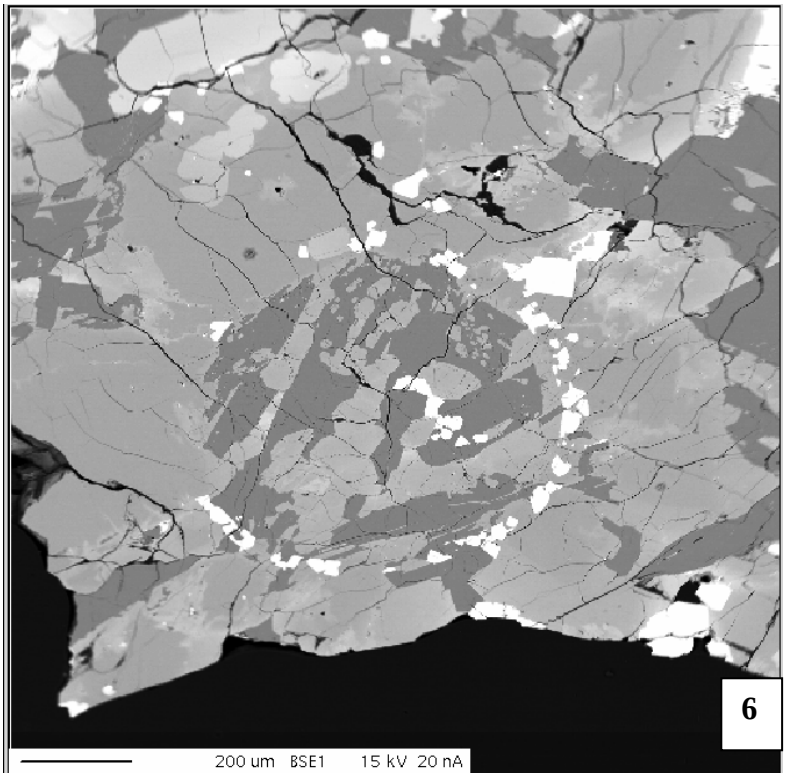

1
200 um BSE1 15 kV 20 nA

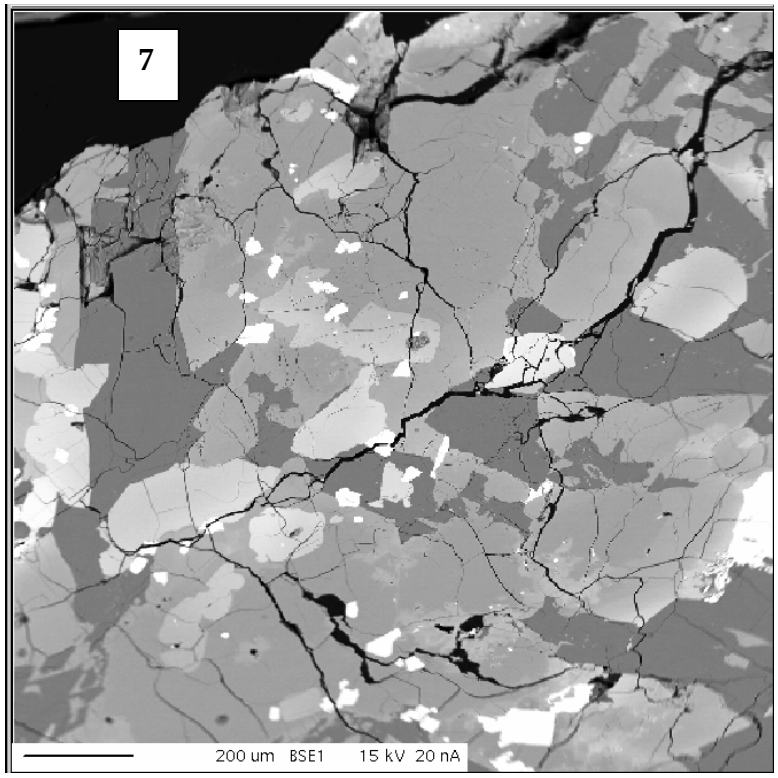

2
200 um BSE1 15 kV 20 nA

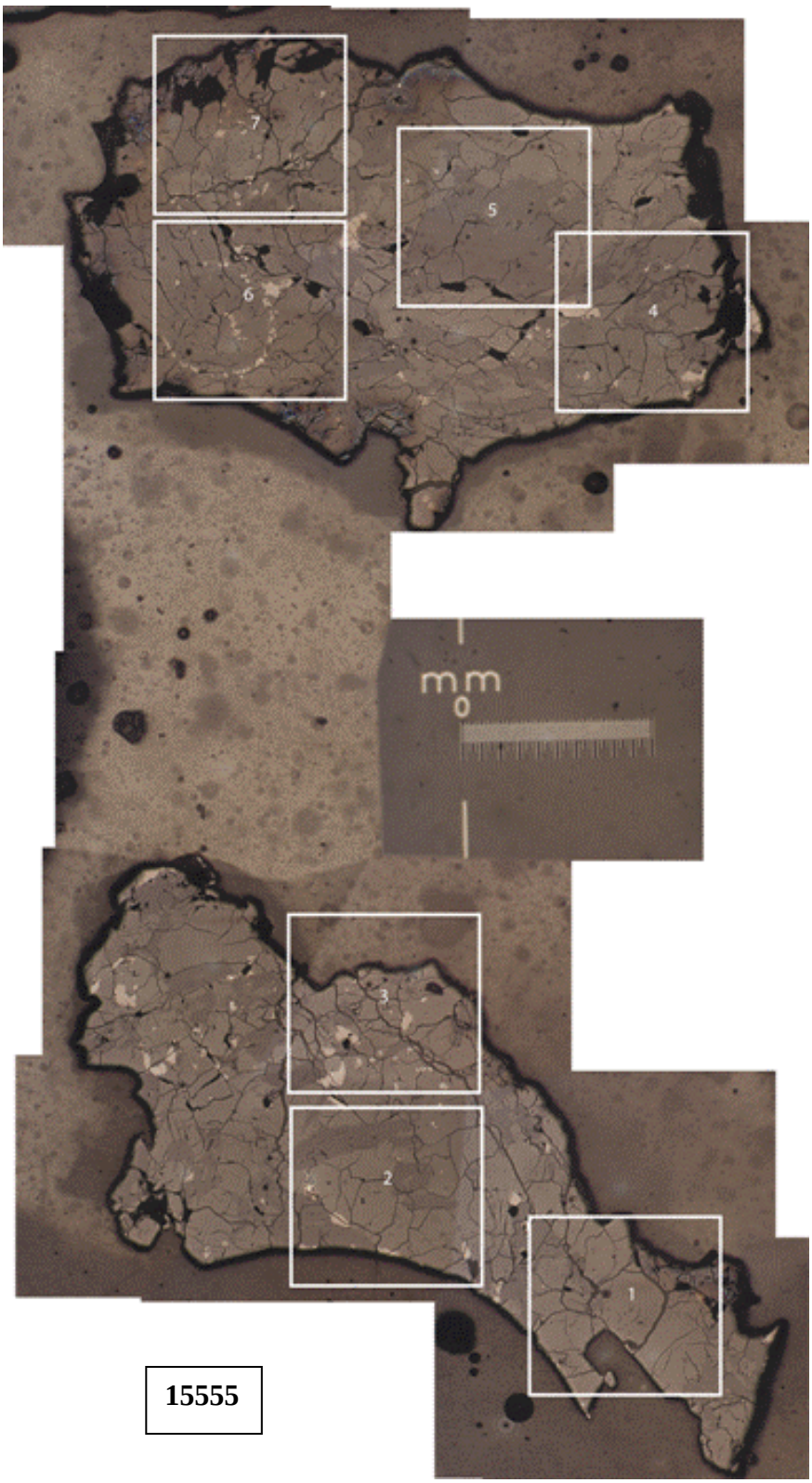

3
200 um BSE1 15 kV 20 nA


4
200 um BSE1 15 kV 20 nA

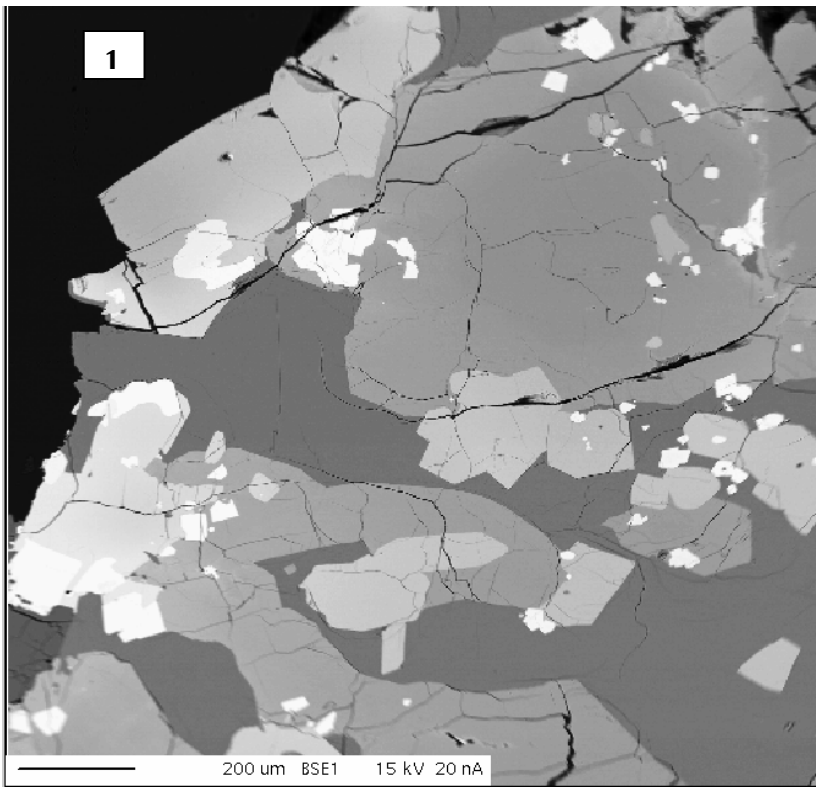

5
200 um BSE1 15 kV 20 nA

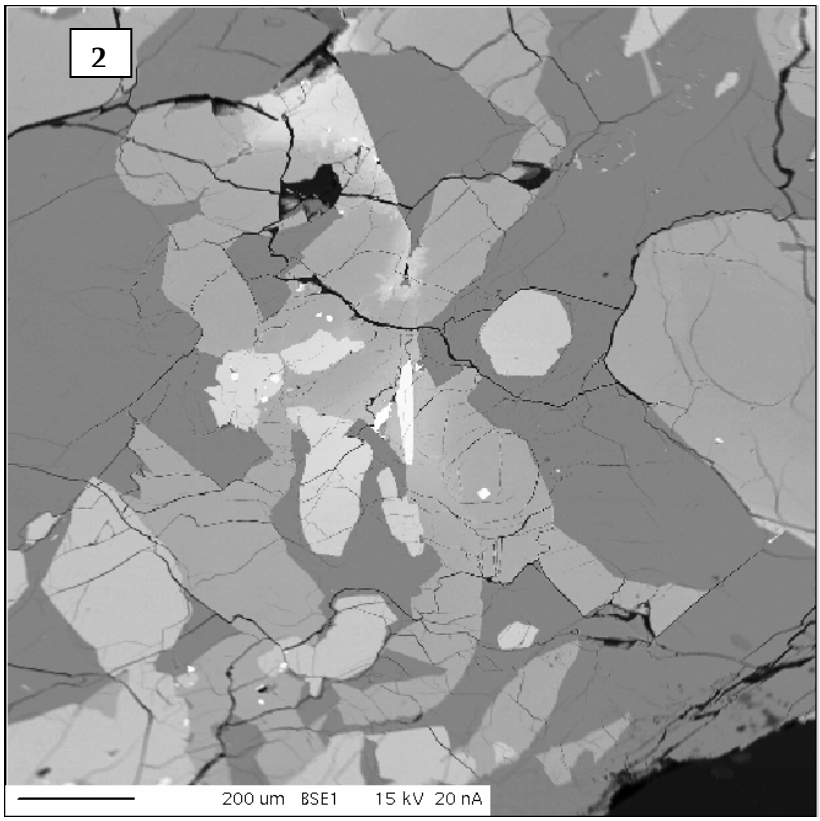

6
200 um BSE1 15 kV 20 nA

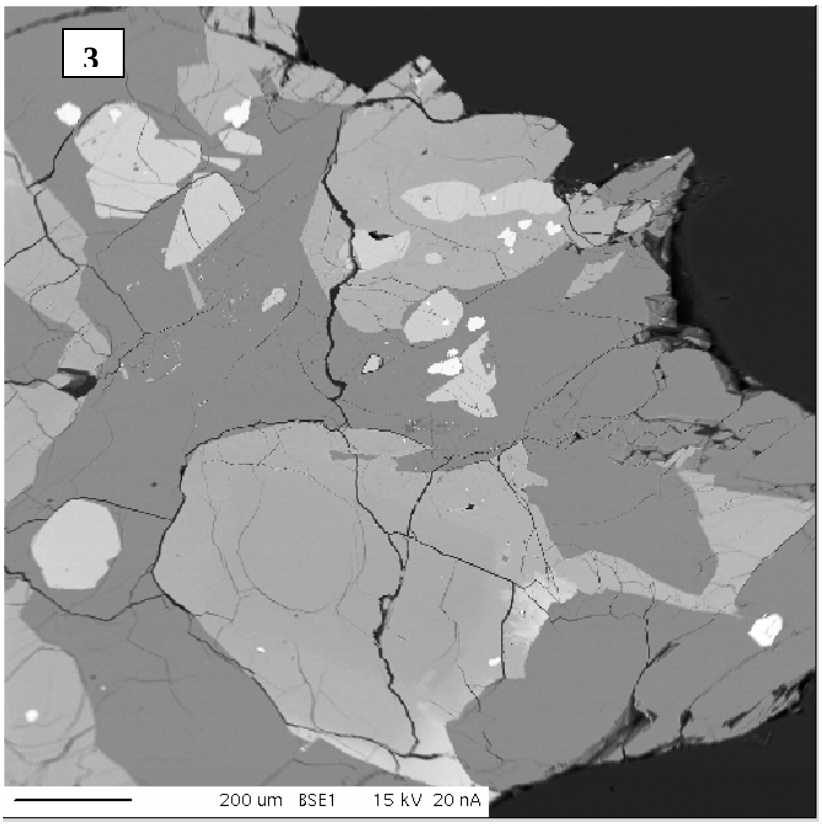

7
200 um BSE1 15 kV 20 nA

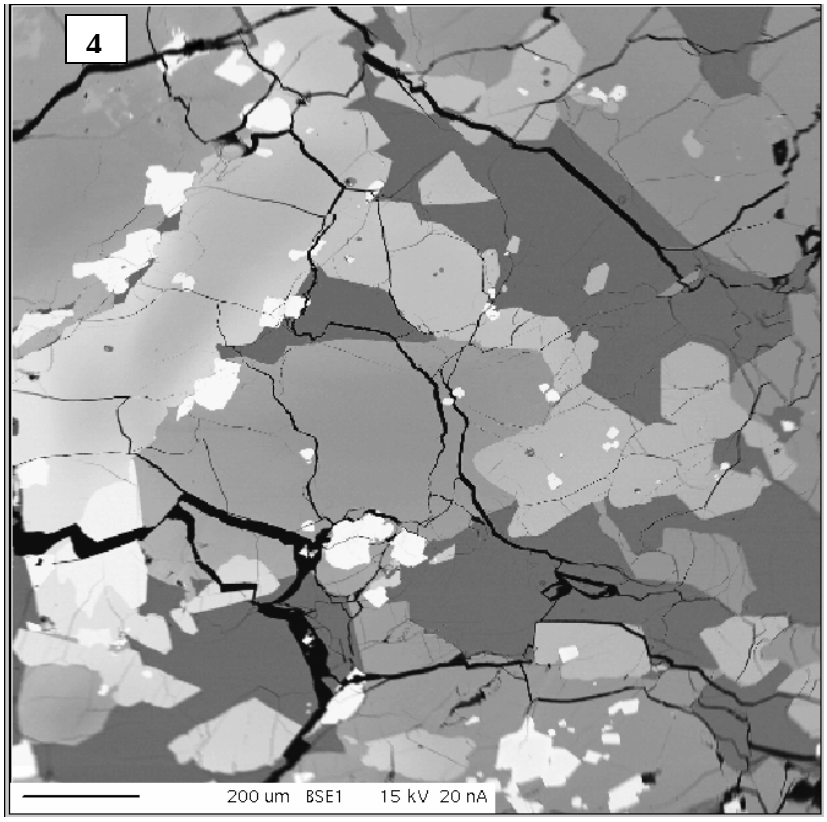


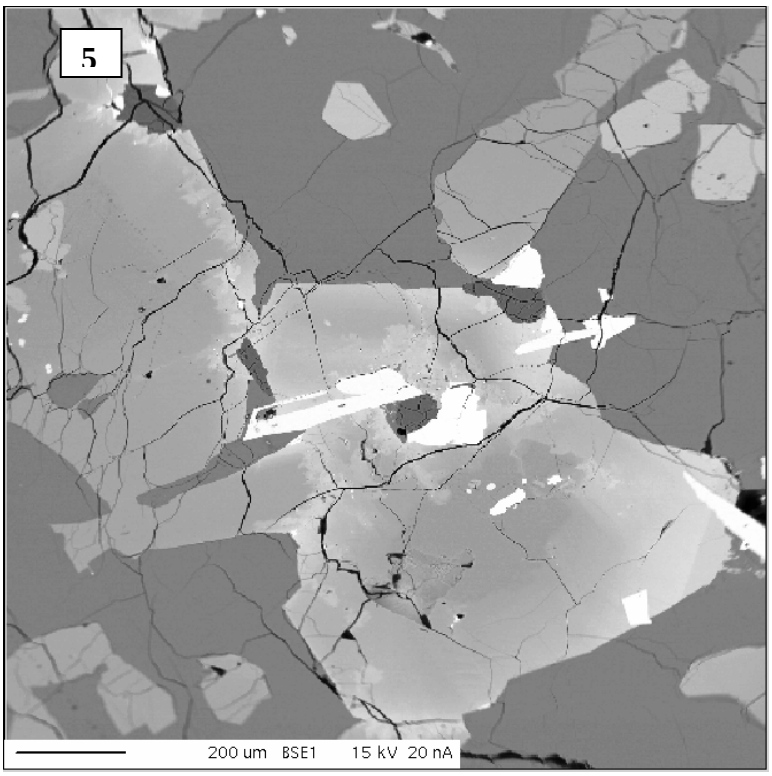
15555

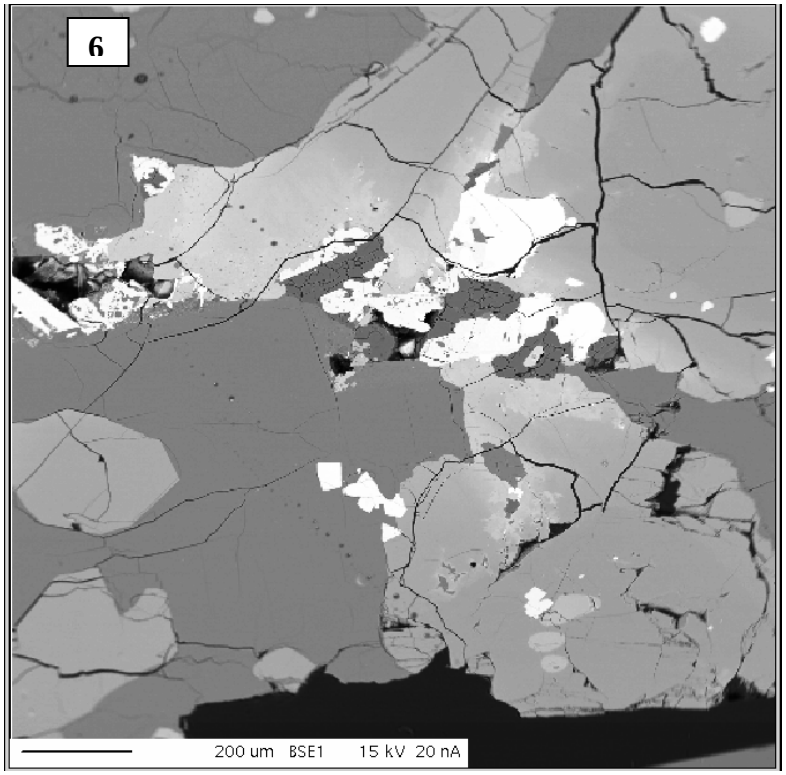

1
200 um BSE1 15 kV 20 nA

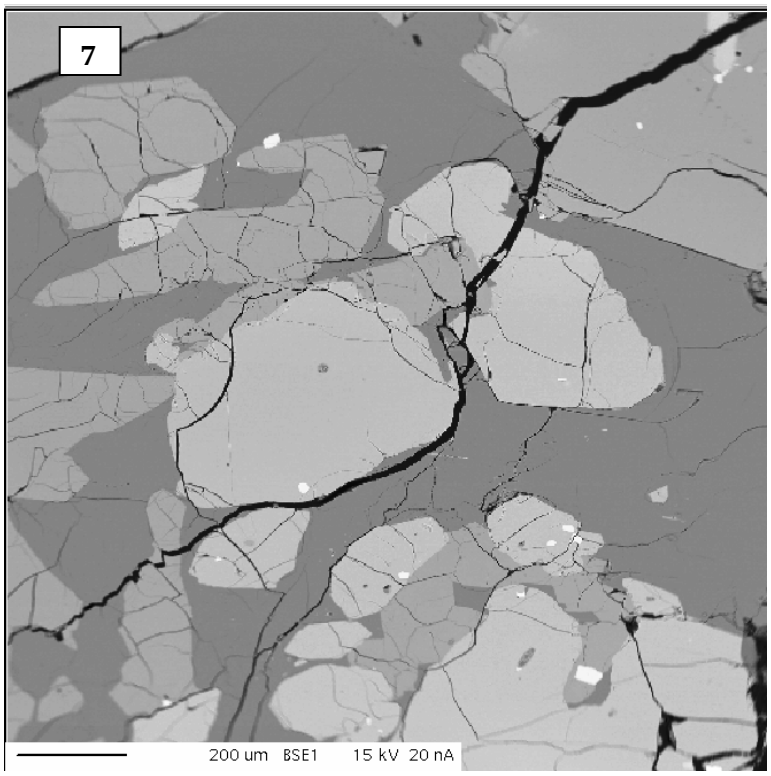

2
200 um BSE1 15 kV 20 nA

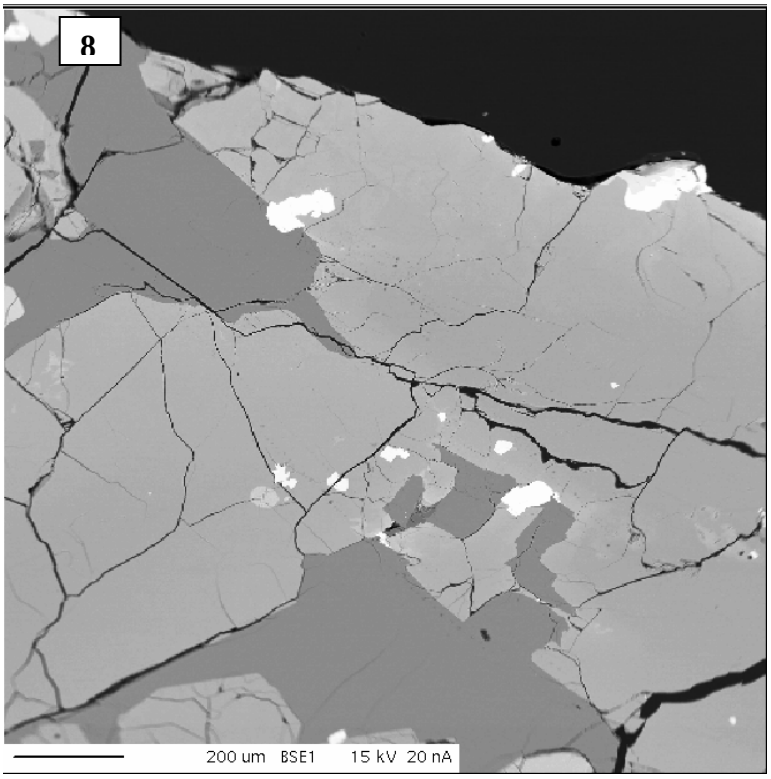

3
200 um BSE1 15 kV 20 nA

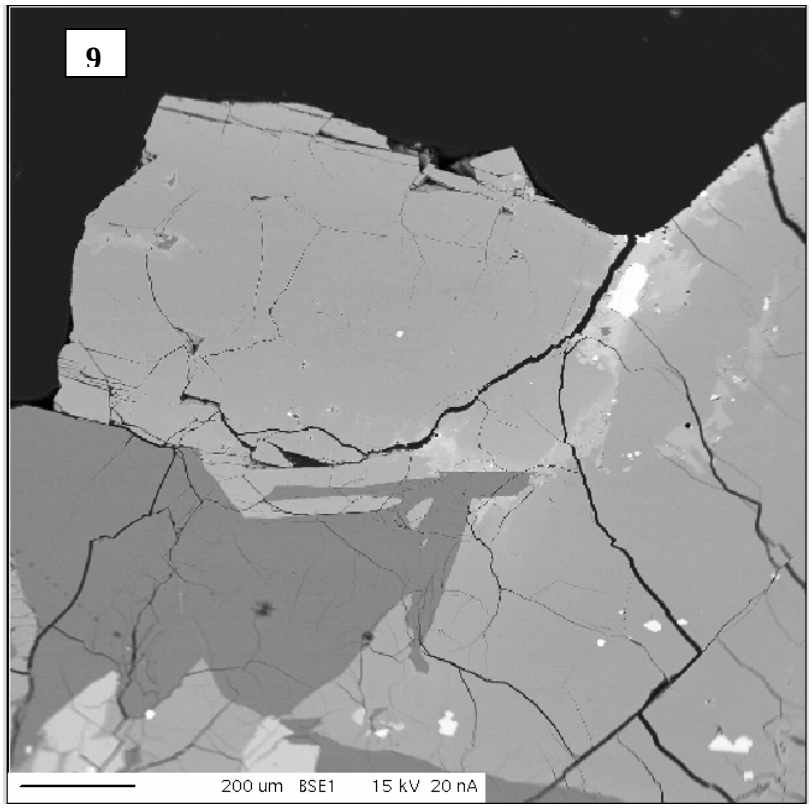

4
200 um BSE1 15 kV 20 nA

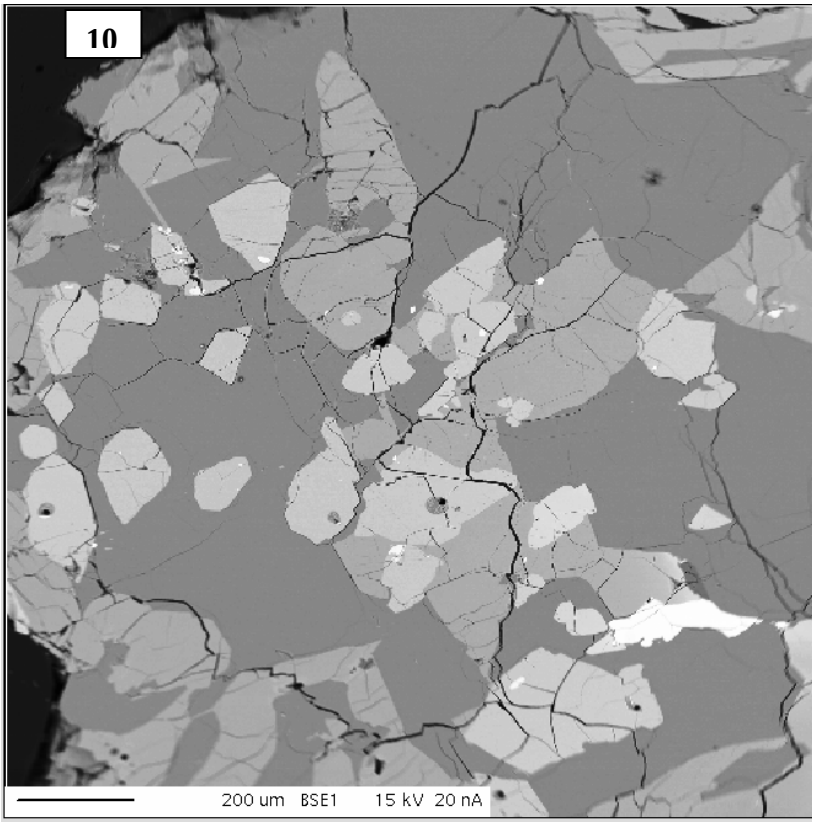

5
200 um BSE1 15 kV 20 nA

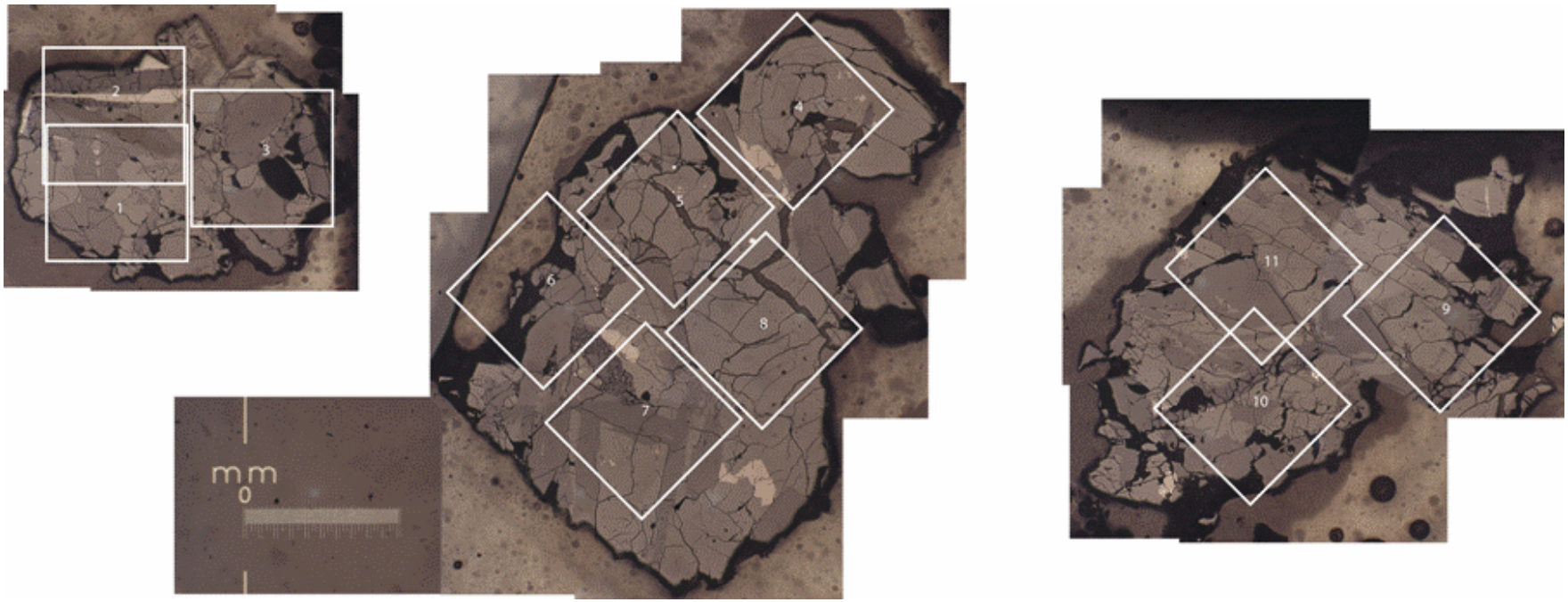

6
200 um BSE1 15 kV 20 nA

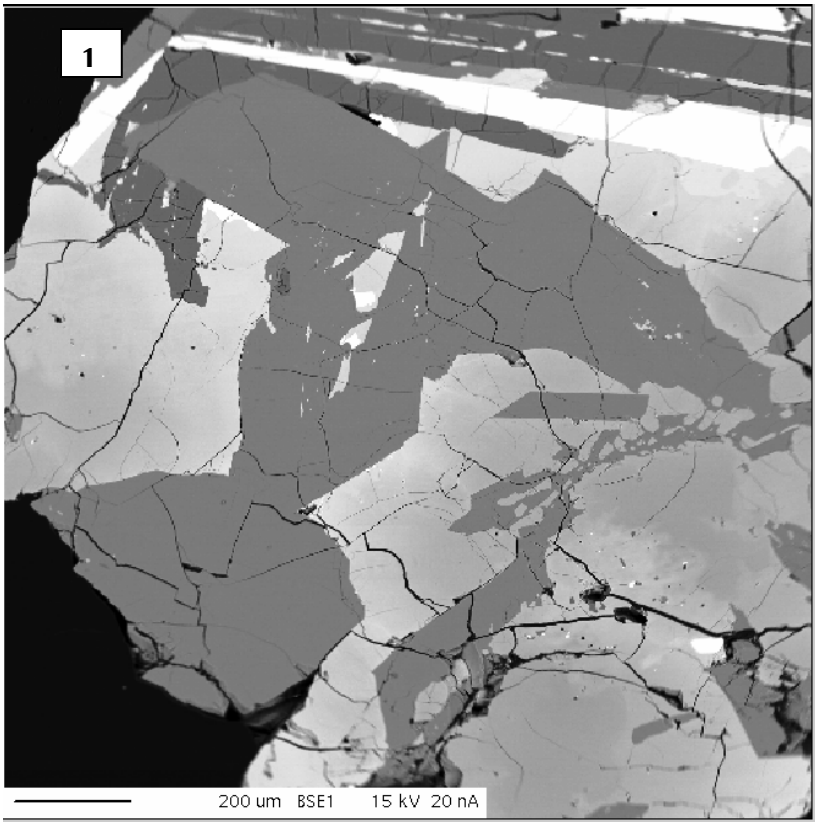

7
200 um BSE1 15 kV 20 nA

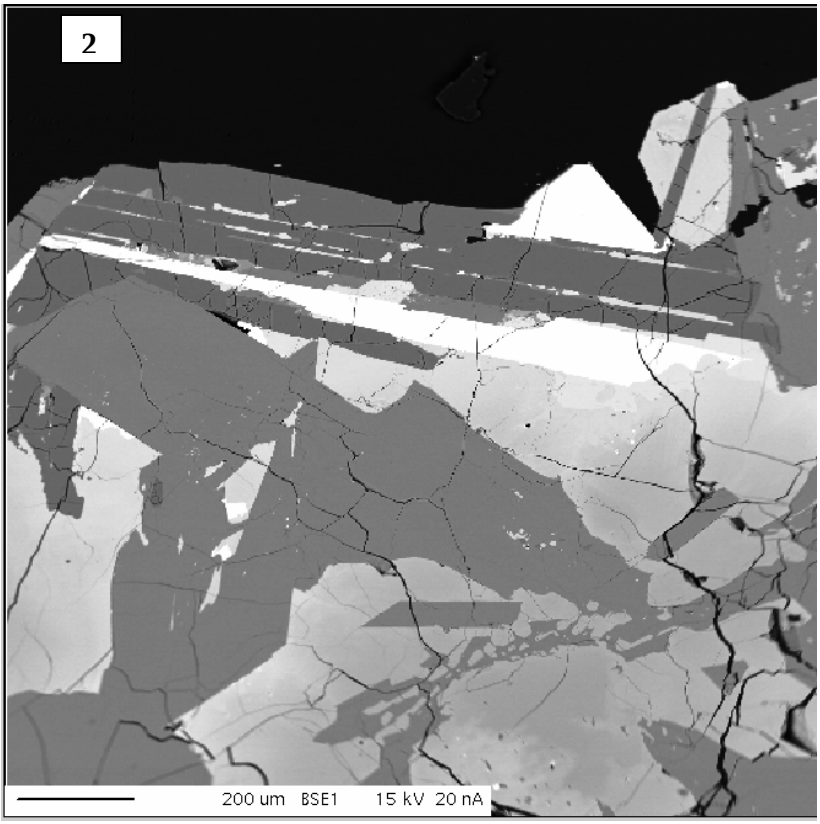

8
200 um BSE1 15 kV 20 nA

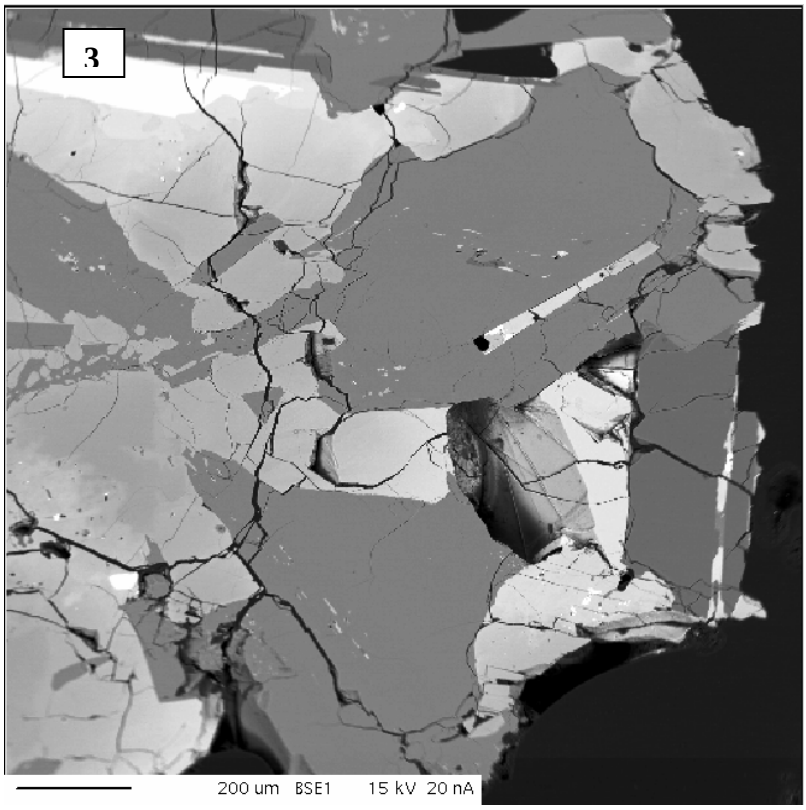

9
200 um BSE1 15 kV 20 nA

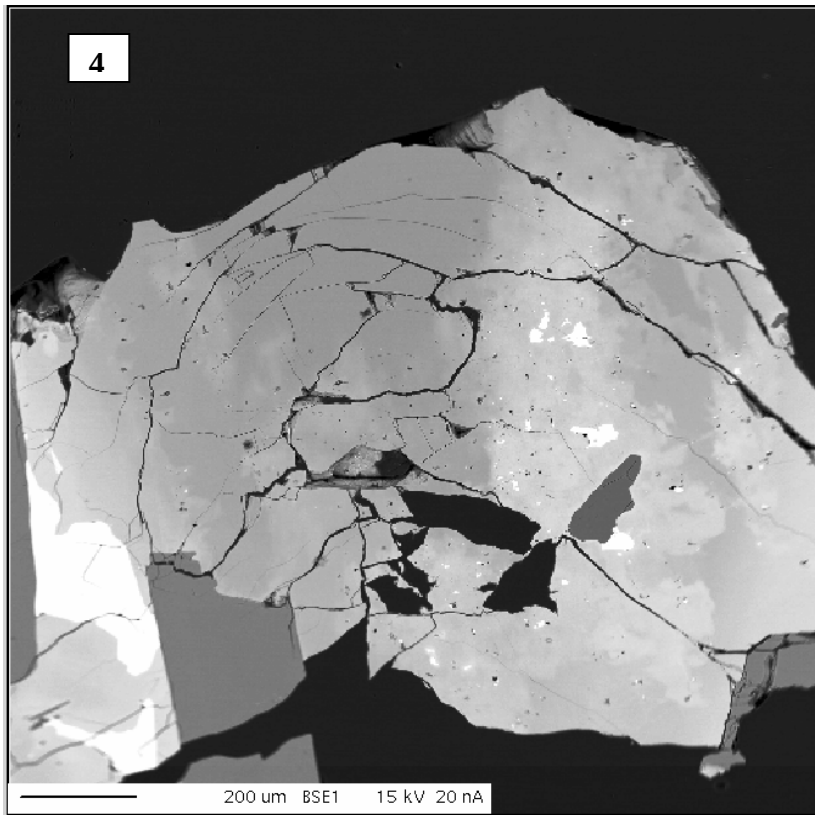

10
200 um BSE1 15 kV 20 nA

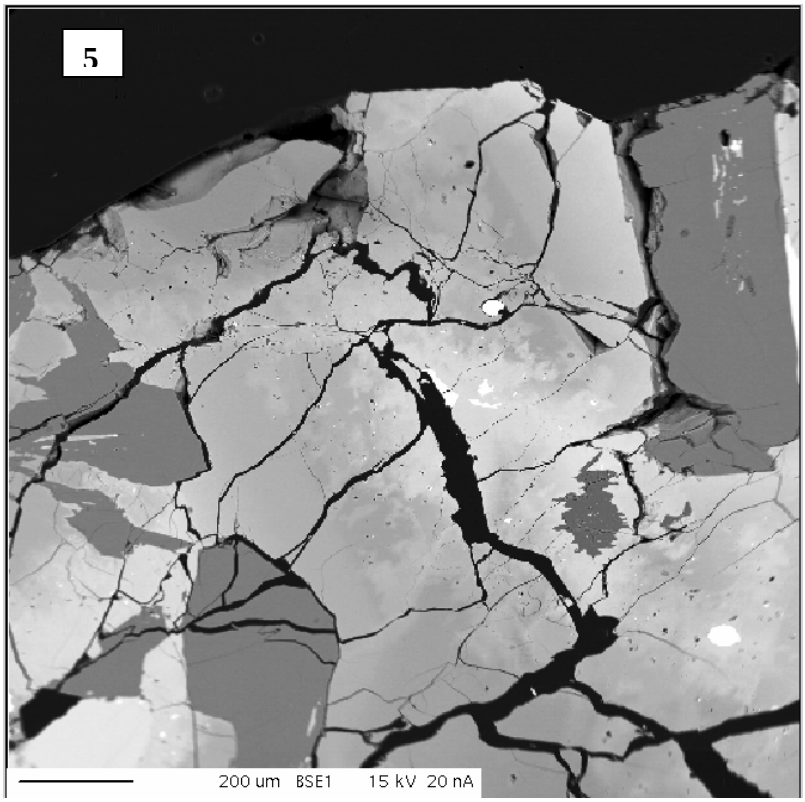

1
2
3
4
5
6
7
8
9
10
11
mm
0

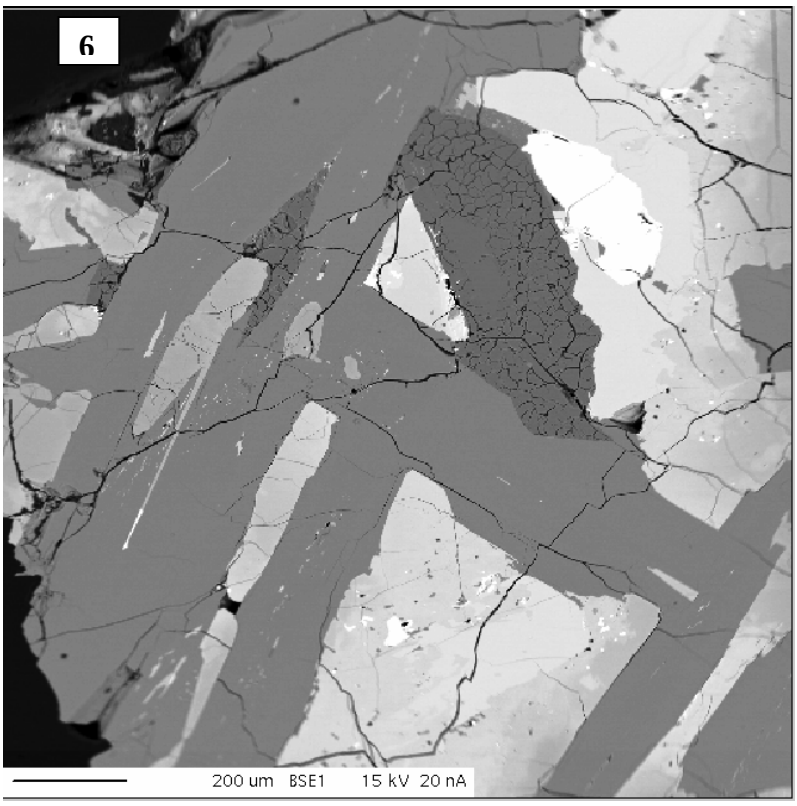

1
200 um BSE1 15 kV 20 nA

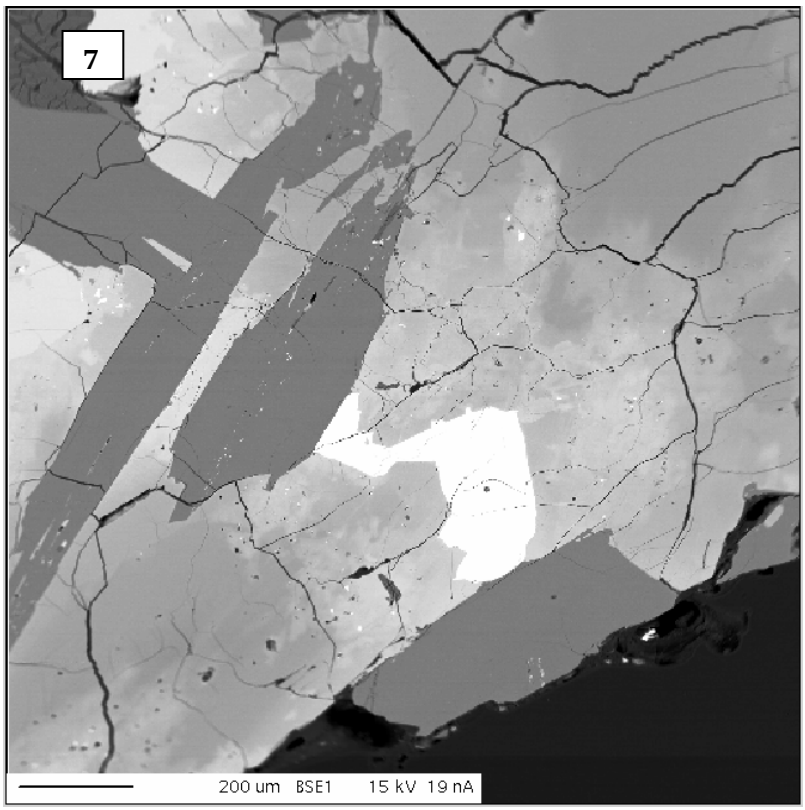

2
200 um BSE1 15 kV 20 nA

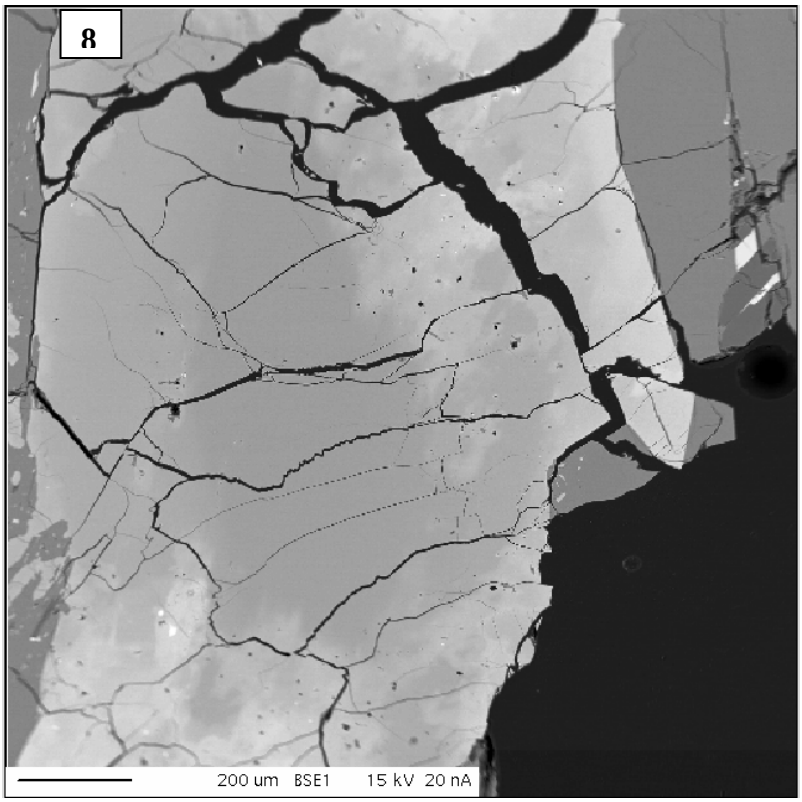

3
200 um BSE1 15 kV 20 nA

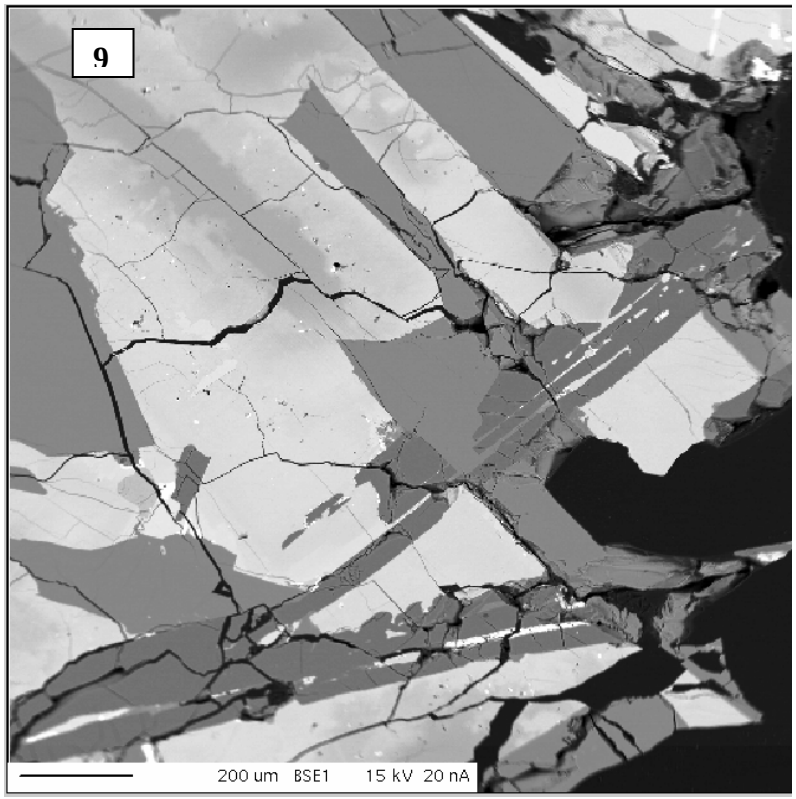

4
200 um BSE1 15 kV 20 nA

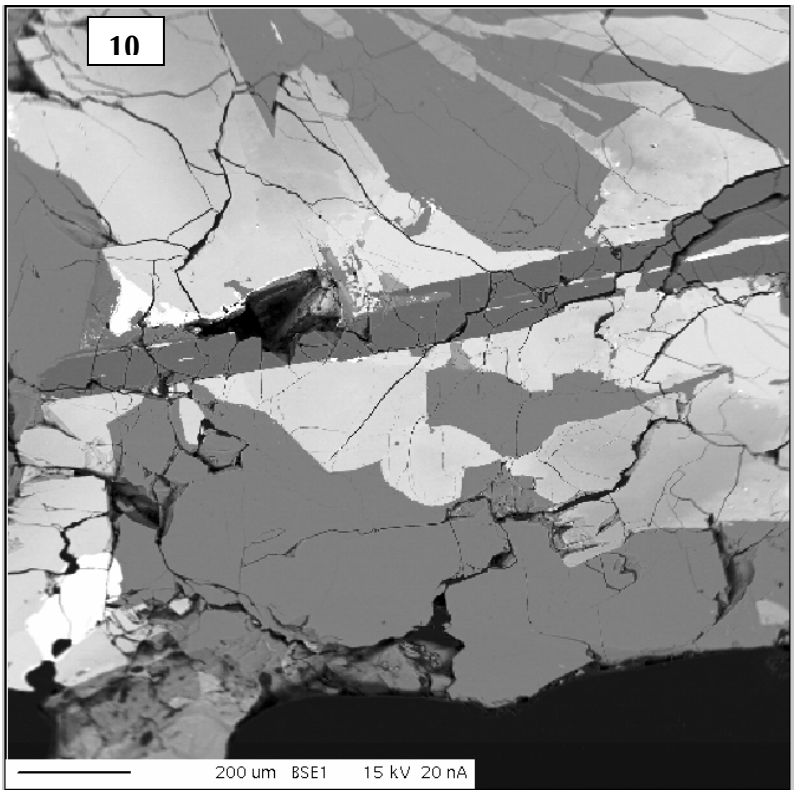

5
200 um BSE1 15 kV 20 nA

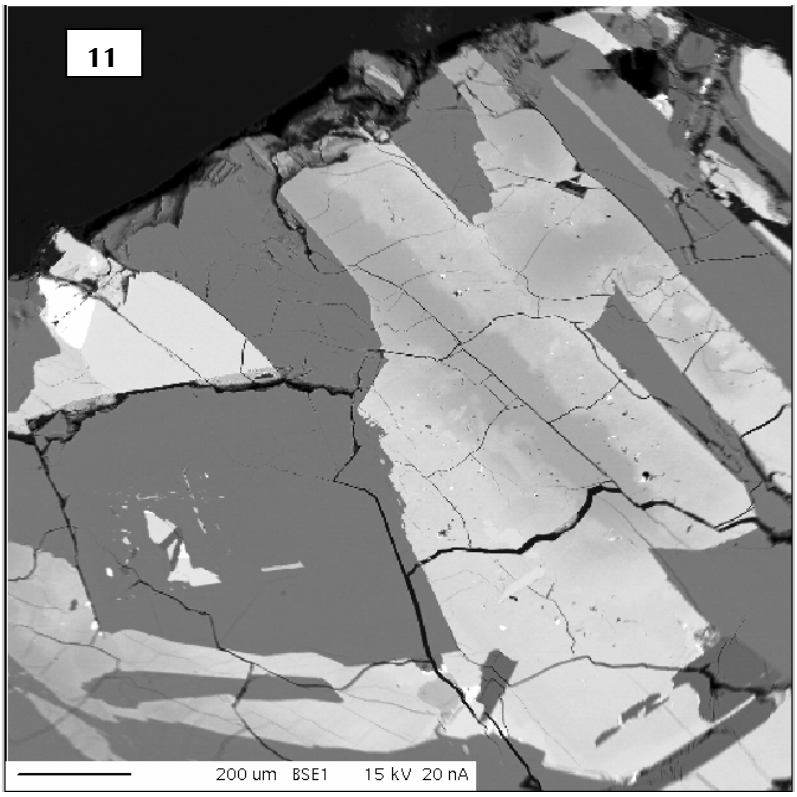

6
200 um BSE1 15 kV 20 nA

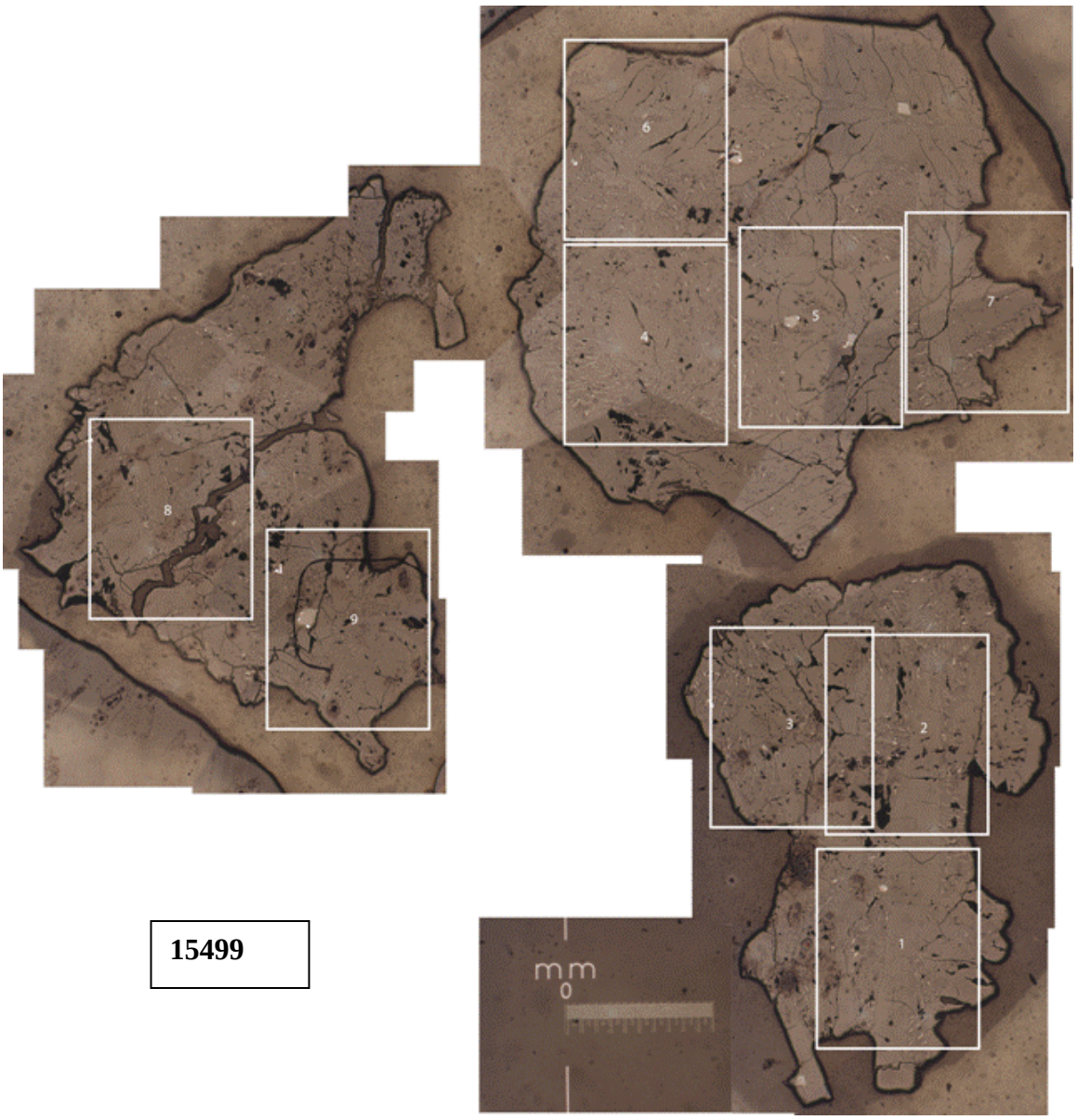

7
200 um BSE1 15 kV 19 nA


8
200 um BSE1 15 kV 20 nA

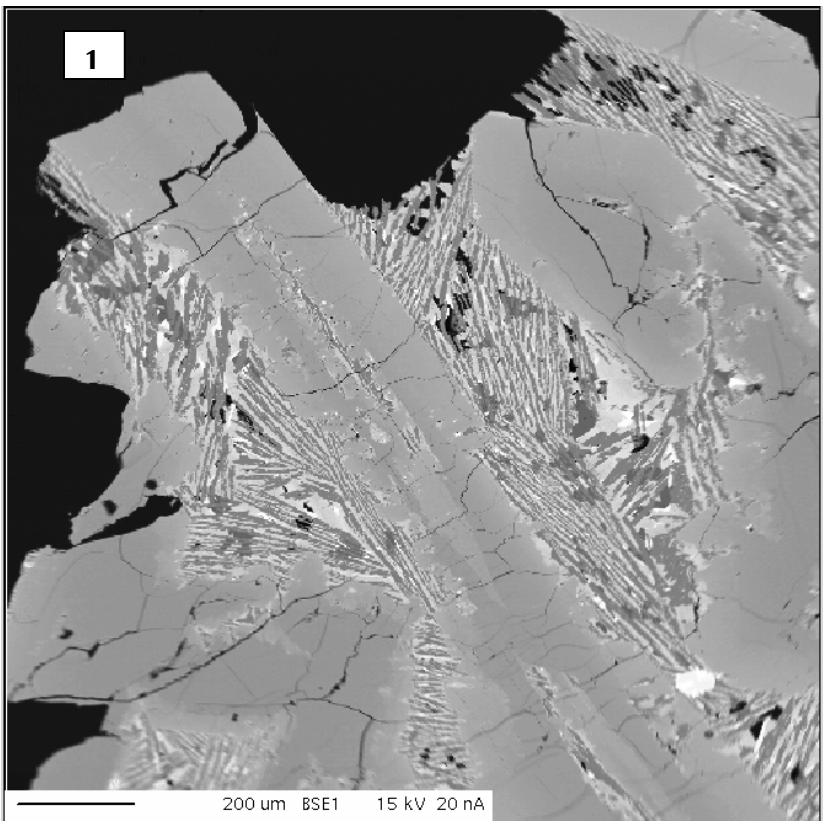

9
200 um BSE1 15 kV 20 nA

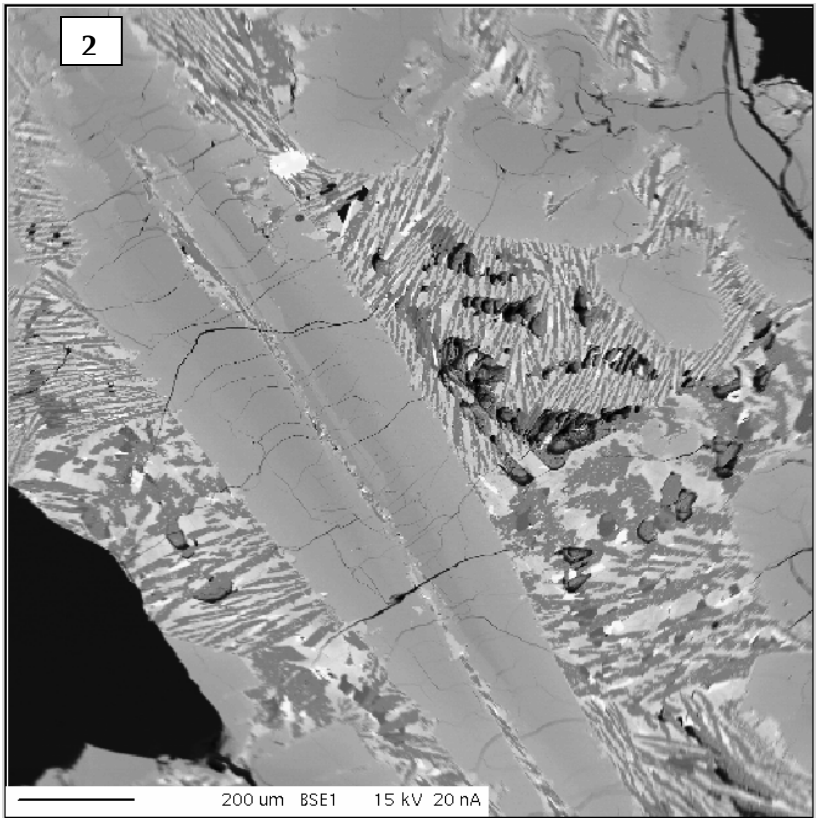

10
200 um BSE1 15 kV 20 nA

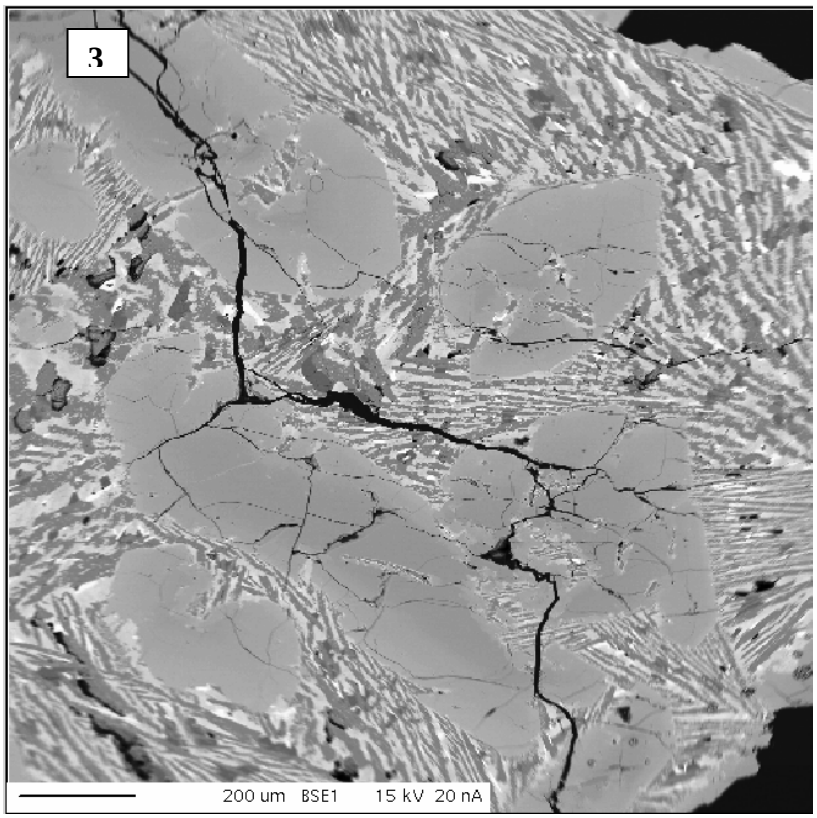

11
200 um BSE1 15 kV 20 nA

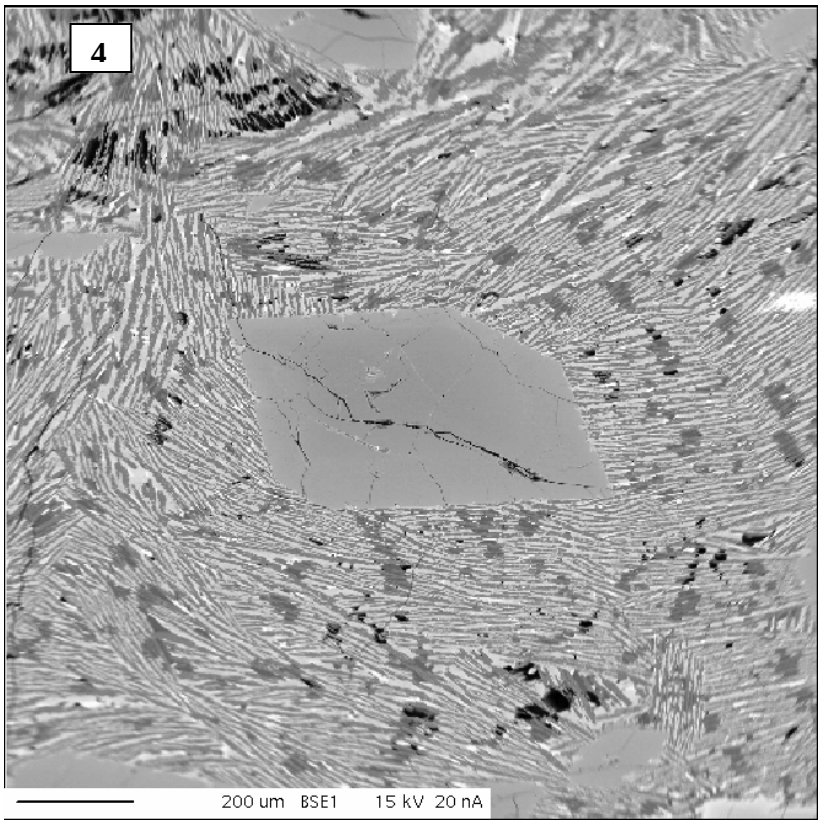


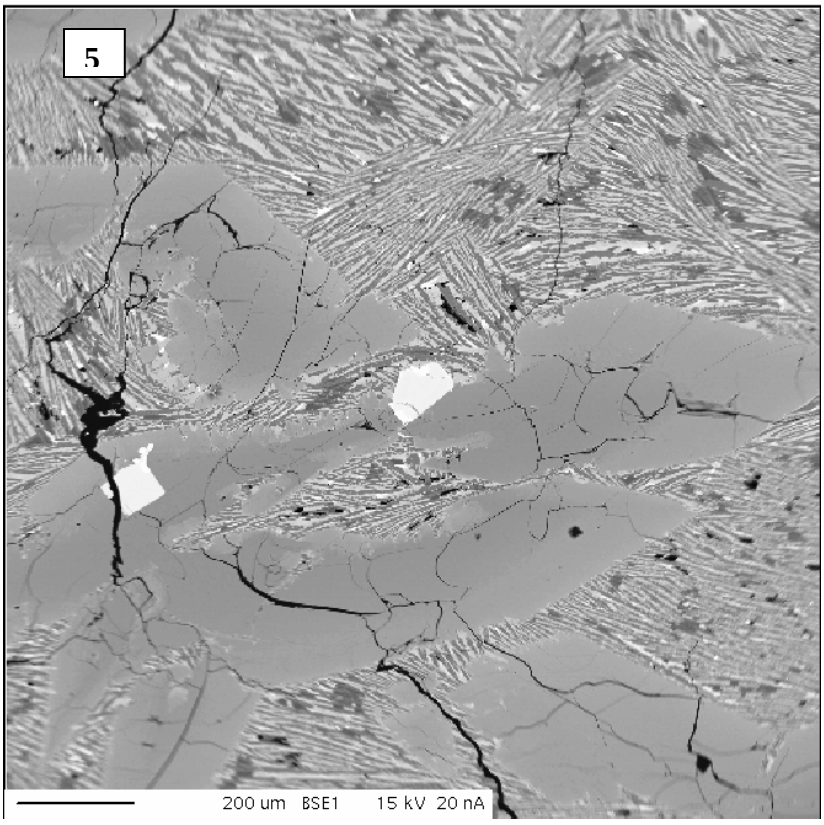
15499

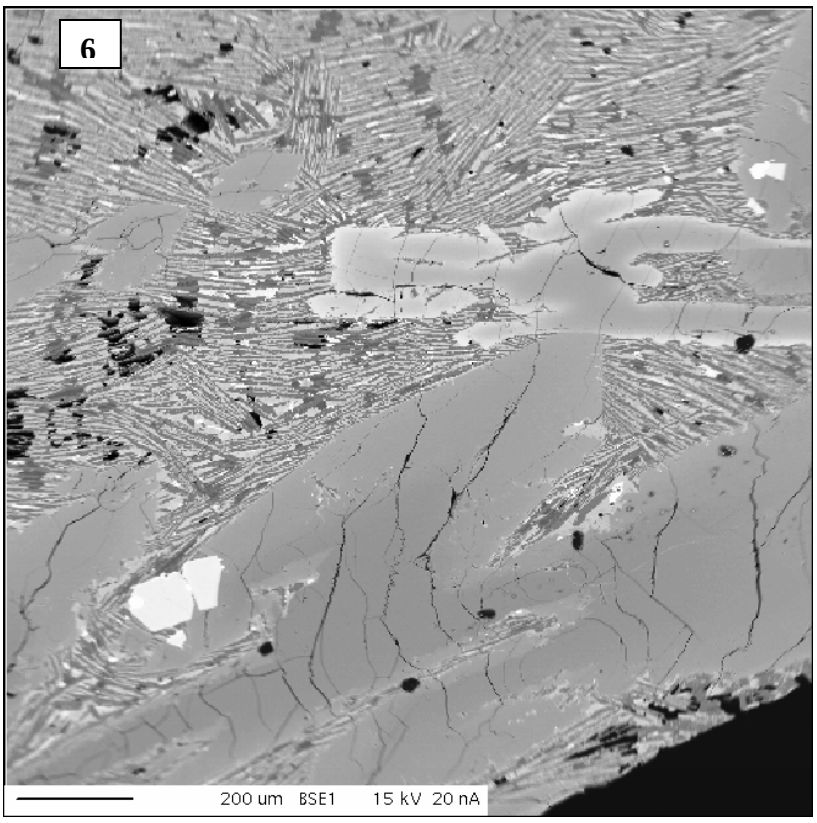

1
200 um BSE1 15 kV 20 nA

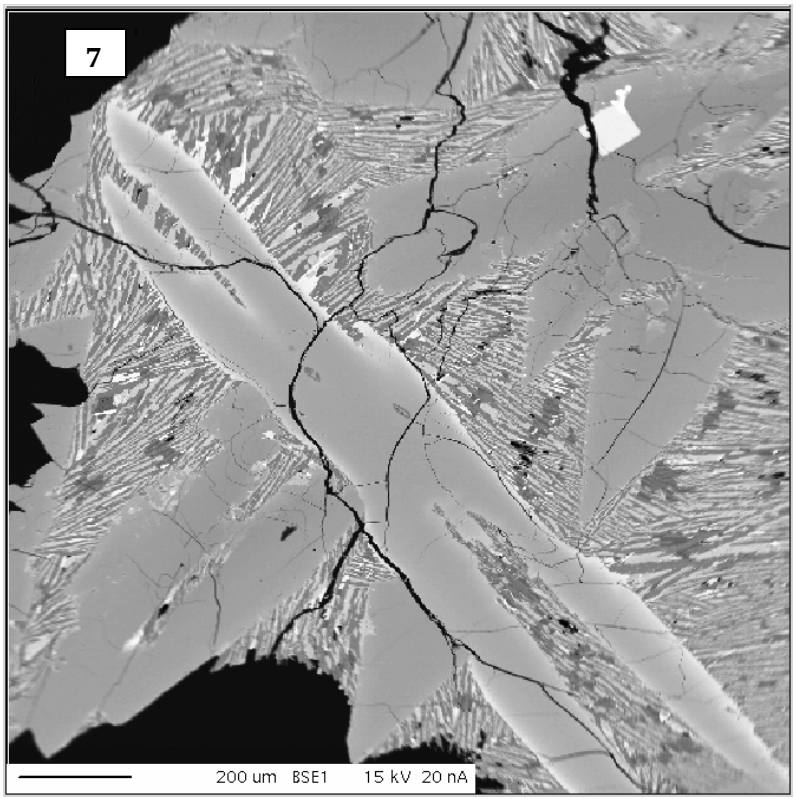

2
200 um BSE1 15 kV 20 nA

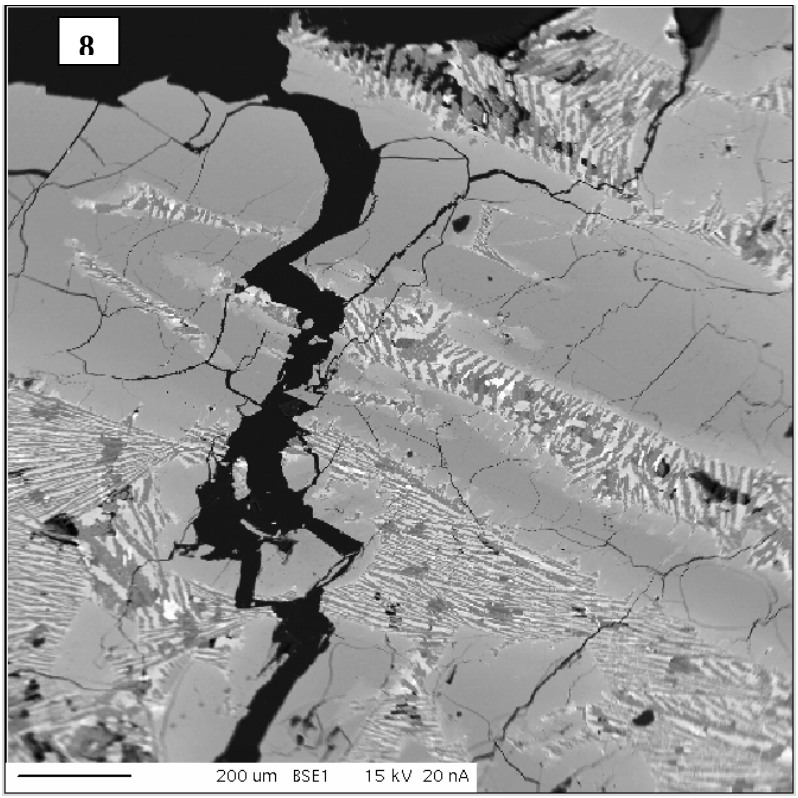

3
200 um BSE1 15 kV 20 nA

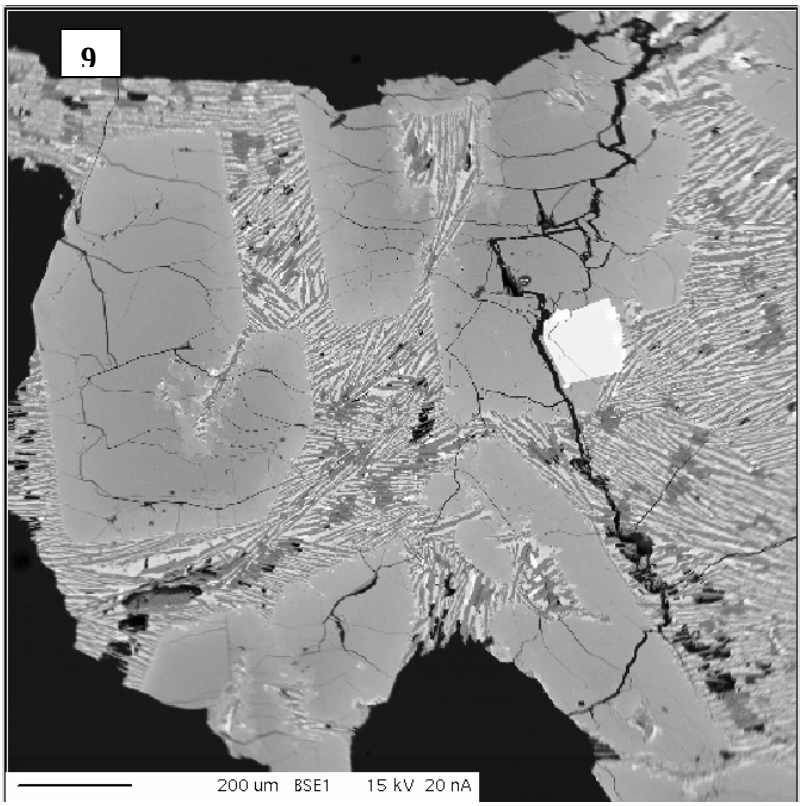

4
200 um BSE1 15 kV 20 nA


5
200 um BSE1 15 kV 20 nA


6
200 um BSE1 15 kV 20 nA


7
200 um BSE1 15 kV 20 nA


8
200 um BSE1 15 kV 20 nA


9
200 um BSE1 15 kV 20 nA

A-3 Mineral Data

All elements are in ppm, All Oxides are in wt. %.

Major- and Trace-Element Chemistry for Sample 15016 Pyroxenes

	a1	a2	a3	a4	a5	a6	a7	a8	a9	a10
Sc	56.5	89.7	39.8	90.4	54.4	52.0	71.3	76.8	60.6	82.1
Ti	3438	5640	2427	5610	4995	3659	6898	4829	3905	5343
V	371	558	280	576	82	323	104	494	385	544
Cr	4424	6594	2950	6528	1499	3818	1896	5952	4388	6025
Mn	1986	2750	1032	2728	2353	1719	2804	2637	1632	1805
FeO	13.8	18.7	6.8	19.1	20.1	12.0	23.7	18.4	11.4	12.0
Co	33.3	45.0	16.9	46.2	38.8	28.4	45.4	43.3	27.6	30.1
Ni	14.7	20.8	8.6	21.3	15.4	13.2	18.7	19.4	13.0	16.5
Ga	0.79	1.18	0.49	1.24	0.87	0.84	1.24	0.99	0.83	1.09
Rb	<0.034	<0.035	<0.022	<0.051	0.171	0.03	0.024	<0.034	<0.029	<0.039
Sr	1.38	3.58	1.68	3.14	2.60	5.76	3.84	1.74	2.77	4.37
Y	5.51	9.93	4.15	9.49	10.90	6.57	15.50	7.73	6.70	9.84
Zr	3.75	7.21	3.38	7.03	6.66	7.71	9.91	5.10	5.30	8.23
Nb	0.049	0.082	0.034	0.076	0.030	0.26	0.038	0.084	0.056	0.075
Ba	0.016	0.071	0.006	0.012	0.007	2.09	0.008	<0.011	<0.0058	<0.0051
La	0.048	0.131	0.061	0.113	0.119	0.277	0.156	0.060	0.101	0.165
Ce	0.304	0.69	0.34	0.63	0.627	0.965	0.913	0.377	0.514	0.774
Pr	0.064	0.164	0.078	0.166	0.152	0.172	0.203	0.092	0.126	0.185
Nd	0.547	1.18	0.592	1.14	1.08	1.14	1.66	0.669	0.942	1.35
Sm	0.339	0.726	0.334	0.555	0.717	0.557	0.959	0.489	0.502	0.796
Eu	0.039	0.054	0.033	0.06	0.061	0.076	0.097	0.042	0.059	0.073
Gd	0.684	1.35	0.591	1.21	1.32	0.939	1.96	0.898	0.861	1.48
Tb	0.142	0.266	0.12	0.277	0.285	0.185	0.406	0.187	0.186	0.292
Dy	1.02	1.76	0.777	1.68	1.93	1.26	2.89	1.33	1.25	1.94
Ho	0.233	0.406	0.177	0.377	0.419	0.265	0.624	0.306	0.272	0.41
Er	0.63	1.04	0.459	1.01	1.13	0.709	1.69	0.844	0.718	1.06
Yb	0.625	0.916	0.4	0.978	1.22	0.674	1.65	0.872	0.623	0.974
Lu	0.092	0.144	0.059	0.139	0.18	0.096	0.247	0.132	0.093	0.123
Hf	0.188	0.38	0.207	0.389	0.354	0.303	0.517	0.28	0.313	0.424
Ta	<0.0037	<0.0064	<0.0021	<0.0096	<0.0042	0.015	<0.0039	<0.0079	<0.0047	0.0071
Th	<0.0078	<0.014	<0.0039	<0.018	0.0079	0.023	<0.0092	<0.0060	<0.0061	<0.0069
U	<0.0060	<0.0073	<0.0043	<0.0088	<0.0040	<0.0051	<0.0062	<0.0067	<0.0039	<0.0056
SiO2	50.3	49.2	52.3	49.3	47.5	50.1	46.7	50.8	50.4	51.1
TiO2	0.64	0.94	0.36	0.86	0.87	0.758	1.25	0.79	0.74	0.95
Al2O3	2.09	2.68	0.88	2.55	1.47	2.26	1.40	2.27	2.11	2.80
Cr2O3	0.72	0.92	0.52	0.95	0.44	0.85	0.23	0.90	0.78	1.06
MgO	18.7	16.0	20.4	16.6	15.2	16.8	10.9	18.3	18.4	16.3
CaO	6.71	13.7	5.90	12.3	7.22	12.3	10.2	9.21	9.30	13.9
MnO	0.35	0.23	0.36	0.29	0.32	0.27	0.34	0.27	0.29	0.28
FeO	19.1	14.3	19.1	14.9	24.2	15.1	25.8	17.1	16.9	13.9
Na2O	0.01	0.01	0.02	0.03	0.02	0.03	0.06	0.03	0.02	0.04
Total	98.6	98.0	99.9	97.8	97.1	98.4	96.9	99.6	99.0	100.2

a11	a12	a13	a14	a16	a17	a18	a19	a20	a21
97.8	151.0	79.4	74.3	69.1	60.8	58.1	60.1	31.1	56.5
5988	12596	5489	5163	6139	5211	3470	3452	1729	5531
665	453	455	417	422	149	263	425	166	97
7638	8743	5549	4919	5080	2794	3875	4886	2473	1629
3252	8191	2751	2270	2140	2793	3357	2728	2183	2819
23.1	66.6	20.3	16.5	15.3	23.4	25.4	19.7	16.5	25.7
56.4	140.0	45.3	37.0	34.8	47.6	57.0	46.7	38.9	49.4
30.7	58.0	18.2	17.0	15.2	19.9	25.0	21.9	16.5	52.4
1.16	2.05	1.19	1.07	1.13	0.88	0.79	0.67	0.36	1.08
<0.038	<0.084	0.272	<0.048	0.058	<0.035	<0.039	<0.027	<0.027	0.131
2.31	4.06	10.10	4.71	6.46	1.31	1.08	0.89	0.39	6.99
9.31	18.40	12.60	10.20	8.55	8.04	5.43	4.85	2.22	16.30
7.06	13.10	20.40	11.20	11.60	4.69	2.54	2.98	0.91	21.80
0.086	0.24	1.49	0.32	0.67	0.049	0.053	0.062	0.024	0.79
0.011	0.995	57.1	2.19	3.49	<0.0073	0.013	<0.0098	0.0048	6.9
0.110	0.232	0.82	0.362	0.421	0.055	0.034	0.022	0.0093	0.941
0.54	0.935	2.56	1.28	1.39	0.307	0.184	0.181	0.048	2.66
0.129	0.191	0.427	0.249	0.252	0.081	0.041	0.049	0.015	0.455
1	1.63	2.78	1.56	1.51	0.632	0.399	0.37	0.133	2.78
0.578	0.946	1.11	0.741	0.749	0.383	0.244	0.27	0.071	1.26
0.058	0.088	0.136	0.091	0.09	0.035	0.029	0.024	0.014	0.15
1.09	1.89	1.77	1.45	1.18	0.895	0.551	0.442	0.227	2.18
0.252	0.422	0.365	0.279	0.241	0.2	0.132	0.118	0.049	0.427
1.66	3.19	2.51	1.94	1.55	1.31	0.846	0.795	0.39	2.91
0.373	0.723	0.514	0.411	0.328	0.327	0.212	0.178	0.095	0.654
1.08	1.97	1.36	1.08	0.911	0.93	0.583	0.551	0.26	1.75
0.966	2.42	1.29	0.985	0.862	0.98	0.622	0.526	0.401	1.74
0.154	0.352	0.176	0.154	0.134	0.14	0.095	0.087	0.061	0.241
0.434	0.661	0.652	0.483	0.417	0.228	0.154	0.181	0.076	0.774
<0.0051	<0.022	0.054	0.022	0.039	<0.0053	<0.0059	<0.0059	0.005	0.057
<0.014	<0.026	0.097	0.027	0.03	<0.0077	<0.0077	<0.0088	<0.0076	0.077
<0.0063	0.014	0.024	<0.0069	0.01	<0.0052	<0.0085	<0.0069	<0.0059	0.023
50.7	50.3	50.4	50.9	50.2	49.9	51.7	51.6	52.3	45.8
0.91	0.95	0.82	0.92	0.76	1.01	0.50	0.67	0.37	0.78
2.54	2.67	2.46	2.74	2.37	1.33	1.35	2.04	0.99	0.67
0.90	0.74	0.92	0.88	0.77	0.34	0.54	0.82	0.44	0.067
17.2	16.6	17.3	17.0	17.5	14.5	18.0	19.2	19.9	6.4
11.3	10.3	11.7	10.6	9.74	6.51	8.42	6.82	5.59	7.58
0.27	0.34	0.33	0.31	0.24	0.37	0.31	0.32	0.4	0.44
15.4	17.9	15.0	16.8	17.3	26.1	18.9	18.7	19.7	36.2
0.03	0.03	0.04	0.04	0.04	0.02	0.03	0.03	0.00	0.01
99.3	99.9	98.9	100.1	99.0	100.1	99.7	100.2	99.7	97.9

Major- and Trace-Element Chemistry for Sample 15555 Pyroxenes

	b1	b2	b3	b4	b5	b6	b7	b8	b9	b10
Sc	54.7	48.5	129	78.2	74.8	50.6	38	50	84.5	103
Ti	3643	2879	7691	5632	4426	3375	2627	3837	7663	8987
V	353	347	905	388	531	229	136	147	137	152
Cr	3978	4126	11721	4999	6182	3417	2344	2457	2446	2584
Mn	1636	2194	6907	2466	3270	2765	2342	2333	3566	2863
FeO	11.3	16.3	51.2	18.2	24.2	21.3	19	19.4	31.3	24.2
Co	29.3	43.9	140	44.5	65.1	51.7	45	43.7	60.5	50.3
Ni	13	20.5	63.7	17.9	29.1	19.7	17.2	16.5	19.6	18.7
Ga	0.762	0.558	1.47	1.03	0.845	0.616	0.423	0.573	1.64	1.56
Rb	<0.043	<0.050	<0.168	<0.058	<0.059	<0.048	<0.056	<0.048	0.168	<0.082
Sr	2.02	0.572	1.74	2.57	0.883	0.731	0.618	1.36	12.5	6.38
Y	5.95	3.46	8.78	8.49	5.37	4.21	3.31	5.29	20	17.2
Zr	3.42	1.64	3.73	6.17	2.68	1.98	1.33	2.86	33.3	13
Nb	0.038	0.037	0.099	0.058	0.054	0.039	0.024	0.034	1.45	0.074
Ba	<0.0057	<0.0097	<0.015	0.02	<0.012	<0.0086	0.0063	0.027	12.7	0.337
La	0.057	0.012	0.033	0.097	0.025	0.02	0.012	0.052	1.48	0.352
Ce	0.311	0.075	0.196	0.47	0.137	0.124	0.089	0.263	4.27	1.54
Pr	0.069	0.023	0.055	0.131	0.038	0.035	0.026	0.055	0.69	0.342
Nd	0.621	0.185	0.515	0.877	0.352	0.27	0.187	0.438	4.26	2.43
Sm	0.378	0.146	0.422	0.596	0.26	0.194	0.168	0.294	1.84	1.36
Eu	0.042	0.014	0.028	0.055	0.023	0.017	<0.0074	0.025	0.219	0.128
Gd	0.693	0.298	0.839	1.06	0.493	0.4	0.321	0.536	2.82	2.29
Tb	0.154	0.078	0.181	0.236	0.113	0.097	0.076	0.131	0.56	0.501
Dy	1.11	0.593	1.51	1.55	0.961	0.753	0.581	0.957	3.87	3.29
Ho	0.236	0.149	0.343	0.345	0.222	0.174	0.128	0.215	0.803	0.72
Er	0.66	0.4	0.937	0.902	0.625	0.475	0.374	0.582	2.17	1.81
Yb	0.605	0.468	1.16	0.898	0.688	0.516	0.401	0.651	2.23	1.74
Lu	0.093	0.072	0.188	0.128	0.112	0.078	0.066	0.09	0.297	0.25
Hf	0.185	0.089	0.204	0.308	0.138	0.107	0.08	0.146	1.03	0.679
Ta	<0.0075	<0.0059	<0.015	<0.0063	<0.010	<0.0075	<0.0055	<0.0057	0.096	0.0075
Th	<0.013	<0.0097	<0.040	<0.013	<0.015	<0.0095	<0.0075	<0.0097	0.156	0.017
U	<0.0051	<0.0059	<0.031	<0.0082	<0.015	<0.0070	<0.0059	<0.0058	0.029	<0.0095
SiO2	50.8	52.2	50.7	50.4	51.8	51.7	51.4	50.4	49.3	48.7
TiO2	0.90	0.54	0.90	0.95	0.64	0.49	0.45	0.76	1.23	1.47
Al2O3	1.75	1.34	2.36	2.22	1.61	1.14	0.91	1.37	1.62	1.94
Cr2O3	0.63	0.75	0.84	0.79	0.89	0.53	0.49	0.45	0.31	0.39
MgO	16.2	20.5	15.2	17.0	19.5	18.9	17.9	16.4	12.5	11.6
CaO	9.4	5.0	15.8	10.1	7.7	6.1	4.8	5.9	11.1	14.1
MnO	0.24	0.34	0.27	0.34	0.37	0.35	0.34	0.39	0.36	0.39
FeO	19.6	19.2	13.0	17.7	17.9	20.6	23.0	23.9	23.1	20.0
Na2O	0	0.02	0.03	0.04	0.05	0.02	0.01	0.03	0.03	0.04
Total	99.5	99.8	99.2	99.5	100.5	99.8	99.3	99.7	99.5	98.7

b11	b12	b13	b14	b15	b16	b17	b18	b19	b20	b21	b22
50.8	39.8	50.3	56.8	54	36.5	38	61.9	60.7	81.1	63.1	64.9
3252	2610	3751	4225	3903	2330	2567	4684	3583	6055	3674	3737
213	162	27.1	228	218	242	197	253	438	414	457	498
3544	2714	505	3618	3273	2450	2591	3695	4852	4867	5148	5388
3318	2605	1607	2710	2237	816	1544	2445	2424	1815	2563	2450
26.5	20.8	15.7	22.1	17.9	5.87	12	19.6	19.1	14	20.1	18.7
63.1	49.4	25.7	51.3	41.7	14.9	28.3	44.5	47.3	32.6	50.6	47.7
21.9	17.1	6.31	18.7	14.6	7.08	11	18	22	14.1	24.5	25.1
0.518	0.45	0.847	0.748	0.722	0.514	0.501	0.841	0.682	1.22	0.756	0.708
<0.083	<0.066	<0.028	<0.066	<0.045	<0.019	<0.031	<0.047	<0.038	<0.059	<0.043	<0.064
0.726	0.546	3.74	1.03	1.03	1.95	1.08	1.48	1.05	6.87	0.756	1.05
3.98	3.13	14.3	5.34	5.48	3.91	3.65	6.52	4.63	10.4	4.77	5.27
1.46	1.21	10.3	2.81	3.04	2.7	2.08	3.86	2.39	8.88	2.33	2.58
0.036	0.026	0.025	0.039	0.029	0.028	0.029	0.044	0.042	0.16	0.05	0.05
<0.0088	<0.0052	0.051	<0.0081	<0.0055	<0.0046	0.046	<0.0079	<0.0082	1.03	<0.010	<0.010
<0.012	0.01	0.204	0.026	0.033	0.063	0.032	0.052	0.035	0.26	0.024	0.031
0.09	0.062	1.07	0.196	0.201	0.297	0.169	0.253	0.146	1.06	0.135	0.192
0.024	0.017	0.245	0.045	0.05	0.07	0.044	0.071	0.046	0.219	0.024	0.042
0.212	0.167	1.88	0.334	0.388	0.562	0.296	0.503	0.351	1.65	0.324	0.427
0.129	0.106	1.11	0.237	0.318	0.324	0.218	0.403	0.249	0.828	0.222	0.308
0.022	0.014	0.099	0.023	0.026	0.037	0.018	0.029	0.017	0.118	0.023	0.024
0.316	0.302	1.99	0.557	0.606	0.559	0.386	0.754	0.499	1.56	0.487	0.588
0.084	0.065	0.386	0.108	0.126	0.111	0.099	0.179	0.108	0.322	0.103	0.133
0.587	0.507	2.72	0.925	1.03	0.78	0.658	1.21	0.809	2.02	0.806	0.908
0.156	0.13	0.584	0.205	0.219	0.154	0.144	0.275	0.191	0.421	0.186	0.206
0.448	0.363	1.5	0.583	0.639	0.399	0.411	0.73	0.503	1.14	0.554	0.546
0.537	0.388	1.55	0.676	0.69	0.404	0.412	0.683	0.53	0.963	0.626	0.562
0.08	0.064	0.227	0.111	0.097	0.056	0.064	0.117	0.082	0.135	0.095	0.091
0.087	0.057	0.493	0.178	0.16	0.148	0.103	0.185	0.128	0.373	0.142	0.129
<0.0083	<0.0050	0.0032	<0.0087	<0.0058	<0.0023	<0.0043	<0.0060	<0.0070	0.01	0.0065	<0.0053
<0.024	<0.0065	<0.0043	<0.0096	<0.011	<0.0055	<0.0084	<0.015	<0.010	<0.012	<0.017	<0.013
<0.0090	<0.0089	<0.0048	<0.0051	<0.011	<0.0043	<0.0045	<0.0089	<0.0073	<0.0087	<0.0073	<0.011
50.8	51.5	50.8	50.4	50.3	50.5	51.2	50.4	51.2	50.0	50.6	49.7
0.65	0.46	0.64	0.77	0.78	0.85	0.52	0.77	0.60	1.01	0.59	0.60
1.36	0.90	1.29	1.59	1.65	1.68	1.14	1.62	1.68	2.40	1.63	1.63
0.51	0.46	0.53	0.56	0.68	0.58	0.4	0.66	0.80	0.85	0.73	0.76
17.4	18.3	17.4	16.7	16.6	17.5	18.4	16.7	18.8	14.7	18.8	18.6
6.5	5.0	6.0	6.5	7.1	6.2	5.2	7.6	6.8	14.3	6.4	7.2
0.38	0.44	0.37	0.36	0.35	0.31	0.31	0.39	0.36	0.23	0.31	0.38
21.6	22.0	22.4	21.6	21.7	21.3	21.3	21.1	18.1	15.2	18.9	18.0
0.04	0.03	0.01	0.01	0	0.03	0.05	0.00	0.00	0.02	0.01	0.01
99.2	99.1	99.4	98.6	99.1	99.0	98.5	99.2	98.3	98.8	98.0	96.9

Major- and Trace-Element Chemistry for Sample 15475 Pyroxenes

	c1	c2	c3	c4	c5	c6	c7	c8	c9	c10	c11
Sc	102	110	72.9	35.8	49.9	110	102	85.9	32.2	80.5	71.4
Ti	5884	6182	3839	1856	2267	7017	6600	5582	1599	5011	3804
V	48.8	51.5	227	235	280	103	121	30.8	263	191	223
Cr	621	672	3691	2791	3998	1457	1828	364	5842	3333	3621
Mn	2824	2704	2854	1022	2060	3064	3106	3040	2255	2903	2792
FeO	28.6	27.9	25	7.93	16.7	30.8	31.3	32.7	19.3	27.3	24.6
Co	36	34.4	43.4	17.2	34.7	41.2	42.7	35.7	58.2	42.9	41.5
Ni	4.15	4	5.53	3.49	5.38	5.05	5.18	3.98	31.9	5.85	5.51
Ga	1.07	1.25	0.822	0.478	0.597	1.19	1.12	1.24	0.406	0.919	0.774
Rb	<0.043	<0.049	<0.058	0.087	<0.039	<0.039	<0.052	0.042	<0.052	<0.054	<0.051
Sr	6.23	7.3	1.59	6.82	1.13	6.12	5.76	9.66	1.27	2.98	1.91
Y	17	19.5	7.41	4.52	4.29	15.7	14.1	25	1.97	9.38	7.24
Zr	10.5	13.3	3.67	6.91	2.3	9.64	9.09	23	1.76	4.94	3.59
Nb	0.023	0.029	0.039	0.376	0.048	0.026	0.047	0.404	0.12	0.04	0.044
Ba	0.0098	0.016	<0.0095	7.02	0.075	0.01	0.592	4.34	0.619	<0.0083	<0.0081
La	0.258	0.313	0.057	0.393	0.035	0.209	0.246	0.637	0.055	0.095	0.046
Ce	1.38	1.68	0.328	1.17	0.181	1.15	1.14	2.68	0.189	0.476	0.324
Pr	0.311	0.409	0.074	0.181	0.044	0.278	0.254	0.546	0.032	0.122	0.076
Nd	2.45	2.99	0.6	1.03	0.34	2.04	1.98	3.89	0.173	0.893	0.594
Sm	1.35	1.6	0.344	0.426	0.226	1.23	1.09	2.09	0.123	0.59	0.414
Eu	0.136	0.172	0.042	0.072	0.027	0.116	0.1	0.206	0.015	0.061	0.044
Gd	2.33	2.76	0.853	0.646	0.503	2.06	1.83	3.45	0.172	1.11	0.786
Tb	0.483	0.55	0.168	0.128	0.093	0.421	0.366	0.688	0.03	0.231	0.179
Dy	3.1	3.72	1.29	0.851	0.747	2.98	2.58	4.64	0.305	1.62	1.28
Ho	0.673	0.786	0.296	0.19	0.162	0.617	0.554	1.02	0.07	0.381	0.293
Er	1.78	2.08	0.855	0.462	0.481	1.63	1.51	2.66	0.219	1.03	0.836
Yb	1.9	2.09	0.892	0.474	0.494	1.68	1.55	2.6	0.286	1.05	0.8
Lu	0.287	0.322	0.13	0.07	0.073	0.274	0.248	0.417	0.041	0.166	0.124
Hf	0.459	0.679	0.167	0.221	0.117	0.462	0.435	0.886	0.058	0.239	0.164
Ta	0.0056	<0.0062	<0.0067	0.024	<0.0083	<0.0066	0.0042	0.028	0.007	<0.0078	<0.0041
Th	<0.0083	<0.0085	<0.0086	0.036	<0.013	<0.0093	<0.012	0.051	<0.014	<0.012	<0.0070
U	<0.0092	<0.0075	<0.0097	0.012	<0.0058	<0.0062	<0.0058	<0.0069	0.0053	<0.012	<0.0080
SiO2	47.7	47.4	50.1	51.2	51.5	45.6	46.7	46.0	51.4	47.1	47.7
TiO2	0.87	1.19	0.65	0.39	0.35	1.06	1.00	0.93	0.23	0.88	0.65
Al2O3	0.82	1.29	1.50	1.38	1.37	1.24	1.22	0.72	0.97	1.23	1.44
Cr2O3	0.09	0.10	0.56	0.68	0.70	0.33	0.42	0.05	0.80	0.48	0.57
MgO	6.9	6.7	14.9	19.8	19.7	8.2	9.0	3.7	23.7	11.0	14.6
CaO	11.2	12.2	7.6	5.9	6.0	12.4	11.8	10.3	2.9	10.0	8.3
MnO	0.41	0.43	0.40	0.29	0.35	0.38	0.38	0.41	0.25	0.36	0.38
FeO	31.1	29.9	23.8	19.1	19.3	27.5	26.6	36.5	18.2	26.7	23.9
Na2O	0.04	0.04	0.02	0.02	0.02	0.04	0.02	0.02	0.03	0.03	0.02
Total	99.1	99.2	99.5	98.8	99.3	96.8	97.2	98.6	98.4	97.8	97.6

c12	c13	c14	c15	c16	c17	c18	c19	c20	c21	c22	c23
63.4	82	51.6	44.5	31.6	36.5	36.9	39.3	93.2	91.7	70	97.3
3625	5197	2306	2264	1477	1614	1693	4494	5442	5238	2948	6415
189	35.8	2.56	2.8	263	297	291	6.26	28.2	27.6	3.96	84.7
3147	505	20.2	22.6	6520	6943	6438	65.5	407	409	35.2	1388
2397	2835	3940	3839	2238	2214	2370	2122	3300	3244	4676	3871
22.1	31	44.4	45.8	18.9	18.7	19.9	29.2	36.4	36	44.4	38.2
36.1	33.1	15.1	17.6	60.5	60.1	57.2	14.6	35.6	35.4	21.3	50.3
4.96	3.39	<0.151	0.376	55.9	52.5	21.6	0.305	3.27	3.47	0.393	5.94
0.725	1.17	1.35	2	0.327	0.352	0.39	2.08	1.4	1.41	0.825	1.06
<0.044	<0.029	0.148	0.121	<0.057	<0.045	<0.064	<0.034	<0.031	0.035	0.058	<0.062
2.87	5.49	6.71	5.4	0.197	0.207	0.276	21.9	7.36	10.1	3.22	5.36
7.22	20.6	204	373	1.56	1.9	1.95	56.5	30	30.6	137	13.9
3.83	13.5	54.8	156	0.668	0.828	0.863	62.8	20.4	21.2	29.2	8.63
0.044	0.029	0.34	0.157	0.054	0.066	0.059	0.081	0.068	0.124	0.046	0.139
0.209	0.011	3.37	2.54	<0.0055	<0.010	<0.0057	0.08	0.047	2.66	0.109	1.98
0.099	0.29	1.2	1.56	<0.0058	0.0079	<0.0085	1.9	0.492	1.05	0.404	0.335
0.48	1.44	5.83	9.54	0.02	0.041	0.032	9.11	2.41	3.95	2.43	1.21
0.114	0.337	1.44	2.61	<0.0059	0.0087	0.0081	2.05	0.563	0.819	0.652	0.217
0.936	2.51	11.7	22.2	0.066	0.066	0.052	13.6	3.96	5.5	6.17	1.72
0.568	1.48	7.77	15.4	0.045	<0.044	0.058	6.78	2.19	2.65	4.56	0.922
0.056	0.132	0.637	1.02	<0.0079	<0.011	<0.0095	0.608	0.212	0.262	0.328	0.092
0.903	2.62	17.4	33	0.102	0.162	0.182	9.86	3.86	4.25	10.2	1.76
0.184	0.559	3.97	7.76	0.037	0.035	0.037	1.84	0.77	0.833	2.44	0.354
1.26	3.69	31.1	58.5	0.227	0.335	0.331	11.4	5.36	5.72	19.5	2.4
0.3	0.833	7.82	14.2	0.066	0.077	0.072	2.29	1.17	1.23	5.23	0.554
0.803	2.22	23.6	41.6	0.171	0.227	0.276	5.73	3.2	3.32	16.4	1.53
0.742	2.35	26.9	40.5	0.212	0.304	0.266	5.04	3.44	3.31	21.1	1.66
0.123	0.377	4.24	5.79	0.04	0.048	0.049	0.756	0.544	0.507	3.53	0.268
0.154	0.624	2	6.35	0.026	0.049	0.054	2.91	0.93	0.908	1.26	0.376
<0.0040	<0.0072	0.014	0.013	<0.0085	<0.0088	<0.0052	0.0079	<0.0066	0.008	<0.0065	<0.0088
<0.012	<0.0099	0.037	0.013	<0.016	<0.0069	<0.015	<0.0092	0.0085	0.072	<0.011	0.023
<0.0096	<0.0074	0.0088	<0.011	0.0083	0.0068	<0.0075	0.0069	0.0083	0.02	<0.0070	<0.011
48.9	45.8	45.5	45.9	53.9	53.6	53.7	47.6	46.5	47.2	45.6	47.6
0.68	0.79	0.42	0.43	0.25	0.24	0.26	1.20	0.96	0.87	0.48	1.01
1.07	0.70	0.30	0.34	0.90	0.97	1.03	1.11	0.95	0.87	0.28	0.96
0.48	0	0.02	0	0.85	0.79	0.92	0.12	0.09	0.08	0.00	0.10
12.1	3.7	1.4	1.1	24.7	25.0	23.6	7.2	3.0	3.9	1.5	6.5
9.3	8.6	6.1	5.4	2.6	2.6	3.1	11.5	9.8	11.5	6.1	10.9
0.44	0.48	0.50	0.53	0.30	0.25	0.27	0.41	0.42	0.47	0.62	0.51
26.0	38.3	44.9	45.9	17.2	17.3	18.0	30.9	37.9	35.1	43.9	31.5
0.04	0.02	0.00	0.00	0.00	0.01	0.02	0.03	0.02	0.02	0.00	0.03
98.9	98.5	99.1	99.7	100.7	100.8	100.8	100.1	99.7	99.9	98.4	99.1

Major- and Trace-Element Chemistry for Sample 15499 Pyroxenes

	d1	d2	d3	d4	d5	d6	d7	d8	d9	d10	d11
Sc	74.9	168	108	112	113	106	125	41.9	81.8	108	87.8
Ti	3800	8248	7680	8479	8697	6922	7707	2026	3929	5989	4933
V	454	1055	348	322	411	434	475	290	563	583	538
Cr	7908	18636	6243	5771	7269	8054	8023	5547	10777	10093	9119
Mn	2472	6128	2048	1988	1887	2276	2324	2020	3618	2845	2551
FeO	20.5	52.4	17.3	17	15.8	18.8	19.3	17.5	30.7	23.2	21.4
Co	48.5	126	33.6	32.5	31.6	39	38.9	47.3	84.1	53.5	49.2
Ni	13.8	38.6	7.88	7.3	6.85	9.41	9.58	20.2	43.2	15.4	13.6
Ga	1.03	2.25	1.98	2.09	2.21	1.79	2.07	0.529	0.999	1.59	1.22
Rb	<0.062	<0.134	<0.054	<0.060	<0.051	<0.084	<0.064	<0.040	<0.088	<0.074	<0.054
Sr	1.13	2.48	5.98	6.82	6.6	8.36	6.3	1.1	0.982	4	1.65
Y	8.18	16.4	20.9	22.4	22.4	18.8	22.2	3.61	7.67	14.9	9.81
Zr	6.9	12.6	26.4	31.2	33.8	22.8	26.3	2.76	4.38	14.6	11.4
Nb	0.092	0.227	0.085	0.103	0.146	0.276	0.124	0.092	0.112	0.123	0.103
Ba	<0.0094	0.308	0.018	0.044	<0.012	1.8	0.059	0.495	<0.017	0.08	0.045
La	0.066	0.138	0.376	0.464	0.47	0.513	0.393	0.067	0.039	0.232	0.101
Ce	0.332	0.606	1.93	2.31	2.31	2.08	2.11	0.206	0.215	1.15	0.519
Pr	0.085	0.159	0.453	0.525	0.508	0.462	0.465	0.038	0.062	0.267	0.112
Nd	0.609	1.23	3.45	3.87	3.92	3.34	3.64	0.295	0.459	1.87	0.969
Sm	0.473	0.766	1.78	2.13	2.03	1.63	1.87	0.166	0.379	1.12	0.606
Eu	0.043	0.073	0.153	0.143	0.175	0.165	0.141	0.016	0.03	0.094	0.038
Gd	0.818	1.71	3.22	3.52	3.55	2.72	3.37	0.332	0.732	1.91	1.16
Tb	0.198	0.349	0.609	0.677	0.702	0.536	0.649	0.077	0.16	0.414	0.256
Dy	1.41	2.73	3.87	4.27	4.33	3.62	4.15	0.645	1.38	2.59	1.76
Ho	0.343	0.684	0.863	0.952	0.943	0.788	0.915	0.134	0.325	0.616	0.418
Er	0.942	1.98	2.17	2.45	2.26	1.95	2.29	0.413	0.791	1.62	1.04
Yb	1.01	2.11	2.02	1.93	1.97	1.82	2.23	0.47	0.893	1.63	1.23
Lu	0.145	0.313	0.281	0.278	0.285	0.255	0.31	0.082	0.145	0.222	0.167
Hf	0.384	0.584	1.26	1.53	1.75	1.08	1.28	0.12	0.234	0.755	0.692
Ta	<0.010	<0.029	<0.0090	0.014	0.016	0.02	<0.0090	<0.0067	<0.018	<0.0092	0.0084
Th	<0.011	<0.026	<0.019	<0.016	0.011	0.03	<0.016	<0.012	<0.022	<0.014	<0.019
U	<0.0094	<0.021	<0.013	<0.011	<0.011	<0.016	<0.010	<0.012	<0.015	<0.013	<0.012
SiO2	50.3	47.9	47.8	48.0	47.1	48.3	48.1	52.2	52.6	49.2	49.5
TiO2	0.60	1.23	1.34	1.45	1.57	1.16	1.36	0.39	0.34	0.89	0.74
Al2O3	2.52	4.41	4.46	4.67	5.17	4.23	4.58	1.67	1.52	3.20	3.14
Cr2O3	1.21	1.17	0.84	1.09	0.94	1.02	0.92	1.00	1.00	1.37	1.18
MgO	18.8	13.2	12.5	12.7	11.8	12.9	12.0	22.4	23.2	15.1	17.5
CaO	7.1	14.5	15.5	16.1	15.7	16.0	16.2	3.6	3.2	13.5	8.1
MnO	0.29	0.29	0.33	0.28	0.24	0.29	0.25	0.33	0.27	0.25	0.32
FeO	18.3	15.5	15.8	14.7	15.9	15.2	15.9	17.8	17.1	15.5	17.9
Na2O	0.02	0.04	0.06	0.07	0.05	0.05	0.07	0.02	0.01	0.03	0.03
Total	99.1	98.3	98.6	99.1	98.5	99.1	99.2	99.4	99.3	99.0	98.5

d12	d13	d14	d15	d16	d17	d18	d19	d20	d21	d22
103	52.9	21.6	100	98	49.8	94.6	103	54.5	105	52.9
6406	2629	1409	7947	7871	2326	6910	6453	2622	6993	2495
538	406	99.9	257	343	345	363	514	404	391	415
9585	7672	1954	5040	7191	6526	7362	9322	7938	7478	7595
2338	2220	416	1962	1859	2314	1828	2042	2413	1836	2142
19	19.1	3.37	16.9	14.8	19.7	14.6	16.1	21	14.8	18.5
42.7	57.2	7.69	33.1	30.4	54.1	30	36.1	63	30.5	56.4
11.1	41.5	1.98	6.72	7.52	23.1	7.62	9.66	43.4	8.44	43.2
1.57	0.69	0.382	1.97	1.93	0.653	1.7	1.73	0.67	1.96	0.612
<0.064	<0.058	<0.014	<0.053	<0.089	<0.048	<0.054	<0.051	<0.074	<0.060	<0.054
3.53	0.449	1.28	7.17	6.28	0.407	5.33	4.84	0.366	7.01	0.325
15	4.14	3.93	22	20.3	4.01	18.2	17.1	3.87	20.1	3.68
20.5	3.75	4.95	27.9	29.4	2.37	25.4	20.7	2.91	28.3	2.89
0.13	0.109	0.024	0.108	0.107	0.069	0.106	0.121	0.082	0.366	0.078
0.012	0.163	0.013	0.209	<0.015	<0.013	0.098	<0.0093	<0.012	1.59	<0.0070
0.222	0.037	0.079	0.45	0.42	0.016	0.34	0.265	0.021	0.903	0.01
1.14	0.16	0.392	2.24	2.1	0.09	1.73	1.44	0.093	3.26	0.092
0.29	0.036	0.088	0.518	0.498	0.025	0.392	0.343	0.028	0.622	0.021
2.12	0.28	0.678	3.62	3.49	0.21	3.01	2.49	0.214	4.13	0.19
1.17	0.184	0.329	2.02	1.92	0.178	1.58	1.39	0.107	1.91	0.134
0.088	0.016	0.025	0.151	0.151	0.014	0.133	0.125	<0.014	0.157	0.011
1.99	0.371	0.599	3.41	3.09	0.346	2.62	2.41	0.334	3.17	0.335
0.386	0.088	0.109	0.649	0.568	0.086	0.513	0.505	0.08	0.586	0.067
2.73	0.739	0.763	4.2	3.91	0.666	3.49	3.34	0.614	3.92	0.599
0.622	0.17	0.164	0.891	0.838	0.154	0.724	0.702	0.161	0.858	0.15
1.61	0.484	0.41	2.35	2.08	0.44	1.81	1.8	0.456	2.16	0.421
1.45	0.584	0.381	2	1.85	0.504	1.74	1.7	0.472	1.79	0.509
0.213	0.096	0.052	0.283	0.286	0.095	0.239	0.26	0.09	0.252	0.089
1.11	0.185	0.249	1.38	1.44	0.121	1.31	1.18	0.165	1.37	0.184
<0.010	<0.0090	0.0025	<0.013	<0.015	<0.0071	0.012	0.016	<0.010	0.039	<0.0094
<0.012	<0.019	<0.0022	0.019	<0.028	<0.024	<0.019	0.016	0.01	0.035	<0.011
<0.010	<0.011	<0.0028	<0.011	<0.019	<0.0075	<0.014	<0.014	<0.011	<0.014	<0.0067
49.2	52.4	52.4	47.9	48.3	52.3	48.5	48.3	52.4	48.4	52.5
0.93	0.38	0.37	1.29	1.23	0.38	1.25	1.16	0.43	1.11	0.40
3.41	1.65	1.58	4.49	4.70	1.60	4.47	4.19	1.65	4.51	1.82
1.30	1.01	1.08	0.86	1.17	1.01	1.39	1.31	0.98	1.01	1.26
15.5	23.1	23.2	11.9	13.2	21.8	14.1	13.6	22.4	12.9	23.7
11.7	3.4	3.2	16.2	15.5	4.0	14.1	14.3	3.4	16.3	3.0
0.33	0.26	0.34	0.26	0.26	0.28	0.30	0.28	0.30	0.25	0.3
16.2	17.0	17.4	15.6	14.4	18.4	14.9	15.3	18.1	14.0	17.3
0.04	0.02	0.01	0.02	0.03	0.02	0.04	0.04	0.03	0.06	0.01
98.6	99.3	99.6	98.5	98.8	99.8	99.1	98.5	99.7	98.6	100.3

Major- and Trace-Element Chemistry for Sample 15016 Plagioclase

	pa1	pa2	pa3	pa5	pa6	pa7	pa8	pa9	pa10	pa12
Sc	3.17	3.02	3.05	2.85	1.74	2.1	3.02	2.91	3.01	3.09
Ti	296	350	275	352	201	290	418	321	278	294
V	0.747	3.05	1.6	2.98	1.62	2.72	3.25	2.16	2.35	1.56
Cr	3.45	6.32	4.78	7.24	2.99	6.36	8.84	5.31	3.06	4.29
Mn	69.7	73.5	66.3	72.5	42.7	53.4	79.7	69	66.8	68.1
FeO	0.647	0.618	0.514	0.609	0.36	0.44	0.668	0.562	0.522	0.554
Co	1.12	1.07	0.929	1.1	0.712	0.747	0.91	1.03	0.999	0.909
Ni	0.464	0.615	0.471	<0.399	0.316	0.24	0.498	0.351	1.07	0.359
Ga	11.7	6.74	9.67	6.31	4.22	4.62	6.34	8.48	7.93	9.69
Rb	0.096	<0.103	<0.098	<0.080	<0.051	<0.055	<0.083	<0.075	<0.097	<0.105
Sr	446	249	309	239	136	162	240	277	261	320
Y	0.338	0.192	0.22	0.212	0.158	0.138	0.192	0.2	0.182	0.242
Zr	<0.025	<0.047	<0.023	0.034	0.111	<0.020	<0.045	0.109	0.038	<0.041
Nb	<0.020	<0.018	<0.021	<0.032	0.017	<0.015	<0.018	0.017	<0.016	<0.023
Ba	47.9	18.5	24.5	19.5	9.4	11.7	18.9	19.7	16.9	26.7
La	0.475	0.236	0.273	0.235	0.142	0.185	0.266	0.237	0.195	0.285
Ce	1.12	0.632	0.661	0.609	0.356	0.418	0.66	0.534	0.463	0.685
Pr	0.137	0.068	0.086	0.071	0.04	0.052	0.072	0.074	0.061	0.089
Nd	0.6	0.349	0.402	0.296	0.164	0.201	0.423	0.25	0.329	0.356
Sm	0.188	<0.128	0.089	<0.117	<0.048	0.054	<0.098	<0.090	0.109	<0.094
Eu	2.88	1.42	1.85	1.4	0.823	0.907	1.4	1.7	1.57	1.99
Gd	0.145	0.095	0.083	<0.089	0.043	0.046	<0.061	<0.083	0.103	0.073
Tb	0.022	<0.026	<0.014	<0.019	<0.0091	<0.0084	<0.013	<0.014	<0.019	<0.017
Dy	<0.072	0.063	<0.052	<0.047	<0.034	0.024	0.046	0.045	<0.045	<0.070
Ho	0.021	<0.017	<0.017	0.014	<0.0087	<0.012	0.0096	<0.014	<0.014	<0.015
Er	<0.038	<0.053	<0.055	<0.032	<0.014	<0.035	<0.023	<0.045	<0.038	<0.045
Yb	0.067	<0.090	<0.067	<0.178	<0.049	<0.057	<0.059	<0.062	<0.044	<0.097
Lu	<0.013	<0.015	<0.0088	<0.015	<0.0054	<0.0059	<0.011	<0.017	0.011	<0.013
Hf	<0.052	<0.051	<0.030	<0.065	<0.017	<0.028	<0.040	<0.036	<0.059	<0.064
Ta	<0.013	<0.018	<0.013	<0.019	<0.0081	<0.0094	0.012	<0.010	<0.016	<0.011
Th	<0.027	<0.030	<0.014	<0.041	<0.015	<0.017	<0.044	<0.015	<0.027	<0.022
U	<0.017	<0.029	<0.021	<0.019	<0.0072	<0.012	<0.015	<0.011	<0.015	<0.017
SiO2	46.0	45.3	45.1	46.8	44.9	47.5	48.4	44.7	45.3	46.1
Al2O3	32.1	33.1	33.2	32.3	32.2	32.1	31.2	33.4	32.9	32.9
CaO	18.0	18.5	18.6	18.0	18.1	17.5	16.7	18.5	18.4	18.2
FeO	0.58	0.50	0.54	0.80	0.71	0.75	0.79	0.68	0.59	0.73
Na2O	1.00	0.76	0.77	1.05	0.97	1.25	1.33	0.76	0.87	0.98
K2O	0.07	0.03	0.02	0.00	0.03	0.02	0.03	0.02	0.03	0.06
Total	97.7	98.3	98.2	98.9	97.0	99.1	98.4	98.0	98.0	99.0

Major- and Trace-Element Chemistry for Sample 15555 Plagioclase

	pb1	pb2	pb3	pb4	pb5	pb6	pb7	pb8	pb9	pb10	pn11	pb12
Sc	3.5	3.37	3.34	3.21	3.19	3	2.95	3.03	3.01	2.96	2.91	2.89
Ti	373	332	317	339	317	299	341	335	348	308	291	303
V	0.842	0.598	2.77	2.7	3.61	6.06	3.81	4.04	1.82	4.69	5.43	3.73
Cr	2.41	3.57	5.14	6.01	8.9	12.1	7	10	5.55	13.9	9.76	7.66
Mn	70.4	74.2	67.5	66.7	69.8	70	67.4	75.2	67.8	74.6	72.1	70
FeO	0.599	0.756	0.486	0.503	0.522	0.512	0.48	0.55	0.556	0.543	0.519	0.544
Co	1.44	1.55	1.08	1.13	1.16	1.27	1.13	1.16	1.17	1.24	1.12	1.18
Ni	<0.386	<0.484	0.657	0.908	0.551	0.748	<0.516	0.574	<0.534	0.919	0.514	<0.397
Ga	10.7	13.3	8.53	8.59	7.78	6.34	7.56	7.38	8.87	7.47	6.67	7.53
Rb	0.177	0.147	<0.165	<0.163	<0.195	<0.158	<0.156	<0.128	<0.088	<0.146	<0.132	0.151
Sr	385	503	280	285	250	212	239	232	311	234	215	252
Y	0.237	0.371	0.183	0.155	0.149	0.123	0.151	0.152	0.192	0.153	0.139	0.157
Zr	<0.028	0.043	<0.030	<0.038	<0.031	<0.025	0.031	<0.024	<0.027	0.023	0.022	<0.035
Nb	<0.013	<0.017	<0.014	<0.015	<0.015	<0.018	<0.018	<0.018	<0.015	<0.019	<0.018	<0.016
Ba	34.1	56.9	18	18.7	16.6	12.4	13.3	14.2	22.9	13	11.1	16.5
La	0.345	0.545	0.217	0.204	0.18	0.227	0.183	0.24	0.257	0.179	0.18	0.185
Ce	0.785	1.27	0.487	0.493	0.476	0.388	0.412	0.46	0.588	0.44	0.393	0.479
Pr	0.088	0.152	0.064	0.051	0.053	0.046	0.064	0.062	0.077	0.054	0.047	0.063
Nd	0.354	0.65	0.255	0.275	0.337	0.264	0.228	0.302	0.359	0.267	0.264	0.324
Sm	<0.091	0.141	<0.083	<0.079	<0.093	<0.103	<0.078	0.072	0.108	<0.107	<0.073	<0.089
Eu	2.42	3.38	1.61	1.62	1.31	1.09	1.35	1.28	1.8	1.31	1.15	1.45
Gd	<0.085	0.112	<0.101	<0.078	<0.096	<0.110	<0.070	0.084	<0.087	<0.116	0.089	<0.078
Tb	<0.029	0.022	<0.015	<0.015	<0.018	<0.017	<0.019	<0.015	<0.019	<0.017	<0.017	<0.024
Dy	0.082	<0.071	<0.057	<0.069	<0.060	<0.044	0.063	<0.053	<0.057	<0.059	<0.057	<0.063
Ho	<0.027	0.017	<0.012	0.015	<0.018	<0.015	<0.013	<0.017	<0.018	<0.015	<0.013	<0.015
Er	<0.035	<0.035	0.045	<0.064	<0.033	<0.033	<0.044	<0.032	<0.040	<0.040	<0.041	<0.041
Yb	<0.082	<0.095	<0.079	<0.103	<0.063	<0.116	<0.095	<0.129	<0.094	<0.086	<0.130	<0.093
Lu	<0.015	<0.011	<0.013	0.012	<0.024	<0.018	<0.013	<0.022	<0.0088	<0.019	<0.013	<0.020
Hf	<0.051	<0.050	<0.063	<0.043	<0.052	<0.036	<0.082	<0.056	<0.030	<0.046	<0.049	<0.033
Ta	<0.015	<0.017	<0.021	<0.021	<0.016	<0.0099	<0.017	<0.019	<0.023	<0.017	<0.021	<0.015
Th	<0.033	<0.040	<0.039	<0.027	<0.033	<0.032	<0.036	<0.028	<0.028	<0.022	<0.040	<0.023
U	<0.023	<0.024	<0.026	<0.014	0.014	<0.018	<0.025	<0.028	<0.023	<0.021	<0.026	<0.019
SiO2	46.8	48.2	45.9	45.6	45.8	45.4	45.1	46.1	45.4	45.0	44.6	44.0
Al2O3	32.9	31.6	33.1	33.4	33.3	32.8	33.1	33.2	33.1	33.5	32.7	32.9
CaO	17.7	16.9	18.4	18.3	18.4	18.1	18.2	18.4	18.1	18.8	18.2	18.6
FeO	0.62	0.81	0.58	0.49	0.49	0.52	0.45	0.59	0.55	0.49	0.53	0.50
Na2O	1.22	1.36	0.93	0.90	0.80	0.92	0.86	0.88	1.00	0.77	1.08	0.81
K2O	0.06	0.14	0.05	0.05	0.01	0.02	0.03	0.02	0.01	0.01	0.01	0.02
Total	99.3	99.0	99.0	98.7	98.8	97.7	97.8	99.1	98.1	98.5	97.1	96.8

Major- and Trace-Element Chemistry for Sample 15475 Plagioclase

	pc1	pc2	pc3	pc4	pc5	pc6	pc7	pc8	pc9	pc10	pc11
Sc	2.65	2.81	2.86	2.69	2.76	3.22	2.72	2.61	2.75	2.91	2.74
Ti	166	266	225	169	170	343	179	252	168	196	166
V	2.73	3.43	1.2	3.21	2.68	3.55	3.17	3.57	3.1	3.33	3.16
Cr	<2.41	9.01	<1.76	3.78	4.63	7.61	3.82	6.26	5.53	7.15	5.76
Mn	65.2	83.2	66.1	69	66.9	82.5	68.4	71.9	67.9	75.3	70.1
FeO	0.543	0.735	0.647	0.529	0.565	0.807	0.535	0.61	0.538	0.6	0.561
Co	0.55	0.861	0.547	0.291	0.694	1.05	0.592	0.57	0.505	0.495	0.573
Ni	<0.495	0.423	0.461	0.719	0.527	0.577	<0.446	0.526	<0.419	<0.289	0.457
Ga	8.61	7.15	10.3	8.14	8.7	7.03	7.79	6.7	8.66	7.6	8.26
Rb	<0.187	<0.123	<0.128	<0.138	<0.118	<0.104	<0.127	<0.125	<0.083	<0.106	<0.138
Sr	271	260	367	256	286	263	260	233	263	255	255
Y	0.127	0.212	0.175	0.127	0.144	0.188	0.141	0.166	0.161	0.15	0.132
Zr	<0.034	<0.026	0.531	<0.028	<0.036	0.025	<0.029	0.03	<0.031	<0.036	<0.036
Nb	<0.015	0.012	<0.012	<0.020	<0.011	<0.010	<0.019	<0.013	<0.013	<0.026	<0.0088
Ba	15.8	19.4	28.3	15.1	18.4	20.7	15	12.9	15.4	14.9	14.6
La	0.183	0.241	0.236	0.185	0.201	0.274	0.161	0.191	0.156	0.186	0.178
Ce	0.386	0.581	0.579	0.388	0.46	0.649	0.381	0.458	0.425	0.448	0.386
Pr	0.041	0.078	0.073	0.053	0.066	0.073	0.04	0.05	0.056	0.058	0.045
Nd	0.29	0.354	0.352	0.241	0.274	0.37	0.264	0.284	0.274	0.229	0.239
Sm	0.075	<0.072	<0.105	<0.077	<0.139	<0.098	<0.099	<0.095	<0.119	<0.117	<0.117
Eu	1.55	1.51	2.19	1.45	1.67	1.43	1.51	1.37	1.53	1.49	1.5
Gd	0.079	0.066	<0.090	<0.081	<0.075	<0.076	0.072	<0.087	<0.083	<0.086	<0.077
Tb	<0.017	<0.012	<0.013	<0.019	<0.016	<0.018	0.013	<0.014	<0.016	<0.016	<0.015
Dy	0.101	<0.054	0.073	0.045	<0.080	<0.076	<0.099	<0.052	<0.059	<0.070	<0.054
Ho	<0.012	<0.014	0.012	0.014	<0.016	0.014	<0.016	0.013	0.017	<0.011	<0.019
Er	<0.042	<0.041	<0.048	<0.038	<0.028	<0.051	<0.045	<0.047	<0.026	<0.034	<0.049
Yb	<0.083	<0.050	<0.069	<0.067	<0.060	<0.055	<0.080	<0.079	<0.061	<0.064	<0.097
Lu	<0.014	<0.016	<0.014	<0.010	<0.010	<0.021	<0.011	<0.010	<0.016	<0.018	<0.013
Hf	<0.037	<0.037	<0.053	<0.048	<0.044	<0.054	<0.034	<0.042	<0.047	<0.058	<0.049
Ta	<0.012	<0.017	<0.018	<0.013	<0.017	<0.012	<0.015	<0.013	<0.011	<0.018	<0.019
Th	<0.038	<0.022	<0.019	<0.033	<0.029	<0.025	<0.022	<0.026	<0.027	<0.020	<0.039
U	<0.028	<0.020	<0.017	<0.026	<0.021	<0.020	<0.022	<0.021	<0.026	<0.020	<0.026
SiO2	45.6	46.1	46.0	43.4	43.1	46.4	44.0	47.4	44.3	44.6	44.8
Al2O3	33.4	33.3	33.4	32.1	33.1	31.2	33.4	32.0	33.0	33.4	32.8
CaO	18.6	18.5	17.8	18.7	18.7	17.3	18.7	17.2	18.5	19.0	18.8
FeO	0.58	0.59	0.53	0.51	0.45	0.70	0.53	0.59	0.41	0.48	0.51
Na2O	0.91	0.96	1.06	0.85	0.78	1.41	0.75	1.40	0.72	0.80	0.79
K2O	0.03	0.00	0.04	0.03	0.01	0.03	0.02	0.02	0.01	0.01	0.03
Total	99.028	99.406	98.795	95.54	96.115	97.061	97.374	98.598	96.973	98.27	97.78

Major- and Trace-Element Chemistry for Sample 15016 Olivine

	oa1	oa2	oa3	oa4	oa5	oa6	oa7
Sc	10.2	9.8	9.6	44.5	8.7	8.1	10.3
Ti	278	286	224	2930	250	191	320
V	46.9	44.8	63	316	44.3	47.2	32.1
Cr	887	867	1178	6047	887	920	675
Mn	2711	2915	2646	2988	2839	2279	3150
FeO	37.2	40.1	34.5	31.3	39.8	30.8	44.5
Co	101	106	104	95.4	103	86.2	109
Ni	89.6	64.1	124	80.9	68.5	82.9	58.3
Ga	0.128	<0.083	0.07	0.697	0.059	0.066	0.064
Rb	<0.040	<0.039	<0.038	<0.038	<0.033	<0.031	<0.038
Sr	<0.0096	0.0087	0.0063	1.92	<0.0077	0.034	0.114
Y	1.11	1.47	0.78	4.66	0.77	0.388	1.11
Zr	0.115	0.104	0.076	3.68	0.069	0.063	0.207
Nb	0.015	0.0091	0.015	0.097	<0.011	0.013	0.0083
Ba	<0.0091	<0.0056	<0.0076	0.09	<0.0066	<0.0061	0.028
La	<0.011	<0.0048	<0.0069	0.091	<0.0071	<0.0052	<0.0058
Ce	<0.0083	<0.0072	<0.0063	0.421	<0.0050	0.004	<0.0097
Pr	<0.0069	<0.0045	<0.0073	0.085	<0.0046	<0.0050	<0.0076
Nd	0.023	<0.019	<0.020	0.647	<0.024	<0.026	<0.027
Sm	<0.042	<0.042	<0.030	0.337	<0.021	0.023	<0.031
Eu	<0.0084	<0.010	<0.0061	0.032	<0.0083	<0.0076	0.0045
Gd	0.061	0.034	<0.029	0.601	0.034	0.023	0.035
Tb	0.017	0.023	0.01	0.134	<0.0083	0.0087	0.016
Dy	0.142	0.196	0.114	0.923	0.092	0.047	0.112
Ho	0.035	0.051	0.019	0.191	0.026	0.0092	0.044
Er	0.131	0.184	0.094	0.572	0.104	0.067	0.178
Yb	0.21	0.225	0.157	0.542	0.138	0.095	0.216
Lu	0.024	0.042	0.022	0.064	0.025	0.011	0.044
Hf	<0.024	<0.020	<0.016	0.206	<0.015	<0.015	0.015
Ta	<0.0087	<0.0047	<0.0060	<0.011	<0.0068	<0.0047	<0.0053
Th	<0.0075	<0.010	<0.011	<0.016	<0.011	<0.0075	<0.0092
U	<0.0052	<0.0063	<0.0068	<0.0080	<0.0045	<0.0047	<0.0040
SiO2	33.7	34.3	35.1	36.4	34.3	34.7	34.7
TiO2	0.10	0.09	0.05	0.06	0.05	0.06	0.02
V2O3	0.02	0.02	0.01	0.00	0.03	0.05	0.00
Cr2O3	0.19	0.17	0.17	0.13	0.09	0.22	0.16
MgO	24.8	24.6	27.6	29.4	23.1	22.7	22.4
CaO	0.34	0.31	0.33	0.24	0.34	0.31	0.28
MnO	0.40	0.38	0.40	0.28	0.40	0.39	0.41
FeO	38.7	40.1	36.5	33.7	40.6	42.2	42.1
Total	98.2	99.9	100.1	100.3	98.9	100.7	100.0

Major- and Trace-Element Chemistry for Sample 15555 Olivine

	ob1	ob2	ob3	ob4	ob5	ob6	ob7
Sc	10.9	10.8	11.2	11.1	11.5	11	10.9
Ti	312	523	294	329	289	327	248
V	27.1	40.6	34.7	33.2	48.6	49.4	71.1
Cr	689	1787	755	899	974	1074	1507
Mn	2893	3108	3159	2899	2738	2659	2348
FeO	38.6	41.1	43.2	38	35.3	33.9	31
Co	108	112	119	111	110	112	107
Ni	53.9	50.8	74.2	58.8	54.1	66.9	112
Ga	<0.052	0.156	<0.062	<0.054	<0.060	<0.054	<0.053
Rb	<0.050	<0.071	<0.067	<0.068	<0.062	<0.040	<0.044
Sr	<0.0061	0.009	<0.0062	0.013	<0.0064	0.011	<0.0060
Y	0.486	0.623	0.762	0.414	0.345	0.415	0.258
Zr	0.105	0.129	0.06	0.108	0.065	0.1	0.064
Nb	<0.0091	0.018	<0.0070	0.012	0.0068	0.011	0.015
Ba	<0.0085	0.017	<0.0093	<0.011	<0.0084	0.0042	<0.0060
La	<0.0047	0.008	<0.0048	<0.0064	<0.0068	<0.0056	<0.0081
Ce	<0.0078	0.021	0.0072	<0.0072	<0.0071	<0.0039	<0.0038
Pr	<0.0037	0.0068	<0.0065	<0.0098	<0.0078	<0.0030	<0.0060
Nd	<0.043	<0.040	<0.031	<0.031	<0.030	<0.022	<0.048
Sm	<0.026	<0.023	<0.031	<0.042	<0.030	<0.036	<0.038
Eu	<0.0080	<0.0068	<0.0077	<0.0065	<0.0066	<0.0098	<0.011
Gd	<0.021	0.048	<0.033	<0.031	<0.022	0.024	<0.033
Tb	<0.0073	0.012	0.01	<0.0059	<0.0067	0.006	<0.0078
Dy	0.052	0.068	0.093	0.039	0.026	0.061	0.031
Ho	0.011	0.023	0.034	0.01	0.013	0.013	0.0084
Er	0.063	0.06	0.093	0.064	0.07	0.04	<0.020
Yb	0.082	0.161	0.13	0.119	0.099	0.11	0.05
Lu	0.028	0.026	0.03	0.029	0.02	0.017	0.012
Hf	<0.013	<0.015	<0.023	<0.020	<0.016	<0.022	<0.013
Ta	<0.0064	<0.0085	<0.0075	<0.0079	<0.0077	<0.0076	<0.0069
Th	<0.010	<0.0098	<0.012	<0.016	<0.010	<0.013	<0.0088
U	<0.0084	<0.0092	<0.012	<0.0093	<0.0064	<0.0088	<0.0067
SiO2	33.6	33.1	34.7	33.0	35.2	35.7	35.8
TiO2	0.05	0.03	0.10	0.06	0.09	0.04	0.05
V2O3	0.02	0.00	0.01	0.00	0.03	0.00	0.01
Cr2O3	0.09	0.15	0.08	0.18	0.22	0.14	0.20
MgO	20.0	19.0	22.4	22.1	25.5	26.9	29.0
CaO	0.37	0.43	0.39	0.44	0.41	0.36	0.35
MnO	0.43	0.41	0.40	0.41	0.39	0.36	0.36
FeO	45.2	46.3	42.7	42.1	38.5	37.5	33.5
Total	99.7	99.4	100.7	98.3	100.3	101.0	99.2

Major- and Trace-Element Chemistry for Sample 15499 Olivine

	od1	od2	od3	od4	od5	od6
Sc	15.7	7.85	9.38	9.96	10.2	10.9
Ti	351	122	147	147	201	221
V	74.8	70.3	89.5	91.9	95.9	88
Cr	1648	1884	2375	2588	2607	2376
Mn	4028	1970	2264	2038	2106	2371
FeO	60.6	28.5	32	27.7	29.1	33.5
Co	148	100	114	114	114	115
Ni	38.8	107	94.4	203	157	78.2
Ga	0.199	<0.057	<0.088	<0.063	<0.087	0.068
Rb	0.136	<0.055	<0.049	<0.033	<0.050	<0.053
Sr	3.04	0.013	0.0052	<0.0077	<0.0088	<0.0073
Y	1.21	0.253	0.206	0.223	0.25	0.281
Zr	1.64	0.122	0.098	0.094	0.129	0.112
Nb	0.071	0.016	0.023	0.024	0.022	0.021
Ba	2.89	0.021	<0.0060	<0.0062	<0.013	<0.0082
La	0.217	<0.0078	<0.0053	<0.0072	<0.0093	<0.0086
Ce	0.445	0.009	<0.0074	<0.0067	<0.0072	<0.011
Pr	0.066	<0.0042	<0.0056	<0.0056	<0.0037	<0.0042
Nd	0.287	0.028	<0.033	<0.043	0.049	<0.045
Sm	0.067	<0.033	<0.056	<0.030	<0.059	<0.027
Eu	0.03	<0.0098	<0.0063	<0.011	<0.010	<0.0097
Gd	0.12	<0.038	<0.025	<0.044	<0.033	<0.032
Tb	0.021	<0.0064	<0.0073	<0.0064	0.0055	<0.0045
Dy	0.158	<0.026	<0.033	<0.024	<0.023	0.034
Ho	0.036	0.011	0.015	<0.0053	0.0091	<0.0077
Er	0.164	0.049	0.024	0.029	0.04	0.036
Yb	0.22	0.076	0.046	0.084	0.05	0.087
Lu	0.032	0.016	0.011	0.017	0.012	0.011
Hf	0.052	<0.032	<0.013	<0.017	<0.024	<0.033
Ta	<0.0085	<0.011	<0.0089	<0.0081	<0.0062	<0.0061
Th	0.033	<0.016	<0.018	<0.017	<0.016	<0.015
U	<0.015	<0.0083	<0.011	<0.0089	<0.0096	<0.0091
SiO2			36.4	37.1	36.8	36.5
TiO2			0.05	0.02	0.05	0.03
V2O3			0.01	0.00	0.01	0.00
Cr2O3			0.30	0.46	0.37	0.33
MgO			32.0	34.1	33.4	32.2
CaO			0.31	0.30	0.31	0.33
MnO			0.28	0.33	0.32	0.37
FeO			30.8	27.7	28.3	29.9
Total			100.2	100.0	99.5	99.6

Vita

Darren W. Schnare was born in Hudson, NY on September 14th, 1982. He was raised in Climax, NY, and graduated from Coxsackie-Athens High School in 2000. From there, he went to the State University of New York at Potsdam, where he received a B.A. in Geology in 2004.

Darren is currently pursuing a career in Planetary Science.